Elsevier Editorial System(tm) for Geomorphology

Manuscript Draft

Manuscript Number: GEOMOR-7016R2

Title: Differential sediment trapping abilities of mangrove and saltmarsh vegetation in a subtropical estuary

Article Type: Research Paper

Keywords: Sediment trapping; Mangrove; Saltmarsh; Mudflat

Corresponding Author: Dr. Yining Chen, Ph.D

Corresponding Author's Institution: The Second Institute of Oceanography, SOA, China

First Author: Yining Chen, Ph.D

Order of Authors: Yining Chen, Ph.D; Yan Li; Charlotte Thompson; Xinkai Wang; Tinglu Cai; Yang Chang

Abstract: Saltmarsh and mangrove are common coastal wetland types and their ability to enhance deposition has been investigated extensively, but rarely compared directly. This study carried out in situ observations to compare the sediment transport processes between a bare mudflat, a mangrove stand and a saltmarsh stand within a subtropical estuary. Turbidity variations over the latter portion of a spring tide were recorded, alongside measurements of flow data, to estimate sediment trapping by hydraulic forces under similar hydroperiods. In addition, vegetation was transplanted to compare the direct sediment trapping by high- and short-standing seedlings. The suspended sediment concentration (SSC) time series showed an overall reduction between the bare mudflat and the vegetated flats. Suspended sediment flux estimates revealed that a considerable amount of sediment was trapped by the saltmarsh and the mangrove edges. The flux estimates find that the saltmarsh edge is more efficient than the mangrove edge in trapping sediments transported normal to the edge. The sediment trapping mechanisms were considered based on two approaches: the hydrodynamic related sediment settling and direct trapping by vegetation. The calculation of deposition tendency showed that the presence of vegetation altered the flow direction and the tidal asymmetry of the deposition process, resulting in a higher deposition tendency during the flood phase to enhance sediment settling. In addition to sediment settling, vegetation surfaces were found to trap sediments directly. In combination with rinsing by precipitation, these trapped sediments accumulated on the bed and contributed to the deposition. Against the background of similar inundation periods, the saltmarsh grass showed a greater sediment trapping ability than the mangrove trees, in terms of both the hydraulic sediment trapping and the direct trapping by vegetation surface.

Dear Editor,

Enclosed is the revised manuscript, entitled "Differential sediment trapping abilities of mangrove and saltmarsh vegetation in a subtropical estuary (GEOMOR 7016R1) ", which has been conditionally accepted by your journal.

We would like to thank the editor(s) for their valuable comments on this manuscript. We have revised some details of our paper, following all of the comments provided by the reviewer (editor). Our revision mainly includes English polishing, clarification of statements and the new table requested. Please find the revised manuscript in the submitted documents. We hope that the issues addressed by the reviewer have been clarified after the revision. In addition, we have been aware of the cost for the colour figures and we are willing to purchase this colour image service.

Yours sincerely,

Yining Chen

- Compare sediment transport from bare mudflat across mangrove and saltmarsh boundaries.
- Sediment trapping is caused by hydraulic forces and direct trapping by vegetation.
- The saltmarsh edge is more efficient than the mangrove edge at trapping sediments.

Abstract
Click here to view linked References

Saltmarsh and mangrove are common coastal wetland types and their ability to enhance deposition has been investigated extensively, but rarely compared directly. This study carried out *in situ* observations to compare the sediment transport processes between a bare mudflat, a mangrove stand and a saltmarsh stand within a subtropical estuary. Turbidity variations over the latter portion of a spring tide were recorded, alongside measurements of flow data, to estimate sediment trapping by hydraulic forces under similar hydroperiods. In addition, vegetation was transplanted to compare the direct sediment trapping by high- and short-standing seedlings. The suspended sediment concentration (SSC) time series showed an overall reduction between the bare mudflat and the vegetated flats. Suspended sediment flux estimates revealed that a considerable amount of sediment was trapped by the saltmarsh and the mangrove edges. The flux estimates find that the saltmarsh edge is more efficient than the mangrove edge in trapping sediments transported normal to the edge. The sediment trapping mechanisms were considered based on two approaches: the hydrodynamic related sediment settling and direct trapping by vegetation. The calculation of deposition tendency showed that the presence of vegetation altered the flow direction and the tidal asymmetry of the deposition process, resulting in a higher deposition tendency during the flood phase to enhance sediment settling. In addition to sediment settling, vegetation surfaces were found to trap sediments directly. In combination with rinsing by precipitation, these trapped sediments accumulated on the bed and contributed to the deposition. Against the background of similar inundation periods, the saltmarsh grass showed a greater sediment trapping ability than the mangrove trees, in

terms of both the hydraulic sediment trapping and the direct trapping by vegetation surface.

Editable manuscript
Click here to view linked References

Differential sediment trapping abilities of mangrove and saltmarsh vegetation in a subtropical estuary

Yining Chen[1,2*], Yan Li[1,2], Charlotte Thompson[3], Xinkai Wang [1], Tinglu Cai [1], Yang Chang[1]

[1]Second Institute of Oceanography, SOA, Hangzhou, 310012, China.

[2]State Key Laboratory of Marine and Environmental Science, Xiamen University, Xiamen, 361005, China.

[3]Ocean and Earth Science, University of Southampton, National Oceanography Centre, Southampton, SO14 3ZH, UK.

Corresponding author: Yining Chen (yiningchen5410@hotmail.com; yiningchen@sio.org.cn)

Key Points:

- Compare sediment transport from bare mudflat across mangrove and saltmarsh boundaries.
- Sediment trapping is caused by hydraulic forces and direct trapping by vegetation.
- The saltmarsh edge is more efficient than the mangrove edge at trapping sediments.

Abstract

Saltmarsh and mangrove are common coastal wetland types and their ability to enhance deposition has been investigated extensively, but rarely compared directly. This study carried out *in situ* observations to compare the sediment transport processes between a bare mudflat, a mangrove stand and a saltmarsh stand within a subtropical estuary. Turbidity variations over the latter portion of a spring tide were recorded, alongside measurements of flow data, to estimate sediment trapping by hydraulic forces under similar hydroperiods. In addition, vegetation was transplanted to compare the direct sediment trapping by high- and short-standing seedlings. The suspended sediment concentration (SSC) time series showed an overall reduction between the bare mudflat and the vegetated flats. Suspended sediment flux estimates revealed that a considerable amount of sediment was trapped by the saltmarsh and the mangrove edges. The flux estimates find that the saltmarsh edge is more efficient than the mangrove edge in trapping sediments transported normal to the edge. The sediment trapping mechanisms were considered based on two approaches: the hydrodynamic related sediment settling and direct trapping by vegetation. The calculation of deposition tendency showed that the presence of vegetation altered the flow direction and the tidal asymmetry of the deposition process, resulting in a higher deposition tendency during the flood phase to enhance sediment settling. In addition to sediment settling, vegetation surfaces were found to trap sediments directly. In combination with rinsing by precipitation, these trapped sediments accumulated on the bed and contributed to the deposition. Against the background of similar inundation periods, the saltmarsh grass showed a greater sediment trapping ability than the mangrove trees, in terms of both the hydraulic sediment trapping and the direct trapping by vegetation surface.

Keywords: Sediment trapping; Mangrove; Saltmarsh; Mudflat

1 Introduction

Natural coastal wetlands are widely recognized for their ability to trap sediments (Perillo et al., 2009; Barbier et al., 2011; Moller et al., 2014), as well as for their defense potential against the action of waves and tidal flows (Temmerman et al., 2013; Horstman et al., 2015; Carus et al., 2016). Saltmarshes and mangroves are globally common coastal wetland types, although the latter are mainly restricted to tropical and subtropical regions. In general, mangroves are dominated by halophytic trees and shrubs, whilst saltmarshes are characterized by herbaceous vegetation (Mitsch and Gosselink, 2007). Because of their ability to stabilize the coast by dissipating waves and current energy and enhancing deposition, these two types of habitats can be useful tools for coastal engineers in protecting the coastline (Redfield, 1972; Gedan et al., 2010).

Vegetation occurring along intertidal flats has been recognized as having the ability to stabilize, trap and bind sediments. In general, plants have been observed to directly increase the erosion threshold of bed sediments (Chen et al., 2012), and indirectly trap sediments by providing additional drag force (Leonard and Luther, 1995; Temmerman et al., 2005a; Chen et al., 2016) which mediate flow patterns, and consequently enhance local sediment deposition (Neumeier and Amos, 2006; Horstman et al., 2015). The enhancement of sediment deposition by coastal wetland vegetation has received more extensive attention in recent decades, in part due to the predicted impacts of accelerated sea-level rise due to global warming (van der Wal and Pye, 2004; Cahoon et al., 2006, Arkema et al., 2013; Woodroffe et al., 2016; Kelleyway et al., 2017). For practical purposes, the understanding of the mechanisms of sediment trapping by vegetation is key to the engineering work of coastal stabilization and protection, but the efficiency varies amongst vegetation species (Kathiresan, 2003; Friess et al., 2012; Ortiz et al., 2013).

Previous studies have revealed that heavily vegetated mangrove systems normally trap sediments during the flood tide, and that there is generally no significant export of sediments during the ebb due to the deceleration of the tidal currents by vegetation-induced friction (Wolanski et al., 1990; 2001; Furukawa et al., 1997; Kitheka et al, 2003). At a tidal-scale, field observations also show that mangrove trees are able to create a favorable environment as a sediment sink by modifying flow routing (Horstman et al., 2015). Factors such as vegetation density and biomass, as well as the intertidal position determining submergence/emergence status, and geomorphological settings (e.g., platforms or creeks), all affect the trapping capacity of mangrove trees (Friess et al., 2012).

Saltmarshes and their interaction with sediment dynamics have also been extensively studied (e.g., Leonard and Luther, 1995; Temmerman et al., 2005a; Neumeier and Amos, 2006; Bouma et al., 2007). Previous studies reveal the dampening effects of saltmarsh vegetation on mean flow and turbulent diffusion, resulting in a more favorable environment for deposition (Christiansen et al. 2000; Neumeier and Amos, 2006; Zong and Nepf, 2010; Nepf, 2012). Factors controlling the trapping capacity of saltmarsh grass include density, biomass, the emergence/submergence status and geomorphological setting (Temmerman et al., 2005a, b; Bouma et al., 2007; Nepf, 2012). The differences between the effects of mangroves and saltmarshes are related to the physical structure of the vegetation. The stiff canopy of saltmarshes normally shows a decrease in biomass with height (Neumeier, 2005). The presence of the trunks and aerial roots of mangrove show considerable effects on flow and deposition mediation (e.g. Madza et al., 1995) while the canopy is made up of rigid stems on the bottom and a stiff leaf layer at the top, resulting in an increase in biomass on the top. Therefore, theoretically, the saltmarsh grass shows a more pronounced influence on the bottom of the water column rather

than the top, whilst the mangrove, depending on species, affects the bottom and sometimes the top of the water column, although the regions of the water column affected by vegetation will depend on the relative local tidal levels to the height of trees.

This body of previous work has endeavored to further our understanding of the mechanisms controlling the bio-physical interactions within fluvial systems and coastal wetlands, together with the feedback between vegetation and sediment dynamics. The use of flumes and model vegetation has played an important role in raising our understanding of these detailed mechanisms (Shi et al., 1995; Nepf, 2012; Oritz et al., 2013). However, field observations focused on natural systems and processes are required to further develop these fundamental findings, particularly in regions where different ecosystems overlap. As pointed out by a number of scientists, complex factors such as precipitation, intermittent discharge, bi-directional flows and the consolidation of sediments must also be taken into account during the study of sediment transport on tide-dominated environments (Fagherazzi et al., 2004; Greene and Hairsine, 2004; Chen et al., 2012). These processes drive the evolution of coastal systems over the long term, but cannot be entirely captured by flume observations. Comparisons of the results from field and flume observations (Bouma et al., 2007) found that flume studies are unable to capture all necessary spatial scales, and will always result in some flow artefacts, including lower turbulence intensities than in the field. Vargas-Luna et al. (2015) reviewed a number of physical models in terms of the effects of vegetation on flows and sediment transport and they concluded that 'field measurements are not available, thus, intensive field campaigns including different climatic conditions, vegetation species…are also recommended.' Thus, the aim of this study was to carry out *in situ* observations to compare the sediment transport at the boundaries of a mangrove swamp and an adjacent saltmarsh. The competition between saltmarshes and

mangrove species has been well documented to be associated with the critical bed elevation and the subsequent inundation period (Saintilan et al., 2014). In this study, we focus on a direct comparison between the sediment trapping abilities of the two types of vegetated boundaries with similar inundation periods (i.e. similar bed elevations). A comparison of differences in flow reduction and energy dissipation by saltmarsh and mangrove plants has already been assessed and is presented in a separate paper (Chen et al., 2016).

2 Methods

2.1 Study Site

Yunxiao Mangrove National Natural Reserve, located at the Zhangjiang Estuary in the southeast China coast, was selected as the site to conduct the field measurements (Fig. 1). The tidal flat developing within this reserve is approximately 600 m in width. The upper part of the tidal flat (100-200 m in width) is covered both by mangroves and saltmarshes; the adjacent species make this location an ideal study area for comparative field observations.

The runoff of the Zhangjiang River carries a large amount of fresh water and sediments, with a mean annual water discharge of 9.6×10^8 m^3 and suspended sediment discharge of 3.6×10^8 kg (MICZTWR Office, 1990). The suspended sediment concentration decreases to ~40mg L^{-1} within the estuary and further to ~ 30 mg L^{-1}in Dongshan Bay (MICZTWR Office, 1990; Liu, 1991). The annual precipitation within the estuary region is 700 mm and 80% of it takes place in the wet season (April to September). The study site is home to a tidally-dominated mangrove forest with a fronting saltmarsh; the tidal flat is exposed to irregular semi-diurnal tides with a mean tidal range of 2.3 m. Wave exposure is very limited due to the sheltering effects of Dongshan Bay outside the estuary, except during typhoon seasons which normally occur in

summer. The resulting physical conditions of the estuary therefore favor the deposition of fine-grained sediments, which form a wide range of tidal flats along the main channel (Liu, 1991). The site under investigation is located on a relatively wide tidal flat with a slope of 2-3‰. The bed of this tidal flat consists of fine-grained sediment, mainly clays and silts.

It has been reported that on the southeast coast of China, the rapid spread of the invasive saltmarsh grass *Spartina alterniflora* threatens the local mangroves (Lin, 2001; Zhang et al., 2012). However, the study site is located on a tidal flat that exhibits co-existence of local mangroves and *Spartina alterniflora* saltmarsh. The upper part of the flat is covered by native mangrove species (*Kandelia obovata*, *Aegiceras corniculatum*, and *Avicennia marina*), while the exotic *Spartina alterniflora* occupies part of the mudflat fronting the mangrove forest (Zhang et al., 2012). The saltmarsh grass only covers a small area of the tidal flat during spring and summer, due to human removal as part of managed efforts to maintain a bare mudflat in the lower part of the tidal flat (Zhang et al., 2006).

Fig. 1. Location of study area and field deployment: a) study area: Yunxiao National Mangrove Reserve; b) location of deployments: Site A (bare mudflat), Site B (mangrove boundary) and Site C (saltmarsh boundary)，together with the definition of flow components: U and V are the geographical northing and easting components, V1 and U1 are the components normal and parallel to the mangrove edge, respectively, and V2 and U2 are the components normal and parallel to the saltmarsh edge, respectively; the flood directions of three sites are also marked by arrows: black for mudflat, red for saltmarsh and blue for mangrove; and c) the positions of instruments deployed and the location of seedling transplantation, sites B and C have the same bed elevation, 5 cm above the bed of Site A (the reference for water level measurements)

154

155 The leading edge of the mangrove forest is made up of a mixture of *Kandelia obovata*
156 and *Aegiceras corniculatum*, with a mostly closed canopy (80-90% closed). The mean distance
157 from the bottom of the tree canopy to the bed was 0.4 m. In spring, the trees had a mean height
158 of 1.6 m and a mean canopy width of 1.2 m. Combination of canopy closure percentage and the
159 canopy width gives a density of 0.8 shoots/m^2. The aerial root system is not well developed in
160 the front, due to the presence of young mangrove trees. In addition, aboveground aerial roots of
161 *K. obovata* are generally rare on the mudflats of Southeast China. Seedlings can be observed
162 sparsely within the mangrove forest, with density of 20-30 shoots/m^2.

163 The saltmarsh of *S. alterniflora*, 1.0 m in height, occurs at the seaward front of the
164 mangrove forest, with a high stem density of 580 m^{-2} and a high aboveground biomass (dry) of
165 2.50 kg m^{-2} (Chen et al., 2016). A topographic map of the region indicates a small elevation
166 change (< 0.27%) in the northwest-southeast (NW-SE) direction. When the tidal flat is
167 submerged (2-3 hours every tidal cycle during the observation period, Table 1), the mean water
168 level was 0.43 m above the tidal flat bed, with the maximum water levels reaching 0.76 m (Chen
169 et al., 2016). It should be noted that due to the elevation of the vegetated mudflat, only higher or
170 spring tides are able to reach this part of tidal flat (Fig. 1c).

171 2.2 Location and Time

172 Because spring is the crucial time for the seedlings of mangrove and saltmarsh vegetation
173 to establish, the field observations were carried out during 30th April to 5th May 2014 throughout
174 the latter portion of a spring tide, covering 11 tidal cycles. The weather was cloudy but dry for
175 most of the time, except the second day, during which a moderately heavy rain event (25 mm

over 24 hours) took place, and the last day, during which a short shower took place just before the vegetation samples were collected (after tidal cycle No. 11).

Three locations (Fig. 1) were selected for comparative synchronous measurements, located on the bare mudflat (Site A), within the mangrove edge (Site B) and within the saltmarsh edge (Site C). The distance between the bare mudflat site and the two vegetated flat sites was approximately 35 m. The sites within the mangrove and saltmarsh boundaries are at a distance of 10 m from the vegetation edge, as defined by the start of the closed canopy. The remaining regions between Sites A and B, and Site C are covered by sparse mangrove trees and *Spartina* grass. The fringes of vegetation described in this contribution include both the dense vegetation with closed canopies, as shown in Fig. 1, together with the sparsely vegetated fronting flat. The space between the vegetated sites (B and C) and the bare mudflat location (Site A) confines the vegetation fringes. Site A is 0.05 cm lower in elevation than the other two sites. Site B and Site C have the same elevations as determined by RTK-GPS.

2.3 Sediment Dynamic Observations

The backscatter intensity data of three Acoustic Doppler Velocimeters (ADV) were used to obtain flow data over 9 tidal cycles. The locations were carefully selected to avoid mangrove trees, and the vegetation around the sensors was removed (Chen et al., 2016). These were fixed to stainless steel frames for field deployment. The ADVs (Nortek Vector models, 6MHz) were all positioned 20 cm above the bed to collect data continuously at a frequency of 16Hz. It should be noted that the ADV sensor measures the water volume at a height of 8 cm above the bed (12 cm below the sensor head positioned 20 cm above the bed, Fig. 1c). ADV backscatter intensity data were also used to estimate the suspended sediment concentration (SSC) based on a logarithmic relationship calibrated within the laboratory (Sontek, 1997; Ha and Maa, 2010). The

longest possible data records were extracted and separated into 5-minute intervals to obtain mean values.

The output of the ADV provides three components of current velocity, U, V and W which represent easting, northing and upward components of the flow. A three-dimensional hydrodynamic and sediment transport model has revealed that as long as the water level is below the canopy top, the vegetated areas flood from the unvegetated areas, with flow directions more or less perpendicular to the vegetation edge (Temmerman et al., 2005a*)*. Thus, the flow components are rotated according to the orientation of the vegetation edges for further analyses. The mangrove edge has an orientation of 160°, and the flow components were rotated to generate components parallel (U1)and normal (V1) to this direction. The same procedure was applied to the saltmarsh edge, which has an orientation of 50° (U2 and V2). For simplicity, the three velocity components (u, v and w) of the tidal currents were used in formula as generalized symbols of the velocity components. When the data correlation values exceeded 0.7, the phase-space thresholding method developed by Goring and Nikora (2002) was adopted for despiking noise before the calculation of mean velocities, turbulent velocities and turbidities.

The suspended sediment flux can be expressed as follows (*Wang et al., 2014*):

$$F = \int_T \int_L \int_H C V_0 \, dz \, dx \, dt \qquad (1)$$

Where F is the flux through a cross section with water depth H (dz) and unit width L (dx) over a timescale T (dt) of a flood or ebb flow, C is the SSC converted from ADV backscatter intensity and V_0 is the speed of flow component normal to the vegetation edges. Due to the position of the sensors, the flux only covers the submerged period of a tidal cycle. However, the

data used for the flux calculation were from simultaneous periods, so this will not affect the comparison amongst the three sites.

The TKE (Turbulent Kinetic Energy) density can be estimated as:

$$TKE_{density} = 0.5\rho(\overline{u'^2} + \overline{v'^2} + \overline{w'^2}) \qquad (2)$$

Equation 2 is applied for each 5-minute data section. Here, ρ is the fluid density; u', v' and w' are the turbulent fluctuations deviating from 5-minute average values of the eastward, northward and upward flow components, respectively (Thompson et al., 2004).

The bed shear stress τ_b is estimated using Equation (3), where $C_1 = 0.19$ as suggested by Soulsby (1997), and suited to vegetated beds (Thompson et al., 2004):

$$\tau_b = C_1 TKE_{density} \qquad (3)$$

The shear velocity u_* can be estimated from the bed shear stress and the fluid density ρ_f (Equation 4):

$$u_* = \sqrt{\frac{\tau_b}{\rho_f}} \qquad (4)$$

Fugate and Friedrichs (2002) provided an algebraic equation for estimating tidally-averaged settling velocity w_s using an ADV. Voulgaris and Meyers (2004) further expand this method to resolve the tidal variability of the settling velocity (Equation 5), which was adopted in our study:

$$w_s C = \langle w'C' \rangle \qquad (5)$$

where C is the 5-minute averaged SSC, w' is the vertical fluid velocity fluctuation, C' is the SSC fluctuation estimated from the ADV backscatter strength, and $\langle\ \rangle$ is the symbol indicating time averaging. The settling velocity estimate (Equation 5) can be applied when the

advection transport is minimal compared with the vertical velocity terms (Fugate and Friedrichs, 2002). Using ADV data from pairs of stations, a consistency check was undertaken to evaluate the ratio of the advection term relative to the settling term, as suggested by Fugate and Friedrichs (2002), before the settling velocity was calculated. The flow data and the SSC data obtained by ADV, as well as the distance between the paired stations and the elevations of sensors, were used for this valuation which gives the average ratio of 0.06 ± 0.04 and 0.009 ± 0.006 for the flat-mangrove and flat-saltmarsh sites, respectively. Thus, the advection term is two orders of magnitude smaller than the settling term and it is reasonable to estimate settling velocity using the method of Voulgaris and Meyers (2004).

Bed samples from each site and local water samples were collected to produce a turbidity gradient in the laboratory, for individual calibration of ADV backscatter sensors. SSC was measured by passing a known sample volume through a pre-weighed 0.45 μm poresize glass fiber filter, followed by drying and weighing. Linear relationships were therefore established between the backscatter intensity and the logarithm of SSC for each sensor, as suggested by previous studies (Ha and Maa, 2010, Fig. 2).

Fig. 2. Calibration between backscatter intensity and suspended sediment concentration for (a) bare mudflat; (b) saltmarsh; and (c) mangrove. Note the x in the equations refers to $Log_{10}SSC$, and SSC is in the unit of mg L^{-1}.

2.4 Vegetation Trapping Experiments

More than 50 saltmarsh grass standings and small branches of mangrove trees were randomly marked and cleaned for field observation. Any sediments attached to these vegetation

samples were washed off using clean water in the field before the experiment started. Subsequently, the aboveground parts of 6 vegetation samples (3 mangrove samples and 3 grass samples) were then collected daily using tough scissors after the initial deployment of the instruments. The sediments on the vegetation surface were washed off and collected into cylinders for subsequent filtering and drying to obtain the dry weight of the sediment deposits on the vegetation. The vegetation samples, including leaves and stems, were subsequently dried and weighed to obtain biomass. Note that for conservation purposes, only small branches of the mangrove trees were collected and thus measured weight is mainly from leaves.

The seedlings of mangrove and saltmarsh grass start to grow during this season (Spring). They are much shorter than the natural standings but vital to the development of the ecosystem. In light of the fact that seedlings appear within the near bed whilst the natural standings penetrate the whole water column during the investigation period, it is important to examine the difference between their abilities of trapping sediment using their leaves and stems. *K. obovate* and *S. alterniflora* seedlings were transplanted adjacent to the observation sites and arranged at a density close to the natural status, and used to represent the sediment trapping ability of vegetation at an early stage of life. Seedlings of *K. obovata* and *S. alterniflora* were transplanted into Site B and Site C, respectively. For each site, fifty 20 cm- high seedlings of mangroves or saltmarsh grass, which had been rinsed clean with water, were separately arranged into two quadrates of 200 cm×100 cm, with an individual spacing of 20 cm. Three Samples of each type of seedlings were collected in triplicate every day along the edge of the plots, together with the natural standings of vegetation to measure the sediment trapped by vegetation using the same method as mentioned before. The mangrove seedlings were in a similar density as their natural

status, but that of the *Spartina* seedlings was decreased to allow a comparison between two species.

The instruments recorded from midnight of 29th/30th April until after the first tidal cycle of 4th May (Table 1), the last point at which water levels were sufficiently high to submerge them.

The sediment mass trapped by the vegetation was measured in this study through the period of the 2nd tidal cycle (occurring in the afternoon of 30 April) to the 11th tidal cycle. The samples were collected every day at noon (Table 1).

Table 1. Description of the field observation deployment

Tidal cycle Number	1	2	3	4	5	6	7	8	9	10	11
Time	01:00 - 03:20	13:00 - 15:00	01:50 - 04:00	13:40 - 15:35	02:30 - 04:40	14:20 - 16:00	03:20 - 05:20	14:40 - 16:40	03:40 - 05:50	N/A	N/A
Date	30/4 AM	30/4 PM	1/5 AM	1/5 PM	2/5 AM	2/5 PM	3/5 AM	3/5 PM	4/5 AM	4/5 PM	5/5 AM
Trapping Experiment		Day 1		Day 2		Day 3		Day 4		Day 5	
Instruments	Recording									Off	
Weather	Cloudy but dry		Rain	Cloudy but dry							Rain

2.5 Supporting Measurements

A RTK-GPS (Trimble-SPS881) survey was undertaken to record the relative elevations of the three sites for water level analysis. Plastic accretion stakes (1.5 cm in diameter, 50 cm long, 10 cm exposed, Fig. 1b) were inserted into the bed to monitor deposition rates by measuring the exposed length from May 2012 to May 2014. It is noted that the *Spartina* grass was removed in August 2012 by the local management office and it had recovered by the spring of 2013; as such,

303 the deposition rates of the saltmarsh represent under-estimated values. Surface sediments were
304 collected during instrument deployment for laboratory grain size analysis using a laser grain size
305 analyzer (Helos, manufactured by Sympatec). Biological properties of the vegetation, such as
306 mangrove geometrics (height and diameter of canopy, diameter of trunk), and density and
307 diameter of grass were measured *in situ* using a tape measure. Aboveground biomass of
308 vegetation was measured by harvesting, drying and weighing plant samples.

309 **3 Results**

310 3.1 Tidal-cycle Scale Suspended Sediment Concentration

311 The variation of suspended sediment concentration (SSC) over 9 tidal cycles is displayed
312 in Fig. 3. The SSC data exhibit a strong tidal asymmetry, with one exception of the second tidal
313 cycle on the bare mudflat. The overall SSC is higher during the flood phase than the ebb phase
314 for all three sites, which implies a favorable environment for a net sediment input. On average,
315 there is a considerable reduction in SSC between the bare mudflat and the vegetated sites (Table
316 2). The average SSC reduced nearly 10% from the bare mudflat to the saltmarsh boundary,
317 whilst nearly 20% from the bare mudflat to the mangrove boundary. This pattern implies
318 sediment trapping within the vegetation boundaries at a tidal scale.

319 Deposition rates over a two-year period were recorded by accretion stakes. The readings
320 of 5 or 6 stakes of each site (see Fig. 1 for more details) are averaged and displayed in Table 2.
321 The short-term pattern of SSC variation is generally consistent with long-term deposition rates
322 recorded by stakes on the vegetated area and the mudflat, which shows higher rates at vegetation
323 edges than on the mudflat (Table 2), although the deposition rates may be under-estimated as
324 compaction is not considered.

325

326 Fig. 3. The SSC data series over 9 tidal cycles: (a) SSC time series based on acoustic backscatter
327 (ADV); and (b) water level variation. The detailed time is listed in Table 1.

328

329

330

331 Table 2. Synthesis of the mean parameters associated with suspended sediment transport of the
332 three sites.

Parameter		Flat	Saltmarsh	Mangrove
Grain size (μm)		6.20±0.76	5.79±0.43	6.34±0.90
Deposition rate (cm a^{-1})		1.14±1.20	2.60±0.97*	2.10±0.87
Settling Velocity (mm s^{-1})		1.90	0.87	0.85
SSC (mg L^{-1})		68.8	62.9	56.2
Net SSC flux per tidal cycle (kg/m)	Normal to saltmarsh edge	8.1	3.0	--
	Normal to mangrove edge	4.4	--	3.2
Sediment trapped per tidal cycle (kg/m)		--	5.1	1.2
Deposition tendency	Flood	0. 17	0.21	0.26
	Ebb	0. 23	0.21	0.25
Cumulative S:B ratio	Natural standings	--	0.017	0.016
	Seedlings	--	0.11	0.13

333 *Note: the deposition rate is under-estimated due to the clearing of grass in August 2012. The
334 stake number is 6 in the saltmarsh site, whilst 5 for the other sites.

335

3.2 Tidal-cycle Scale Sediment Transport: A Comparison

Detailed flow information has been published in a separate paper (Chen et al., 2016). Here, we provide a brief summary of the horizontal flow conditions. The horizontal flow speeds of the three sites are shown in Fig. 4. A considerable reduction in flow speed caused by vegetation is readily identified and a rotation of flow direction by vegetation has been related to eddy viscosity and drag forces (Chen et al., 2016).

Fig. 4. The variations of horizontal flow speed and direction throughout 9 tidal cycles (source: Chen et al., 2016): (a) flow speed data; and (b) flow direction data. Note the geographical flow direction uses the north as zero degrees.

Neumeier and Ciavola (2004) noted a relatively uniform vertical velocity profile within saltmarsh grass canopies. Due to the shallow water layer, the SSC is normally regarded as a constant through the vertical profile in modeling or field observations on tidal flats (e.g., Temmerman et al., 2003; Wang et al., 2012). In addition, based on the consideration of small flow speed magnitude and the relatively low turbidity, a uniform profile assumption is used in this study for SSC flux estimate, based on a combination of flow and SSC data using Equation 1. The SSC flux data for each flood and ebb period is displayed in Fig. 5. Due to the flow rotation, the SSC transport normal to the vegetation is mainly presented, but the sediment transport along the vegetation edges is also considered (Fig. 1b). The SSC fluxes of the bare mudflat site are decomposed according to saltmarsh edge and mangrove edge orientations separately (Fig. 5). Diurnal inequality results in higher sediment fluxes during the relatively high tides (odd numbers) than the relatively low tides (even numbers). The sediment fluxes are determined by

both SSC and flow velocity. Although the SSC values of the bare mudflat are not always higher than the vegetated sites, as indicated by Fig. 3 for all tidal cycles, the net sediment trapping of the vegetation edges is likely to be the result of flow reduction by the vegetation.

Overall, the study area is dominated by a net input of sediments. The highest fluxes occur on the bare mudflat site; this is because when the suspended sediments are transported into the vegetation edges, a large amount of sediment is trapped by the vegetation and only part of the sediment flux is able to pass through the vegetation to reach the upper tidal flat. The bare mudflat site shows different SSC fluxes when considering the main transport directions (Fig. 5). This site shows a lower net sediment transport towards the mangrove, because the presence of the mangrove edge deviates the flow (257º in flood) away from the main flow direction of 305º in flood on the tidal flat (Fig. 4b, Chen et al., 2016).

The long-term deposition rates (Table 2) are consistent with the pattern of the flux estimates at tidal cycle scales: relatively low deposition rates are observed on the bare mudflat (1.4 cm a^{-1}) whilst high deposition rates occur at the vegetation edges (> 2 cm a^{-1}); the deposition rate at the saltmarsh edge is higher than that at the mangrove edge, in response to a greater difference in sediment input between the vegetated sites and the bare mudflat site.

Fig. 5. Suspended sediment fluxes per unit width estimated at a tidal cycle scale: (a) sediment flux at the bare mudflat site in the direction normal to saltmarsh edge; (b) sediment flux at the saltmarsh site in the direction normal to saltmarsh edge; (c) sediment flux at the bare mudflat site in the direction normal to mangrove edge; and d) SSC flux at the mangrove site in the direction normal to mangrove edge. The flux was estimated to represent the total mass passing a unit width of bed over a time span of either the ebb or flood flow. North represented by zero degrees.

382

383 The amount of sediment trapped between the vegetated sites and the bare mudflat sites is
384 estimated using the SSC flux data using Equation 1. The sediment trapped at the vegetation
385 boundaries can be estimated by comparing the difference between the fluxes of the mudflat site
386 (with subscript of 'mud') and the vegetated sites (with subscript of 'veg'), as described by
387 following (Equation 6):

388 $$trap = (Flux_{flood,mud} - Flux_{ebb,mud}) - (Flux_{flood,veg} - Flux_{ebb,veg}) \quad (6)$$

389 The values of sediment trapping are given in Table 2. This clearly indicates that the
390 presence of vegetation can increase SSC trapping at their front edges. Further, by comparing the
391 SSC fluxes (Table 2), it can be inferred that considerable amount of the sediments transported
392 from the lower part of the tidal flat towards the upper tidal flat are trapped within the front edges
393 of the vegetation, an area of 35 m wide which includes a combination of mudflat and sparse
394 vegetation. Finally, the saltmarsh front edge, showing a greater trapping ability, is found to be
395 more efficient than the mangrove front edge in trapping sediments. Due to the total amount of
396 sediment flux from the bare mudflat is same for two vegetated sites, coupled with the fact that
397 the mangrove trees trap less sediments normal to their front, more sediments can be transported
398 parallel to the mangrove edge than the saltmarsh edge. The transport in this direction can
399 increase the elevation of the whole system and benefiting the neighboring plants. Remote sensing
400 image analysis (Li et al., 2017) shows the mangrove in this area expands in a direction parallel to
401 its front, whilst the saltmarsh advances in a direction normal to its present front. The sediment
402 transport and trapping pattern might explain the different directions of vegetation expansion.

3.3 Enhanced deposition by vegetation as indicated by deposition tendency

In order to quantitatively evaluate the tendency for particles to deposit or resuspend, the ratio of particle settling velocity to the shear velocity $\frac{w_s}{u_*}$ has been proposed by Ortiz et al. (2013) for saltmarsh environments. The estimates of settling velocity and shear velocity for this study were calculated using Equations 2-5 as described in the Methods section. In general, when $\frac{w_s}{u_*}$ is above 0.1, the environment is considered to be deposition-dominant (Zong and Nepf, 2010)

Mean $\frac{w_s}{u_*}$ ratios calculated for each flood and ebb tide are displayed in Fig. 6. The $\frac{w_s}{u_*}$ ratio of the flood and ebb vary within a range of 0.14 and 0.31 for all sites, implying favorable conditions for deposition. The tidal cycle-averaged values (including flood and ebb phases) of vegetation sites are 0.25 ± 0.03 and 0.21 ± 0.04 for the mangrove site and the saltmarsh site, respectively, whilst this value is 0.20 ± 0.03 for the bare mudflat site.

Fig. 6. Deposition tendency of three sites as indicated by $\frac{w_s}{u_*}$ ratio: (a) mudflat; (b) saltmarsh; and (c) mangrove; the dashed line of 0.1 marks the lower limit for 'deposition favorable' conditions, as suggested by Zong and Nepf (2010).

3.4 Sediment Trapping by Vegetation, and Precipitation Effects

A ratio of sediment mass (S) to biomass (B), S/B, is proposed in this study to allow estimates of the ability of vegetation to trap sediments. The S/B ratio is defined as the value of

422 the dry sediment mass washed from the vegetation divided by the dry biomass of the vegetation
423 itself. We choose this ratio because dry sediment mass and dry biomass can be easily measured
424 in laboratory with high accuracy. Further, the data on dry sediment mass and dry biomass have
425 been used in a large number of studies and this allows us to discuss our results using other data
426 sources. The properties of the two vegetation species are listed in Table 3.

427

428 Table 3. The biological properties of the investigated mangrove trees and saltmarsh grass

Spartina	Height (m)	Stem density (m^{-2})	Biomass (dry, kg m^{-2})	Coverage (%)	Stem diameter (m)
	1.0	580	2.5	90%	0.008
Mangrove	Height (m)	Stand Density (m^{-2})	Canopy biomass (dry, kg m^{-2})	Canopy closure (%)	Trunk diameter (m)
	1.6	0.8	0.22	80-90%	0.1

429

430

431 Because the samples were collected successively, the S/B ratio data are cumulative,
432 indicating the continuous sediment trapping by vegetation over tidal cycles. The cumulative S/B
433 ratio of the natural standings and the transplanted seedlings of mangrove trees and saltmarsh
434 grass for the observation period are illustrated in Fig. 7.

435

436 Fig. 7. The cumulative sediments trapped by vegetation surfaces, as indicated by the S/B ratio
437 over 10 tidal cycles: (a) seedlings and (b) mature standings. The seedling samples were planted
438 in a matrix of 10 x 5 stands within an rectangular area of 100 cm x 200 cm. Three samples of
439 each vegetation type were collected every day to give the average and standard deviation values
440 in this figure.

441

Overall, the S/B ratio of natural, high standings is significantly less than that of the seedlings for both types of vegetation (Fig. 7). This is because the top canopy of the high standings experiences much less submergence than the lower part, and this decreases their efficiency as a sediment trap by unit mass. However, in the light of the large amount of biomass (e.g. aboveground biomass of *Spartina alterniflora* reaches 2.5 kg m^{-2} in this area) of the high standings and the length of time they are present (from Spring to Autumn) compared to the seedlings (only part of the seedlings are able to survive until Autumn), they perform a more important role overall in trapping sediments on the tidal flat.

The S/B ratio of mangrove and saltmarsh seedlings both vary considerably over the 10 tidal cycles while maintaining similar patterns (Fig. 7a). The S/B ratios of the mangrove seedlings are similar to those of the *Spartina* seedlings if the shoot densities are same. The S/B ratio drops to a minimum during tidal cycles 4 and 5, then they increase on the following two days, and decrease slightly again on the last day. This pattern is different from the expected continuous increase and it is highly likely to be associated with precipitation, which took place during tidal cycles 3 and 4, and before tidal cycle 11. The authors observed in the field that the rain drops washed off fine particles attached to the leaves during the low water period. It appears that the sediments become trapped by vegetation during high water levels, and the rain during the emergence hours creates a mechanism to transport sediment downward onto the bed. Without precipitation, the sediments will be accumulated until an upper limit is reached. The presence of precipitation is able to accelerate this downward transport of sediment. This mechanism may be not only important for the sedimentary process on the tidal flat, but also for the growth of seedlings. High standings show a similar pattern as the seedlings (Fig. 7b), except during tidal cycle no. 4-5. In general, the high standings show less diurnal variation, as well as lower

standard deviations amongst samples. The high standings of saltmarsh grass and mangroves show a decreasing trend in S/B ratio, with a low value occurring on the day after the moderately heavy rain (tidal cycles 4 and 5), together with a general increase after that day. Similarly, the short shower also shows its effect at the end of the observation, slightly decreasing the S/B ratio on the last day. The frequency of sampling is not sufficiently high in this study to confirm it, but the lag between surface sediment decreases in successive days (Fig. 7) might imply a lag in response to precipitation.

4 Discussion

A complete understanding of the mechanisms mediating sediment accumulation by tidal flat vegetation, particularly the possible impact of vegetation upon suspended particles, is still illusive (Graham and Manning, 2007). Trapping of suspended particles can be caused by both changes to hydraulic forces and by the direct presence of vegetation leaves and stems. In the following sections, the sediment settling caused by hydraulic forces and by the direct trapping by leaves or stems will be discussed separately, together with limitations of this study.

4.1 Hydraulic Sediment Settling Processes within the Saltmarsh and the Mangrove Fronts

Various devices (e.g., floc cameras) have been used to show that suspended particles settle in a flocculated form within saltmarshes and mangrove swamps (French and Spencer, 1993; Wolanski, 1995; Graham and Manning, 2007). Wolanski (1995) suggested that the settling velocity of suspended particles in mangrove swamps is 1 mm s^{-1} for clay and 5 mm s^{-1} for silt. Voulgaris and Mayers (2004) observed an invariant, tidally-averaged settling velocity of 0.24 mm s^{-1} for flocs on a saltmarsh surface. A more accurate observation of floc settling velocity within a saltmarsh vegetation canopy under turbulent flow conditions was conducted in an

annular flume using a flocs camera (Graham and Manning, 2007), which provides a range of 0.004 ~ 3.36 mm s^{-1}, with a mean value of 0.55 mm s^{-1}. Settling velocities estimated based on ADV observations by this study (Table 2) are within the range of previous observations. However, a decrease in the settling velocity of suspended particles from the bare mudflat to the vegetated sites occurs and further explanation is needed for the settling processes.

The settling of suspended sediments within the vegetation canopy is related to the generation of turbulence and the wake-sheltering effects in the lee of downstream stems (Shi et al., 1995; Nepf, 1999). In general, the deposition tendency ratio, also known as the inverse movability number forming part of the Rouse parameter (Amos et al., 2010), has a range of 0.002 to 0.3 in aquatic environments and a typical value of 0.02 has been used in flume experiments (Ortiz et al., 2013). Relatively high values of the ratio imply a trend for deposition whilst low values suggest a tendency for resuspension. Deposition has been clearly observed in flumes when the deposition tendency ratio is above 0.1 (Zong and Nepf, 2010).

The vegetation below the sensors was cleared in this study and, thus, this observation looked into the sediment settling directly driven by hydrodynamics, but not the direct trapping by the vegetation surface. Meanwhile, more than 80% of the turbulent kinetic energy is dissipated by the vegetation in comparison with the mudflat (Chen et al, 2016). Therefore, it is important to use the $\frac{w_s}{u_*}$ ratio to determine the likelihood of deposition.

The most notable pattern revealed by Fig. 6 is the change of tidal asymmetry in the $\frac{w_s}{u_*}$ ratio by vegetation. On the bare mudflat, the $\frac{w_s}{u_*}$ ratio shows a strong ebb-dominant characteristic throughout the tidal cycles, consistent with the asymmetry in suspended sediment

508 flux (Fig. 5). Paired-sample T tests (by SPSS package) are used to exam three sites in terms of
509 the flood-ebb asymmetry. The results show a significant difference between the bare mudflat and
510 the vegetated sites (P<0.01, Table 4).

511

512

513

514 Table 4. Paired samples tests for tidal asymmetry of deposition tendency

	Std. deviation	Std. error mean	t	df	Sig. (P-value)
flat vs saltmarsh	0.043	0.014	-3.616	8	0.007
flat vs mangrove	0.023	0.075	-8.284	8	<0.001

515

516 Thus, a considerable amount of suspended particles, mostly clay and fine silts (Table 2),
517 are transported into the bare mudflat during the flood stage. These particles tend to settle, as
518 indicated by the $\frac{w_s}{u_*}$ ratio (> 0.1 over 9 tidal cycles) during this stage. During the ebb stage
519 however, the $\frac{w_s}{u_*}$ ratio increases considerably, and consequently the majority of deposition
520 occurs during this stage, resulting in a deposition lag.

521 Tidal asymmetry, as defined by comparing flood and ebb phases through various
522 parameters in relation to hydrodynamic processes, has been widely recognized for its importance
523 in resulting sedimentation processes (Dronkers, 1986; Scully and Friedrichs, 2007; Brown and
524 Davies, 2010), but hardly considered in flume experiments (Zong and Nepf, 2010; Ortiz et al.,
525 2013). The tidal asymmetry in the deposition tendency can be altered by vegetation. Throughout
526 9 tidal cycles in our study, the deposition tendency data shows considerable ebb-dominance

within the bare mudflat site (Fig. 6a) whilst the vegetated sites shows either nearly symmetrical or flood-dominant deposition tendencies (Fig. 6b, c). Differently from the bare mudflat, most of the suspended particles within the vegetated sites therefore deposit during the flood stage when the SSC is high, rather than the ebb stage with low SSC, improving the deposition efficiency. This is likely to be an important mechanism throughout which vegetation enhances deposition by regulating hydrodynamics and the consequent $\frac{w_s}{u_*}$ ratio, but has not been reported by previous studies. The presence of vegetation decreases both the settling velocity (Table 2) and the shear velocity (Chen et al., 2016). The improved deposition efficiency implies that shear velocity reduction is greater than the decrease of settling velocity, as a function of the vegetation.

4.2 The Potential Contribution of Direct Trapping to Deposition

The suspended sediment settling and trapping driven by hydraulics have been extensively studied. However, the sediment directly trapped by vegetation is rarely taken into account. Vegetation occurring on tidal flats has been widely recognized for its ability to increase deposition to adapt to relative sea-level rise. Accelerated deposition rates have been observed in a number of saltmarshes and mangrove swamps, in comparison with unvegetated tidal flats (e.g., Childers and Day, 1990; Furukawa and Wolanski, 1996; Christansen et al., 2000; Alongi et al., 2005; Lovelock et al., 2015). The suspended particles can form larger flocs and settle more rapidly to the seabed as the vegetation creates a more favorable environment for sediment settling (Neumeier and Ciavola, 2004; Graham and Manning, 2007; Nepf, 2012; Ortiz et al., 2013). More recently, leaf transport as a source of particulate organic matter (POM) in ecosystems was observed in flume experiments which compared mimic mangrove forests and seagrass beds, indicating the mangrove roots were more efficient at trapping POM than the

seagrass beds (Gillis et al., 2013). Associated with leaf transport, it can be readily observed in the field that a thick layer of mud can accumulate on the leaf surface. This is another pathway for suspended particles to be trapped by the vegetation system, but is rarely recognized in the literature.

A quantitative measurement of suspended sediment trapped by vegetation stems and leaves in the field has been conducted in this study, and is represented by the S/B ratio (Fig. 7). Moreover, the amount of sediment trapping over a unit area (1 m × 1 m) is estimated based on S/B ratio and the biomass data. On average, the difference in S/B ratio of saltmarsh grass between two successive days reaches a value of 0.003 (based on data reported in Fig. 7), even when considering the rinsing by rainfall. The maximum accumulated S/B ratio over two successive days reaches 0.014. Considering the dry biomass values of 2.5 kg m^{-2} and based on our observations the aboveground biomass, including stems and leaves, has the potential to trap a maximum of 35 g dry sediments per square meter per day (S/B ratio =0.014). The dry density of clay and silt sediments is approximately 1.28 g cm^{-3} and thus the estimated amount of sediments attached to the vegetation surface have the potential to add up to 0.5 cm to the annual deposition rate during its growing season (6 months). This estimate assumes complete deposition from the leaves to the bed, but could be revised if additional factors (e.g., the water content and bulk density) were considered, and may be overestimated.

Spartina alterniflora has been artificially introduced into Chinese tidal flats since 1980s for the purpose of stimulating tidal flat accretion (Chung, 2006). It has been reported that the presence of *Spartina alterniflora* has increased the sedimentation rates of the tidal flats from ~1.5 cm a^{-1} to ~ 3 cm a^{-1} (Wang et al., 2005; Gao et al., 2014). The direct trapping amount of sediments by vegetation, however, remains unknown. Most of the *Spartina alterniflora*

572 saltmarshes appear on the silty or clay mudflats along the east China coast, including Jiangsu
573 Province, Shanghai, Zhejiang Province and Fujian Province (Gao et al., 2014). The total area of
574 this type of saltmarshes sums up to 3.2×10^8 m^2 (Zuo et al., 2012). The aboveground biomass
575 (dry mass) varies within the range of 2000 ~ 2500 g m^{-2} over these regions (Li et al., 2005; Liao
576 et al., 2008; Gao et al., 2016). If the same estimate is undertaken using the S/B ratio of this study
577 (0.014), the *Spartina alterniflora* saltmarshes are expected to result in a maximal direct trapping
578 of 1.9×10^6 tons of sediments over their growing season every year (dry biomass = 2250 g m^{-2}).
579 This value means that the direct trapping of sediments contributes 0.45 cm a^{-1} to the deposition
580 rate; nearly 1/3 of the increased deposition rates reported (Wang et al., 2005; Gao et al., 2014).

581 The sediment trapped by mangrove trees can also be estimated similarly. The mean
582 density of the mangrove trees is 0.8 trees m^{-2}. The total dry biomass of the canopy is
583 approximately 176 g m^{-2}. If half of the canopy is assumed to be submerged (a factor of 0.5
584 applied to the biomass), together with the maximum increase of S/B ratio of 0.028 between two
585 succeeding days (based on Fig. 7), the potential amount of sediment available from the leaves of
586 mangrove trees is 2.5 g m^{-2} per day at a maximum, which may contribute a maximum of 0.07 cm
587 (in dry mass) annually to deposition rate over an annual period. This is negligible when
588 compared to the saltmarsh grass. Therefore, the standings of saltmarsh grass contribute
589 substantially to sediment deposition processes, by trapping the sediments via the leaves and
590 stems and then transported to the bed by rainfall rinsing. In contrast, the mangrove trees are less
591 effective in direct trapping sediments via the canopy. It should be noted that most mature
592 mangrove forests worldwide will only rarely be inundated up to the canopy, with most
593 sedimentation occurring due to the slowing down of hydrodynamics between the aerial
594 roots. Our study only attempts to capture the mechanisms for the expanding pioneer zone of

595 mangrove forests which is occupied by short, young mangrove trees. With the future
596 development of aerial roots, the sediments trapped by mangrove trees may increase substantially.
597 Meanwhile, the net deposition rate increased by the mangrove trees also proves less effective
598 than the saltmarsh grass, although they have more significant influences on the hydrodynamics
599 (Chen et al., 2016). The deposition tendency data in Fig. 6 reveals that mangrove trees are more
600 effective than the saltmarsh grass in enhancing sedimentation by hydraulic alteration, but this
601 part is unable to compensate the difference caused by direct trapping. More importantly, the flow
602 rotation by the mangrove trees remarkably reduces the sediment transport flux into the
603 vegetation edge (Fig. 5b) and leads to a reduced efficiency in trapping sediments in a normal
604 direction.

605 A similar estimate was also used for the amount of sediment trapped by seedlings. The
606 maximum amount of sediment trapped by mangrove seedlings within a day was 4.78 g m^{-2};
607 higher than the 3.7g m^{-2} value found for grass seedlings of same stem density. The important
608 implication from the seedling observations is that the mangrove seedlings are more efficient in
609 directly trapping sediments, when compared to the more mature trees. The amount of sediment
610 trapped by mangrove seedlings per unit area is almost twice that of the canopy (2.5 g m^{-2} per
611 day). It can therefore be inferred that the both seedlings and aerial roots of some mangrove
612 species, which show similar characteristics to the seedlings, will have a fundamental effect on
613 sedimentation processes.

614 Although an aerial root system was not observed at the mangrove boundary under this
615 investigation due to the young age of the forest, the biomass distribution of the typical mangrove
616 species in southeast China has been reported by other studies (Lin et al., 1985; 1990; 1992; 1998,
617 Table 5). For three species in this table, the trunk represents the largest percentage of the total

aboveground biomass. The canopies, mainly consisting of branches and leaves, contain the next largest percentage in the total biomass. The contribution of aboveground roots (or seedlings) varies among species. For these species, the contribution of aboveground roots (or seedlings) is much less than the canopies. If the water level is sufficiently high to reach mangrove canopies, the direct sediment trapping by canopies is more considerable than the aboveground roots (or seedlings). In other words, the relative height of water level to the mangrove trees determines the direct trapping efficiency for these species in Table 5. In contrast, the aboveground roots of *Rhizophora stylosa* show the highest percentage in total aboveground biomass. Therefore, the aboveground root system of *Rhizophora stylosa* is fundamentally important in direct sediment trapping, regardless of water level changes.

Table 5. The typical mangrove species in Southeast China and their biomass constitutes as indicated by the percentage of total aboveground biomass (data source from Lin et al., 1985; 1990; 1992; 1998). Note the seedling of *Kandelia obovate* was reported instead of aboveground roots because *Kandelia obovate* trees rarely develop aboveground roots.

Location	Species	Trunk (%)	Branch (%)	Leaf (%)	Aboveground root (%)
Guangdong	*Aegiceras corniculatum*	74.20	13.68	7.29	4.84
Fujian	*Kandelia obovata*	77.78	15.56	6.52	0.19 (seedling)
Hainan	*Bruguiera sexangula*	69.61	22.95	4.39	3.05
Guangxi	*Rhizophora stylosa*	35.41	23.05	3.49	38.04

In terms of the transport of directly trapped sediments, precipitation may play an important role in this process within vegetated tidal flats. On land, raindrops falling on the sediment surface

636 can cause suspension, saltation and bedload movement, particularly in low slope areas, but the
637 maximum raindrop impacts occur for water depths of less than one raindrop diameter (Moss et
638 al., 1979; Proffitt et al., 1991; Beuselinck et al., 2002). Contrary to the terrestrial environment,
639 on vegetated tidal flats the raindrops have limited impact on sediment resuspension because of
640 the deep water layers during high water periods; and at low tide, the dense vegetation forms a
641 mat to dissipate the kinetic energy of raindrops. Visual observation of the vegetated sites did not
642 indicate the formation of fast overland flow, which is generally the main factor causing sediment
643 movement on land surfaces. However, the raindrops can still work directly on the bare mudflat
644 surface and influence recently deposited, unconsolidated sediments as pointed out by Voulgaris
645 and Meyers (2004).

646 When the vegetated flat was exposed, the rinsing of the vegetation surface by raindrops
647 results in a direct transport of sediments to the bed. Our experiments show the direct trapping of
648 sediments by the vegetation surface. Precipitation creates a pathway for those particles to be
649 moved onto the bed. Furthermore, the thick sediment layer on the vegetation leaf surfaces might
650 cause a problem for seedling growth by different means, such as reducing photosynthesis or
651 increasing the bending of stems. It has been observed by ecologists that the seedlings of
652 saltmarsh grass and mangrove trees can be smothered due to the thick layer of mud on leaf
653 surfaces (Yihui Zhang, *personal communication*). Therefore, rainfall events, especially moderate
654 ones, can be of fundamental importance to the coastal wetland system and further studies on their
655 frequency and seasonality coupled with tidal characteristics should be considered in the future in
656 order to understand the mechanisms driving the change of coastal ecosystems.

4.3 The Limitations of Field Observations

Instrument availability and the restrictions of *in situ* deployment during this study lead to two primary limitations which should be discussed. Firstly, the number of ADVs available restricted the number of observations possible. Three locations were carefully chosen to form a nearly isoceles triangle, so that the mangrove and the saltmarsh were located on the same contour line (Chen et al., 2016*)*, sharing a mutual control site on the bare mudflat. The elevation difference between the two vegetated flats and the bare mudflat bed is only 0.05 m *(*Chen et al., 2016*)*. This small elevation difference has minimal influence on the flow direction and the subsequent suspended sediment transport, which can be confirmed through application of Soulsby's drag coefficient calculations, as derived for bedforms *(*Soulsby, 1997*)*:

$$z_{0b} = a\frac{\Delta H^2}{\lambda} \qquad (7)$$

$$C_{Db} = \left[\frac{0.4}{1+\ln(\frac{z_{0b}}{h})}\right]^2 \qquad (8)$$

where ΔH and λ are the height (0.05 m) and width (35 m), respectively, of the bed form, Z_{0b} is the bed roughness due to bedform, h is the mean water depth and C_{Db} is the drag coefficient attributed to the bedform. The C_{Db} is estimated to be 0.0026 for the 0.05 m elevation difference, which is over an order of magnitude smaller than the drag coefficients (0.04-0.36) associated with the three sites *(*Chen et al., 2016*)*, indicating that the elevation change has very limited contribution to any frictional term and is unlikely to affect flows. The principle reason for the

677 alteration of flows and suspended sediment transport is therefore attributed to the presence of
678 vegetation.

679 Secondly, some assumptions have been made regarding likely sediment transport
680 pathways within the tidal flat. Although we acknowledge that the sediment could be transported
681 into and out of the tidal flat via different routes, this question was addressed using previous
682 observations and modeling results. The tidal flat under investigation features a gently seaward
683 sloping topography, and lacks a well-developed tidal creek system (Chen et al., 2016*)*. Under
684 these circumstances, modeling *(*Temmerman et al., 2005b*)* suggests that flow directions during a
685 tidal cycle are usually perpendicular to the marsh edge with the sedimentation processes
686 controlled by elevation differences and distance from the marsh edge. Thus, our study assumes
687 that suspended sediments are transported into and out of the vegetation via the same route. This
688 assumption might cause some uncertainty of the suspended sediment flux estimates and further
689 work investigating the sediment transport pathway is needed in the future, particularly within
690 coastal wetlands.

691

692 **5 Conclusions**

693 Field observations were made to compare the sediment transport processes occurring
694 between a bare mudflat, a saltmarsh and a mangrove edge, considering both hydrodynamically
695 induced sediment settling and the direct trapping effects of the vegetation surface. The
696 interpretation of the SSC data, together with high-frequency flow measurements, reveals that the
697 saltmarsh grass are more efficient than the mangrove trees at inducing sediment trapping over a
698 tidal-cycle scale. The main findings of this study are summarized in Fig. 8 and outlined below:

699 1) The SSC data exhibit a strong tidal asymmetry. The SSC is higher during the flood phase

than the ebb phase for all three sites, implying a favorable environment for a net sediment input. The mean SSC level is generally high on the mudflat and decreases within the vegetated area, which is generally consistent with the deposition rates of the three sites.

2) Tidal cycle-scale sediment flux estimates show a depositional environment on the studied tidal flat. The presence of vegetation alters the flow direction and the subsequent suspended sediment transported into the system. Sediment transport fluxes indicate that the saltmarsh edge is more efficient than the mangrove edge at trapping sediment. This pattern is further supported by calculations of sediment fluxes at a tidal scale and deposition rates at a longer timescale. Although the SSC reduction is more pronounced at the mangrove site, the flow rotation caused by the mangrove trees reduces the sediment flux into the mangrove edge itself. Instead, a large portion of suspended sediment is transported along the mangrove edge, which is significantly different from the sediment transport pattern of the saltmarsh edge.

3) The mechanism for acceleration of deposition by tidal flat vegetation can be identified by using two approaches: sediment settling driven by local changes in the hydrodynamics and the direct sediment trapping by vegetation surfaces. Particle settling over a tidal scale was evaluated from deposition tendency. Deposition tendency on the bare mudflat is generally higher during ebb tides than flood tides, indicating a tidal asymmetry and a deposition lag during the ebb phase. Tidal flat vegetation is able to mediate the tidal asymmetry of this deposition tendency. Vegetation radically increases this parameter during floods when the SSC is high, and this creates a more favorable environment for deposition. Eventhough it is more efficient in trapping sediment, the saltmarsh grass is found to be less efficient than the mangrove trees at altering the deposition tendency of

723 that sediment (Table 2).

724 4) The sediments trapped on vegetation leaves and stems are also quantified using samples
725 of natural standings and seedlings. Saltmarsh grass has a higher direct sediment trapping
726 ability than mangrove trees. The amount of sediment trapped by the saltmarsh grass
727 surface can contribute a considerable amount to deposition, in particular when associated
728 with rainfall events, whilst the sediment directly trapped by mangrove trees is negligible
729 compared to the observed total annual deposition rate in this particular site where only
730 young mangrove trees occupy the front and very limited biomass is found close to the
731 bed. A new mechanism of direct sediment trapping by the vegetation surface, in
732 combination with precipitation, is proposed by this study, as a supplement to the
733 mechanisms associated with hydrodynamic mediation by vegetation.

734

735 Fig. 8. A summary of the main findings of this study: 1) the suspended sediments are transported
736 from the bare mudflat to the vegetated edges with similar inundation periods, the fluxes can be
737 decomposed into normal and parallel components; 2) a considerable amount of sediment was
738 trapped at the front of the saltmarsh and the mangrove; 3) the saltmarsh front is more efficient
739 than the mangrove front due to the flow rotation caused by the mangrove; and 4) the sediment
740 trapping is associated with two mechanisms: hydrodynamically induced sediment settling and
741 direct trapping by the vegetation surfaces. The size of the arrow and the circle provides the
742 information on relative magnitudes of these mechanisms.

743

Acknowledgments

We would like to thank Dr. Yihui Zhang at Xiamen University and Prof. Dong-Ping Wang at State University of New York at Stony Brook for their valuable comments on inspiring this manuscript. Mr. Yi Li and Mr. Yang Yang (SIO, SOA) are thanked for their support in fieldwork. Thanks extend to the Management Office of Yunxiao Mangrove National Nature Reserve, for the site access. The data used are listed in the tables and figures. This work is funded by NSFC Projects (Grant no. 41006047 and 41776096) and a Fundamental Research Fund of Second Institute of Oceanography (No. JT1505). The authors also thank the anonymous reviewers for their time and thoughtful comments.

References

Alongi, D.M., Pftitzner, J., Trott, L.A., Tirendi, F., Dixon, P., and D.W., Klumpp, 2005.Rapid sediment accumulation and microbial mineralization in forests of the mangrove Kandelia candel in the Jiulongjang Estuary, China. Estuarine. Coastal and Shelf Science 63, 605–618.

Amos, C. L., Villatoro, M., Helsby, R., Thompson, C. E. L., Zaggia, L., and G.,Umgiesser, *et al*., 2009. The measurement of sand transport in two inlets of venice lagoon, italy. Estuarine Coastal & Shelf Science, 87(2), 225-236.doi: 10.1016/j.ecss.2009.05.016.

Arkema, K.K.,Guannel, G., Verutes, G., Wood, S.A., Guerry, A., Ruckelshaus, M., Kareiva, P., Lacayo, M. and J.M., Silver, 2013. Coastal habitats shield people and property from sea-level rise and storms Nature Climate Change, 3, 913-918. doi: 10.1038/NCLIMATE1944

765 Barbier, E.B., Hacker, S.D., Kennedy, C., Koch, E.W., Stier and A.C.B., Silliman, 2011.The
766 value of estuarine and coastal ecosystem services. Ecological Monographs, 81(2), 169-
767 193. doi: 10.1890/10-1510.1

768 Beuselinck, L., G.,Govers, P. B., Hairsine, G.C., Sander, and M. Breynaert, 2002. The influence
769 of rainfall on sediment transport by overland flow over areas of net deposition. Journal of
770 Hydrology, 257, 145-163.doi:10.1016/S0022-1694(01)00548-0.

771 Bouma, T. J., L. A. van Duren, S. Temmerman, T. Claverie, A. Blanco-Garcia, T. Ysebaert, and
772 P. M. J. Herman, 2007. Spatial flow and sedimentation patterns within patches of
773 epibenthic structures: Combining field, flume and modelling experiments, Continental
774 Shelf Research, 27(8), 1020-1045, doi:10.1016/j.csr.2005.12.019.

775 Brown, J.M. and A.G., Davies, 2010. Flood/ebb tidal asymmetry in a shallow sandy estuary and
776 the impact on net sand transport. Geomorphology 114 (2010) 431–439.
777 doi:10.1016/j.geomorph.2009.08.006

778 Cahoon, D. R., Hensel, P. F., Spencer, T., Reed, D. J., McJee, K. and N. Saintilan, 2006. Coastal
779 Wetland Vulnerability to Relative Sea-Level Rise: Wetland Elevation Trends and Process
780 Controls. Verhoeven, J.T.A., Beltman, B., Bobbink, R.,and D.F. Whigham (eds.),
781 Wetlands and Natural Resource Management, Volume 190 of the series Ecological
782 Studies, 271-292.

783 Carus, J., Paul, M., and B., Schroder, 2016. Vegetation as self-adaptive coastal protection:
784 Reduction of current velocity and morphologic plasticity of a brackish marsh pioneer.
785 Ecology and Evolution 2016; 6(6), 1579–1589. doi: 10.1002/ece3.1904

786 Chen, Y., C. E. L. Thompson, and M. B. Collins, 2012. Saltmarsh creek bank stability:
787 Biostabilisation and consolidation with depth, Continental Shelf Research, 35, 64-74, doi:
788 10.1016/j.csr.2011.12.009.

789 Chen, Y., Li, Y., Cai, T., Thompson, C. E. L., and Y. Li, 2016. A comparison of
790 biohydrodynamic interaction within mangrove and saltmarsh boundaries. Earth Surface
791 Processes and Landforms, 41(13): 1967-1979. doi: 10.1002/esp.3964.

792 Childers, D. L., and J. W. Day, 1990. Marsh-water column interactions in two Louisiana
793 sstuaries. I. sediment dynamics. Estuaries, 13(4), 393-403.

794 Christiansen, T., P. L. Wiberg, and T. G. Milligan, 2000. Flow and Sediment Transport on a
795 Tidal Salt Marsh Surface, Estuarine, Coastal and Shelf Science, 50(3), 315-331,
796 doi:10.1006/ecss.2000.0548.

797 Chung, C.H., 2006. Forty years of ecological engineering with Spartina plantations in China.
798 Ecological Engineering, 27, 49–57. doi:10.1016/j.ecoleng.2005.09.012

799 Dronkers, J., 1986. Tidal asymmetry and estuarine morphology. Netherlands Journal of Sea
800 Research, 20 (2/3), 117-131.

801 Fagherazzi, S., Marani, M., and L.K., Blum, 2004. The ecogeomorphology of tidal marshes.
802 Washington, DC: American Geophysical Union, Coastal and Estuarine Studies, 268pp.

803 French, J.R., and T., Spencer, 1993. Dynamics of sedimentation in a tide-dominated back barrier
804 salt marsh, Norfolk, UK. Marine Geology, 110, 315-331.

805 Friess, D. A., K.W. Krauss, E.M. Horstman, T. Balke, T.J. Bouma, D. Galli, and E.L. Webb,
806 2012. Are all intertidal wetlands naturally created equal? Bottlenecks, thresholds and

knowledge gaps to mangrove and saltmarsh ecosystems. Biological Reviews, 87, 346–366. doi:10.1111/j.1469-185X.2011.00198.x

Furukawa, K., and E. Wolanski, 1996. Sedimentation in mangrove forests. Mangroves and Salt Marshes, 1, 3-9.

Furukawa, K., Wolanski, E., and H.Mueller, 1997. Currents and sediment transport in mangrove forests. Estuarine Coastal and Shelf Science, 44(3), 301-310. doi:10.1006/ecss.1996.0120

Fugate, D. C., and C. T. Friedrichs, 2002. Determining concentration and fall velocity of estuarine particle populations using ADV, OBS and LISST, Continental Shelf Research, 22(11-13), 1867-1886, doi:Pii S0278-4343(02)00043-2.

Fugate, D. C., and C. T. Friedrichs, 2003. Controls on suspended aggregate size in partially mixed estuaries, Estuarine, Coastal and Shelf Science, 58(2), 389-404, doi:10.1016/s0272-7714(03)00107-0.

Gao, J., Feng, Z., Chen, L., Wang, Y., Bai, F. and J., Li, 2016. The effect of biomass variations of Spartina alterniflora on the organiccarbon content and composition of a salt marsh in northern JiangsuProvince, China. Ecological Engineering 95, 160–170. doi: 10.1016/j.ecoleng.2016.06.088

Gao, S., Du, Y.F., Xie, W.J., Gao, W.H., Wang, D.D. and X.D., Wu, 2014. Environment-ecosystem dynamic processes of Spartina alterniflora salt-marshes along the eastern China coastlines. Science China: Earth Sciences, 57, 2567–2586, doi: 10.1007/s11430-014-4954-9

Gedan, K. B., M. L.,Kirwan, E., Wolanski, E. B., Barbier, and B. R. Silliman, 2010. The present and future role of coastal wetland vegetation in protecting shorelines: answering recent

challenges to the paradigm. Climatic Change, 106(1), 7-29. doi: 10.1007/s10584-010-0003-7

Gillis, L. G., T. J. Bouma, W. Kiswara, A. D. Ziegler, and P. M. J. Herman, 2014. Leaf transport in mimic mangrove forests and seagrass beds, Mar Ecol Prog Ser, 498, 95-102, doi:10.3354/meps10615.

Goring D. G., and V. I. Nikora, 2002. Despiking acoustic Doppler velocimeter data. Journal of Hydraulic Engineering, ASCE 128: 117-126. doi:10.1061/(ASCE)0733429(2002)128:1(117)

Graham, G. W., and A. J. Manning, 2007. Floc size and settling velocity within a *Spartina anglica* canopy, Continental Shelf Research, 27(8), 1060-1079. doi:10.1016/j.csr.2005.11.017.

Greene, R. S. B. and P. B. Hairsine, 2004. Elementary processes of soil–water interaction and thresholds in soil surface dynamics: a review. Earth Surface Processes and Landforms, 29,1077-1091. doi: 10.1002/esp.1103.

Ha, H. K., and J. P. Y. Maa, 2010. Effects of suspended sediment concentration and turbulence on settling velocity of cohesive sediment, Geosciences Journal, 14(2), 163-171, doi:10.1007/s12303-010-0016-2.

Horstman, E.M., Dohmen-Janssen, C.M., Bouma, T.J., and S. J. M. H. Hulscher, 2015. Tidal-scale flow routing and sedimentation in mangrove forests: Combining field data and numerical modelling, Geomorphology, 228, 244-262. doi:10.1016/j.geomorph.2014.08.011.

Kathiresan, K., 2003. How do mangrove forests induce sedimentation? Revista de Biologia Tropical 51, 355-360.

Kelleway, J.J., Saintilan, N., Macreadie, P.I., Baldock, J.A. and P.J. Ralph, 2017. Sediment and carbon deposition vary among vegetation assemblages in a coastal salt marsh. Biogeosciences, 14, 3763–3779. doi:10.5194/bg-14-3763-2017

Kitheka, J.U., Ongwenyi, G.S., and K.M., Mavuti, 2003. Fluxes and exchange of suspended sediment in tidal inlets draining a degraded mangrove forest in Kenya. Estuarine, Coastal and Shelf Science, 56, 655–667.doi:10.1016/S0272-7714(02)00217-2

Leonard, L.A., and M.E. Luther, 1995. Flow hydrodynamics in tidal marsh canopies. Limnology and Oceanography 40: 1474–1484.

Li, J., Xu, J., Zhang, D., Yan, X., Tong, Y. and Y., Shen. 2005. Function of Spartina alterniflora salt march and its eco-economic value in south coast of Hangzhou Bay. Areal Research and Development, 24, 58-62. (In Chinese with English abstract).

Li, Y., Y., Chen, Y., Li, 2017. Remote sensing analysis of the changes in the junction region of mangrove forests and *Spartina alterniflora* saltmarshes. Marine Science Bulletin, 36, 348-359.

Liao, C.Z., Luo, Y.Q., Fang, C.M., Chen, J.K., Li, B., 2008. Litter pool sizes, decomposition, and nitrogen dynamics in Spartina alterniflora-invaded and native coastal marshlands of the Yangtze estuary. Oecologia 156, 589–600.

Lin, P., 2001. A review on the mangrove research in China. Journal of Xiamen University (Natural Science), 40(2), 592-603.

871 Lin, P., Hu, H., Zheng, W., Li, Z., and Y., Lin, 1998. A study of biomass and energy of
872 mangrove communities in Shenzhen Bay. Scientia Silvae Sinicae, 34, 18-23. (In Chinese
873 with English abstract)

874 Lin, P., Lu, C., Lin, G., Chen, R., and L., Su, 1985. Study on mangrove ecosystem of
875 Jiulongjiang River estuary. Journal of Xiamen University (Natural Science), 24, 508-514.
876 (In Chinese with English abstract)

877 Lin, P., Lu, C., Wang, G. and H., Chen, 1995. Biomass and productivity of *Bruguiera sexangula*
878 mangrove forest in Hainan Island, China. Journal of Xiamen University (Natural
879 Science), 29, 209-213. (In Chinese with English abstract)

880 Lin, P., Yin, Y. and C., Lu, 1992. Biomass and productivity of *Rhizophora stylosa* community in
881 Yingluo Bay of Guangxi, China. Journal of Xiamen University (Natural Science), 31,
882 199-202. (In Chinese with English abstract)

883 Liu, Q., 1991. Silt transportation and its influences on submarine scour and silting in Dongshan
884 Bay, Fujian Journal of Oceanography in Taiwan Strait, 10(1), 69-76.

885 Lovelock, C. E., M. F. Adame, V. Bennion, M. Hayes, R. Reef, N. Santini, and D. R. Cahoon ,
886 2015. Sea level and turbidity controls on mangrove soil surface elevation change,
887 Estuarine, Coastal and Shelf Science, 153, 1-9, doi:10.1016/j.ecss.2014.11.026.

888 Luhar, M., and H. M. Nepf, 2013. From the blade scale to the reach scale: A characterization of
889 aquatic vegetative drag, Advances in Water Resources, 51, 305-316,
890 doi:10.1016/j.advwatres.2012.02.002.

891 Mazda, Y., Kanazawa, N., and E.,Wolanski, 1995. Tidal asymmetry in mangrove creeks.
892 Hydrobiologia 295, 51–58.

MICZTWR Office, 1990. Multipurpose Investigation of the Coastal Zone and Tidal Wetland Resources– Report of Fujian Province. 575pp. Ocean Press, China.

Mitsch, W.J., and J.G. Gosselink, 2007. Wetlands. John Wiley & Sons: Chichester, 619pp.

Moller, I., Kudella, M., Rupprecht, F., Spencer, T., Paul, M., van Wesenbeeck, B. K., and S. Schimmels, 2014. Wave attenuation over coastal salt marshes under storm surge conditions. Nature Geoscience, 7(10), 727-731. doi: 10.1038/ngeo2251

Moss, A. J., Walker, P. H., and J. Hutka, 1979. Raindrop-simulated transportation in shallow water flows: an experimental study. Sedimentary Geology, 22, 165-184.

Nepf, H., 1999. Drag, turbulence, and diffusion in flow through emergent vegetation. Water Resources Research, 35(2), 479-489. doi: 10.1029/1998wr900069.

Nepf, H., 2012. Flow and transport in regions with aquatic vegetation. Annual Review of Fluid Mechanics 44: 123–142. doi:10.1146/annurev-fluid-120710-101048.

Neumeier, U., and P. Ciavola, 2004, Flow Resistance and Associated Sedimentary Processes in a Spartina maritima Salt-Marsh, J Coastal Res, 20(2), 435-447, doi:10.2112/1551-5036(2004)020(0435:FRAASP)2.0.CO;2.

Neumeier, U., and C. L. Amos, 2006.The influence of vegetation on turbulence and flow velocities in European salt-marshes. Sedimentology, 53(2), 259-277. doi: 10.1111/j.1365-3091.2006.00772.x

Ortiz, A., Ashton A., and H. Nepf, 2013. Mean and turbulent velocity fields near rigid and flexible plants, and the implications for deposition. Journal of Geophysical Research - Earth Surface 118: 1–15.DOI:10.1002/2013JF002858.

914 Perillo, G. E. M., E. Wolanski, D. R. Cahoon, and M. M. Brinson, 2009. Coastal Wetlands: An
915 Integrated Ecosystem Approach, Elsevier, Elsevier B.V.

916 Proffitt, A. P. B., Rose, C. W., and P. B., Hairsine, 1991. Rainfall detachment and deposition:
917 experiments with low slopes and significant water depth. Soil Science Society of
918 America Journal, 55, 325-332. doi:10.2136/sssaj1991.03615995005500020004x

919 Redfield, A.C., 1972. Development of a New England salt marsh. Ecological Monographs,
920 42,201–237.

921 Saintilan, N., Wilson, N., Rogers, K., Rajkaran, A., and K.W. Krauss, 2014. Mangrove
922 expansion and salt marsh decline at mangrove poleward limits. Global Change Biology,
923 20 (1), 147-157.doi: 10.1111/gcb.12341

924 Scully, M. E., and C. T. Friedrichs, 2007. Sediment pumping by tidal asymmetry in a partially
925 mixed estuary Journal of Geophysical Research, 112, C07028,
926 doi:10.1029/2006JC003784

927 Sheng, J., and A.E.,Hay, 1988. An examination of the spherical scatterer approximation in
928 aqueous suspensions of sand. Journal of the Acoustic Society of America 83 (2), 598–
929 610.

930 Shi, Z., Pethick, J. S., and K., Pye, 1995. Flow structure in and above the various heights of a
931 saltmarsh canopy: a laboratory flume study. Journal of Coastal Research 11(4), 1204–
932 1209.

933 SonTek, 1997. SonTek Doppler current meters: using signal strength data to monitor suspended
934 sediment concentration. SonTek/YSIInc., California, 7pp.

935 Soulsby R., 1997. Dynamics of Marine Sands: A Manual for Practical Applications. Thomas
936 Telford: London, 272pp.

937 Temmerman, S., Bouma, T.J., Govers, G., Wang, Z.B., De Vries, M.B. and P.M.J., Herman,
938 2005a. Impact of vegetation on flow routing and sedimentation patterns: Three-
939 dimensional modeling for a tidal marsh. Journal of Geophysical Research 110, F04019.
940 doi:10.1029/2005JF000301

941 Temmerman, S., Bouma, T.J., Govers, G., and D., Lauwaet, 2005b, Flow paths of water and
942 sediment in a tidal marsh: relations with marsh developmental stage and tidal inundation
943 height. Estuaries 28, 338–352.

944 Temmerman, S., Meire, P., Bouma, T.J., Herman, P.M.J., Ysebaert, T., and H., De Vriend, 2013.
945 Ecosystem-based coastal defence in the face of global change. Nature 504, 79-83.
946 doi:10.1038/nature12859.

947 Thompson, C.E.L., C.L., Amos, and G., Umgiesser, 2004, A Comparison Between Fluid Shear
948 Stress Reduction by Halophytic Plants in Venice Lagoon, Italy and Rustico Bay, Canada
949 - analyses of in situ measurements. Journal of Marine Systems 51, 293-308. Doi:
950 10.1016/j.jmarsys.2004.05.017.

951 van der Wal, D., and K. Pye, 2004. Patterns, rates and possible causes of saltmarsh erosion in the
952 Greater Thames area (UK), Geomorphology, 61(3-4), 373-391,
953 doi:10.1016/j.geomorph.2004.02.005.

954 Vargas-Luna, A., A. Crosato, and W. S. J. Uijttewaal, 2015. Effects of vegetation on flow and
955 sediment transport: comparative analyses and validation of predicting models, Earth Surf
956 ace Processes and Landforms, 40(2), 157-176, doi:10.1002/esp.3633.

957 Vincent, C.E., and A., Downing, 1994. Variability of suspendeds and concentrations, transport
958 and eddy diffusivity under non-breaking waves on the shore face. Continental Shelf
959 Research 14 (2/3), 223–250.

960 Voulgaris, G., and S. T. Meyers, 2004. Temporal variability of hydrodynamics, sediment
961 concentration and sediment settling velocity in a tidal creek, Continental Shelf Research,
962 24, 1659–1683, doi:10.1016/j.csr.2004.05.006.

963 Wang, A., Gao, S., Jia, J., Pan, S., 2005. Contemporary sedimentataion rates on saltmarshes at
964 Wanggang, Jiangsu, China. Journal of Geographical Sciences, 15, 199-209. doi:
965 10.1360/gs050208

966 Wang, A., Ye, X., and J., Chen, 2010. Observations and analyses of floc size and floc settling
967 velocity in coastal salt marsh of Luoyuan Bay, Fujian Province, China. Acta Oceanologia
968 Sinica 29, 116-126. doi: 10.1360/gs050208.

969 Wang, Y., Gao, S., Jia, J., Thompson, C.E.L., Gao J., and Y. Yang, 2012. Sediment transport
970 over an accretional intertidal flat with influences of reclamation, Jiangsu coast, China.
971 Marine Geology 291-294, 147-161. doi:10.1016/j.margeo.2011.01.004.

972 Wang, Y., Gao, S., Jia, J., Liu Y., and J., Gao, 2014. Remarked morphological change in a large
973 tidal inlet with low sediment-supply. Continental Shelf Research 90, 79-95.doi:
974 10.1016/j.csr.2014.02.005

975 Wolanski, E., 1995. Transport of sediment in mangrove swamps, Hydrobiologia, 295, 31-42.

976 Wolanski, E., Mazda, Y., King, B., and S., Gay, 1990. Dynamics, flushing and trapping in
977 Hinchinbrook channel, a giant mangrove swamp, Australia. Estuarine Coastal and Shelf
978 Science, 31, 555–579.

979 Wolanski, E., Mazda, Y., Furukawa, K., Ridd, P., Kitheka, J.,Spagnol, S., and T., Stieglitz, 2001.
980 Water-circulation in mangroves and its implications for Biodiversity. In E. Wolanski
981 (Ed.), Oceanographic processes of coral reefs: physical and biological links in the Great
982 Barrier Reef (pp. 53–76). London: CRC Press.

983 Woodroffe, C.D., Rogers, K., McKee, K.L., Lovelock, C.E., Mendelssohn, I.A. and N. Saintilan,
984 2016. Mangrove Sedimentation and Response to Relative Sea-Level Rise. Annual
985 Review of Marine Science, 8, 243–66. Doi: 0.1146/annurev-marine-122414-034025

986 Zhang, Y., Wang, W., Wu, Q., Fang, B., and P. Lin, 2006. The growth of Kandelia candel
987 seedlings in mangrove habitats of the Zhangjiang estuary in Fujian, China. Acta
988 Ecologica Sinica, 26(6), 1648-1655. doi: 10.1016/s1872-2032(06)60028-0

989 Zhang, Y. H., Huang, G. M., Wang, W. Q., Chen, L. Z., and G.H. Lin, 2012. Interactions
990 between mangroves and exotic Spartina in an anthropogenically disturbed estuary in
991 southern China. Ecology, 93(3), 588-597.

992 Zong, L., and H. Nepf, 2010. Flow and deposition in and around a finite patch of vegetation,
993 Geomorphology, 116(3-4), 363-372, doi:10.1016/j.geomorph.2009.11.020.

994 Zuo, P., Zhao, S., Liu, C., Wang,C. and Y., Liang, 2012. Distribution of Spartina spp. along
995 China's coast. Ecological Engineering, 40,160– 166. doi:10.1016/j.ecoleng.2011.12.014

996

*Revised manuscript with changes marked
Click here to view linked References

Differential sediment trapping abilities of mangrove and saltmarsh vegetation in a subtropical estuary

Yining Chen[1,2*], Yan Li[1,2], Charlotte Thompson[3], Xinkai Wang [1], Tinglu Cai [1], Yang Chang[1]

[1]Second Institute of Oceanography, SOA, Hangzhou, 310012, China.

[2]State Key Laboratory of Marine and Environmental Science, Xiamen University, Xiamen, 361005, China.

[3]Ocean and Earth Science, University of Southampton, National Oceanography Centre, Southampton, SO14 3ZH, UK.

Corresponding author: Yining Chen (yiningchen5410@hotmail.com; yiningchen@sio.org.cn)

Key Points:

- Compare sediment transport from bare mudflat across mangrove and saltmarsh boundaries.
- Sediment trapping is caused by hydraulic forces and direct trapping by~~of~~ vegetation.
- The saltmarsh edge is more efficient than the mangrove edge at trapping sediments.

Abstract

Saltmarsh and mangrove are common coastal wetland types and their ability to enhance deposition has been investigated extensively ~~investigated~~, but rarely compared directly. This study carried out *in situ* observations to compare the sediment transport processes between a bare mudflat, a mangrove stand~~s~~ and a saltmarsh stand~~s,~~ within a subtropical estuary. Turbidity variations over ~~a spring to middle~~ the latter portion of a spring tide~~tidal cycle~~ were recorded, alongside measurements of flow data, to estimate sediment trapping by hydraulic forces under similar hydroperiods. In addition, vegetation was transplanted to compare the direct sediment trapping by high~~- standings~~ and short-standing seedlings. The suspended sediment concentration (SSC) time series showed an overall reduction between the bare mudflat and the vegetated flats. Suspended sediment flux estimates revealed that a considerable amount of sediment was~~ere~~ trapped by the saltmarsh and the mangrove edges. The flux estimates find that the saltmarsh edge is more efficient than the mangrove edge in trapping sediments transported normal to the~~its~~ edge. The sediment trapping mechanisms were considered based on two approaches: the hydrodynamic related sediment settling and direct trapping by vegetation. The calculation of deposition tendency showed that the presence of vegetation altered the flow direction and the tidal asymmetry of the deposition process, resulting in a higher deposition tendency during the flood phase to enhance sediment settling. In addition to~~Besides~~ sediment settling, vegetation surfaces were found to trap sediments directly. In combination with rinsing by precipitation, th~~e~~ose trapped sediments accumulated on the bed and contributed to the deposition. Against the background of similar inundation periods, the saltmarsh grass showed a greater sediment trapping ability than the mangrove trees, in terms of both the hydraulic sediment ~~settling~~ trapping and the direct trapping by vegetation surface.

批注 [RV1]: Not sure what you mean by middle. Mean tide, i.e. neither spring nor neap.

批注 [RV2]: This needs a final proof read once you've implemented the changes.
Also the Abstract needs to be submitted separately. So, please ensure the amended Abstract is uploaded.

Keywords: Sediment trapping; Mangrove; Saltmarsh; Mudflat

1 Introduction

Natural coastal wetlands are widely recognized for their ability to trap sediments (Perillo et al., 2009; Barbier et al., 2011; Moller et al., 2014), as well as for their defense potential against the action of waves and tidal flows (Temmerman et al., 2013; Horstman et al., 2015; Carus et al., 2016). Saltmarshes and mangroves are globally common coastal wetland types, although the latter are mainly restricted to tropical and subtropical regions. In general, mangroves are~~is~~ dominated by halophytic trees and shrubs, whilst saltmarshes are characterized by herbaceous vegetation (Mitsch and Gosselink, 2007). Because of their ability to stabilize the coast by ~~attenuating~~ dissipating waves and current energy~~s~~ and enhancing deposition, these two types of habitats can be useful tools for coastal engineers in protecting the coastline (Redfield, 1972; Gedan et al., 2010).

Vegetation occurring along intertidal flats has been recognized as having the ability to stabilize, trap and bind sediments. In general, plants have been observed to directly increase the erosion threshold of bed sediments (Chen et al., 2012), and indirectly trap sediments by providing additional drag force (Leonard and Luther, 1995; Temmerman et al., 2005a; Chen et al., 2016) which mediate flow patterns, and consequently enhance local sediment deposition (Neumeier and Amos, 2006; Horstman et al., 2015). The enhancement of sediment deposition by coastal wetland vegetation has received more extensive attention in recent decades, ~~against the background~~ in part due to the predicted impacts of accelerated sea-level rise due to global warming (van der Wal and Pye, 2004; Cahoon et al., 2006, Arkema et al., 2013; Woodroffe et al., 2016; Kelleyway et al., 2017). For practical purposes, the understanding of the mechanisms of sediment trapping by vegetation is key to the engineering work of coastal stabilization and

带格式的: 字体: 非倾斜

批注 [RV3]: Please don't use italics in Geomorphology – please correct throughout.

带格式的: 字体: 非倾斜

带格式的: 字体: 非倾斜

批注 [RV4]: Do you mean attenuation? Attenuated waves have shorter wavelength and greater wave height. I don't believe you mean this.

带格式的: 字体: 非倾斜

带格式的: 字体: 非倾斜

带格式的: 字体: 非倾斜

带格式的: 字体: 非倾斜

批注 [RV5]: Not clear what you mean by 'against the background'. This is too vague.

带格式的: 字体: 非倾斜

protection, but the efficiency varies amongst vegetation species (Kathiresan, 2003; Friess et al., 2012; Ortiz et al., 2013).

Previous studies have revealed that heavily vegetated mangrove systems normally trap sediments during the flood tide, and that there is generally no significant export of sediments during the ebb~~,~~ due to the deceleration of the tidal currents by vegetation-induced friction (Wolanski et al., 1990; 2001; Furukawa et al., 1997; ~~Wolanski et al., 2001;~~ Kitheka et al, 2003). At a tidal-scale, field observations also show~~s~~ that mangrove trees are able to create a favorable environment as a sediment sink by modifying flow routing (Horstman et al., 2015). Factors such as vegetation density~~, root system characteristics,~~ and biomass, as well as the intertidal position ~~of the mangrove forest, which determines the~~determining submergence/emergence status, and geomorphological settings ~~such as the presence of~~ (e.g., platforms or creeks), all affect the trapping capacity of mangrove trees (Friess et al., 2012).

Saltmarshes and their interaction with sediment dynamics have also been extensively studied (e.g., Leonard and Luther, 1995; Temmerman et al., 2005a; Neumeier and Amos, 2006; Bouma et al., 2007). Previous studies reveal the dampening effects of saltmarsh vegetation on mean flow and turbulent diffusion, resulting in a more favorable environment for deposition (Christiansen et al. 2000; Neumeier and Amos, 2006; Zong and Nepf, 2010; Nepf, 2012). Factors controlling the trapping capacity of saltmarsh grass include density, biomass, the emergence/submergence status and ~~the~~ geomorphological setting~~s~~ (Temmerman et al., 2005a, b; Bouma et al., 2007; Nepf, 2012). The differences between the effects of mangroves and saltmarshes are related to the physical structure of the vegetation. The stiff canopy of saltmarshes normally shows a decrease in biomass with height (Neumeier, 2005). The presence of the trunks and aerial roots of mangrove show considerable effects on flow and deposition mediation (e.g.

带格式的: 字体: 非倾斜

带格式的: 字体: 非倾斜

带格式的: 字体: 非倾斜

批注 [RV6]: This sentence is too complex to follow. Please sub-divide and simplify.

带格式的: 字体: 非倾斜

带格式的: 字体: 非倾斜

带格式的: 字体: 非倾斜

带格式的: 字体: 非倾斜

批注 [RV7]: Please support with a reference.

带格式的: 字体: 非倾斜

Madza et al., 1995) while the canopy is made up of rigid stems on the bottom and a stiff leaf layer at the top, resulting in an increase in biomass on the top. Therefore, theoretically, the saltmarsh grass shows a more pronounced influence on the bottom of the water column rather than the top, whilst the mangrove, depending on species, affects the bottom and sometimes the top of the water column, although the regions of the water column affected by vegetation will depend on the relative local tidal levels to the height of trees.

This body of previous work has endeavored to further our understanding of the mechanisms controlling the bio-physical interactions within fluvial systems and coastal wetlands, together with the feedback between vegetation and sediment dynamics. The use of flumes and model vegetation has played an important role in raising our understanding of these detailed mechanisms (Shi et al., 1995; Nepf, 2012; Oritz et al., 2013). However, field observations focused on natural systems and processes are required to further develop these fundamental findings, particularly in regions where different ecosystems overlap. As pointed out by a number of scientists, complex factors such as precipitation, intermittent discharge, bi-directional flows and the consolidation of sediments must also be taken into account during the study of sediment transport on tide-al dominated environments (Fagherazzi et al., 2004; Greene and Hairsine, 2004; Chen et al., 2012). These processes drive the evolution of coastal systems over the long term, but cannot be entirely captured by flume observations. , Comparisons of the results from field and flume observations (Bouma et al., 2007) found that flume studies are unable to capture all necessary spatial scales, and will always result in some flow artefacts, including lower turbulence intensities than in the field. Vargas-Luna et al. (2015) reviewed a number of physical models in terms of the effects of vegetation on flows and sediment transport and they concluded that 'field measurements are not available, thus, intensive field campaigns including different

批注 [RV8]: Provide some example referenes.

带格式的: 字体: 非倾斜

带格式的: 字体: 非倾斜

带格式的: 字体: 非倾斜

带格式的: 字体: 非倾斜

带格式的: 字体: 非倾斜

带格式的: 字体: 非倾斜

109 climatic conditions, vegetation species……are also recommended.' Thus, the aim of this study
110 was to carry out *in situ* observations to compare the sediment transport at the boundaries of a
111 mangrove swamp and an adjacent saltmarsh. The competition between saltmarshes and
112 mangrove species has~~ve~~ been well documented to be associated with the critical bed elevation
113 and the subsequent inundation period (Saintilan et al., 2014). In this study, we focus on a direct
114 comparison between the sediment trapping abilities of the two types of vegetated boundaries
115 with similar inundation periods (i.e. similar bed elevations). A comparison of differences in flow
116 reduction and energy dissipation by saltmarsh and mangrove plants has already been assessed
117 and is presented in a separate paper (Chen et al., 2016).

带格式的: 字体: 非倾斜

带格式的: 字体: 非倾斜

118 **2 Methods**

119 2.1 Study Site

120 Yunxiao Mangrove National Natural Reserve, located at the Zhangjiang Estuary in the
121 southeast China coast, was selected as the site ~~for us~~ to conduct the field measurements (Fig.~~ure~~
122 1). The tidal flat developing within this reserve is approximately 600 m in width. The upper part
123 of the tidal flat (100-200 m in width) is covered both by mangroves and saltmarshes; the adjacent
124 species make this location an ideal study area for comparative field observations.

批注 **[RV9]:** Please use Fig. Please apply throughout.

125 The runoff of the Zhangjiang River carries a large amount of fresh water and sediments,
126 with a mean annual water discharge of 9.6×10^8 m^3 and suspended sediment discharge of 3.6×10^8
127 kg (MICZTWR Office, 1990). The suspended sediment concentration decreases to ~40mg L^{-1}
128 within the estuary and further to ~ 30 mg L^{-1}in Dongshan Bay (MICZTWR Office, 1990; Liu,
129 1991). The annual precipitation within the estuary region is 700 mm and 80% of it takes place in
130 the wet season (April to September). The study site is home to a tidally-dominated mangrove

批注 **[RV10]:** Source of data?

带格式的: 字体: 非倾斜

带格式的: 字体: 非倾斜

forest with a fronting saltmarsh; the tidal flat is exposed to irregular semi-diurnal tides with a mean tidal range of 2.3 m. Wave exposure is very limited due to the sheltering effects of Dongshan Bay outside the estuary, except during typhoon seasons which normally occur in summer. The resulting physical conditions of the estuary therefore favor the deposition of fine-grained sediments, which form a wide range of tidal flats along the main channel (Liu, 1991). The site under investigation is located on a relatively wide tidal flat with a slope of 2-3‰. The bed of this tidal flat consists of fine-grained sediment, mainly clays and silts.

It has been reported that on the southeast coast of China, the rapid spread of the invasive saltmarsh grass *Spartina alterniflora* threatens the local mangroves (Lin, 2001; Zhang et al., 2012). However, the study site is located on a tidal flat that exhibits co-existence of local mangroves and *Spartina alterniflora* saltmarsh. The upper part of the flat is covered by native mangrove species (*Kandelia obovata*, *Aegiceras corniculatum*, and *Avicennia marina*), while the exotic *Spartina alterniflora* occupies part of the mudflat fronting the mangrove forest (Zhang et al., 2012). The saltmarsh grass only covers a small area of the tidal flat during spring and summer, due to human removal as part of managed efforts to maintain a bare mudflat in the lower part of the tidal flat (Zhang et al., 2006).

带格式的: 字体: 非倾斜

带格式的: 字体: 非倾斜

带格式的: 字体: 非倾斜

带格式的: 字体: 非倾斜

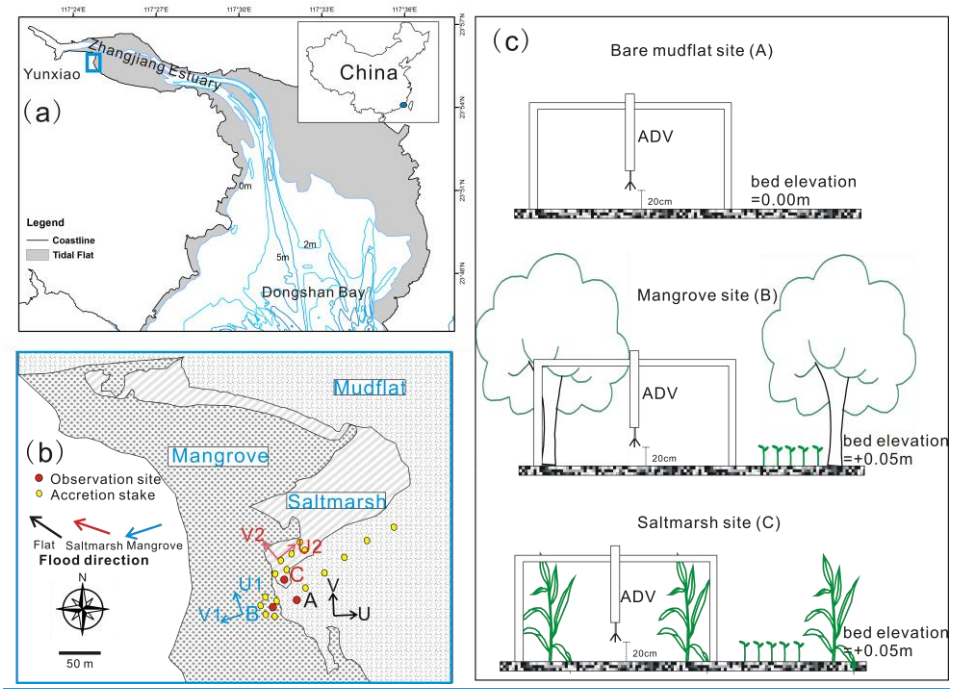

Figure 1. Location of study area and field deployment: a) study area: Yunxiao National Mangrove Reserve; b) location of deployments: Site A (bare mudflat), Site B (mangrove boundary) and Site C (saltmarsh boundary)，together with the definition of flow components: U and V are the geographical northing and easting components, V1 and U1 are the components normal and parallel to the mangrove edge, respectively, and V2 and U2 are the components normal and parallel to the saltmarsh edge, respectively; the flood directions of three sites are also marked by arrows: black for mudflat, red for saltmarsh and blue for mangrove; and c) the positions of instruments deployed and the location of seedling transplantation, sites B and C have the same bed elevation, 5 cm above the bed of Site A (the reference for water level measurements)

批注 [RV11]: Please note, colour Fig.s only appear in the online version unless you are willing and able to meet the additional production costs for the print version. If not, please provide equivalent greyscale images in which the same features and contrasts can be seen equally clearly. In addition, your Fig. captions will need to be sensitive to the fact that colour Fig.s only appear online. Referring to colour directly is problematic in this case.

Please address throughout.

批注 [CYN12R11]: We understand the cost and we will pay for the colour fiigures of this manuscript. We also noticed a minor problem for the arrows in Fig.1 and have uploaded a new figure

The leading edge of the mangrove forest is made up of a mixture of *Kandelia obovata* and *Aegiceras corniculatum*, with a mostly closed canopy (80-90% closed). The mean distance from the bottom of the tree canopy to the bed was 0.4 m. In spring, the trees had a mean height of 1.6 m and a mean canopy width of 1.2 m. Combination of canopy closure percentage and the canopy width gives a density of 0.8 shoots/ ~~-~~m^{-2}. The aerial root system is not well developed in the front, due to the presence of young mangrove trees ~~in the front~~. In addition, ~~-~~ aboveground aerial roots of *K. obovata* are generally rare on the mudflats of Southeast China. S~~s~~eedlings can be observed sparsely within the mangrove forest, with density of 20-30 shoots/ ~~-~~m^{-2}.

The saltmarsh of *S. alterniflora*, 1.0 m in height, ~~occurred~~ occurs at the seaward front of the mangrove forest, with a high stem density of 580 m^{-2} and a high aboveground biomass (dry) of 2.50 kg m^{-2} (Chen *et al.*, 2016). A topographic map of the region ~~*(Chen et al., 2016)*~~ indicates a small elevation change (< 0.27%) in the northwest-southeast (NW-SE) direction. When the tidal flat is submerged (2-3 hours every tidal cycle during the observation period, Table 1), the mean water level was 0.43 m above the tidal flat bed, with the maximum water levels reaching 0.76 m (Chen et al., 2016). It should be noted that due to the elevation of the vegetated mudflat, only higher or ~~middle to~~ spring tides are able to reach this part of tidal flat (Fig. ~~ure~~ 1c).

2.2 Location and Time

Because spring is the crucial time for the seedlings of mangrove and saltmarsh vegetation~~s~~ to establish, the field observations were carried out during 30th April to 5th May 2014 throughout ~~a period of spring to middle tides~~ the latter portion of a spring tide, covering 11 tidal cycles. The weather was cloudy but dry for most of the time, except the second day, during which a moderately heavy rain event (25 mm over 24 hours) took place, and the last day, during

带格式的： 字体：非倾斜

批注 [RV13]: As before, I'm not sure what you mean by 'middle'.

批注 [RV14]: As previously. Do you mean spring and neap tides?

which a short shower took place just before the vegetation samples were collected (after tidal cycle No. 11).

Three locations (~~Figur~~Fig. 1) were selected for comparative synchronous measurements, located on the bare mudflat (Site A), within the mangrove edge (Site B) and within the saltmarsh edge (Site C). The distance between the bare mudflat site and the two vegetated flat sites was approximately 35 m. The sites within the mangrove and saltmarsh boundaries are at a distance of 10 m from the vegetation edge, as defined by the start of the closed canopy. The remaining regions between Sites A and B, and Site C are covered by sparse mangrove trees and *Spartina* grass. The fringes of vegetation described in this contribution include both the dense vegetation with closed canopies, as shown in ~~Figure~~Fig. 1, together with the sparsely vegetated fronting flat. The space between the vegetated sites (B and C) and the bare mudflat location (Site A) confines the vegetation fringes. Site A is 0.05 cm lower in elevation than the other two sites. Site B and Site C have the same elevations as determined by RTK-GPS.

2.3 Sediment Dynamic Observations

The backscatter intensity data of three Acoustic Doppler Velocimeters (ADV) were used to obtain flow data over 9 tidal cycles. The locations were carefully selected to avoid mangrove trees, and the vegetation around the sensors was removed (Chen et al., 2016). These were fixed to stainless steel frames for field deployment. The ADVs (Nortek Vector models, 6MHz) were all positioned 20 cm above the bed~~,~~ to collect data continuously at a frequency of 16Hz. It should be noted that the ADV sensor measures the water volume~~-~~ at a height of 8 cm above the bed (12 cm below the sensor head positioned 20 cm above the bed, ~~Figure~~Fig. 1c). ADV backscatter intensity data were also used to estimate the suspended sediment concentration (SSC) based on a logarithmic relationship calibrated within the laboratory (Sontek, 1997; Ha and Maa, 2010). The

带格式的：字体：非倾斜

带格式的：字体：非倾斜

longest possible data records were extracted and separated into 5-minute intervals to obtain mean values.

The output of the ADV provides three components of current velocity, U, V and W which represent easting, northing and upward components of the flow. A three-dimensional hydrodynamic and sediment transport model has revealed that as long as the water level is below the canopy top, the vegetated areas flood from the unvegetated areas, with flow directions more or less perpendicular to the vegetation edge (Temmerman et al., 2005a). Thus, the flow components are rotated according to the orientation of the vegetation edges for further analyses. The mangrove edge has an orientation of 160°, and the flow components were rotated to generate components parallel (U1)~~normal (V1)~~ and normal (V1)~~parallel (U1)~~ to this direction. The same procedure was applied to the saltmarsh edge, which has an orientation of 50° (~~V2~~ U2 and ~~U2~~V2). For simplicity, the three velocity components (u, v and w) of the tidal currents were used in formula as generalized symbols of the velocity components. When the data correlation values exceeded 0.7, the phase-space thresholding method developed by Goring and Nikora (2002) was adopted for despiking noise before the calculation of mean velocities, turbulent velocities and turbidities.

带格式的: 字体: 非倾斜

带格式的: 字体: 非倾斜

带格式的: 字体: 非倾斜

The suspended sediment flux can be expressed as follows (*Wang et al., 2014*):

$$F = \int_T \int_L \int_H C V_0 dz dx dt \quad (1)$$

Where F is the flux through a cross section with water depth H (dz) and unit width L (dx) over a time-scale T (dt) of a flood or ebb flow, C is the SSC converted from ADV backscatter intensity and V_0 is the speed of flow component normal to the vegetation edges. Due to the position of the sensors, the flux only covers the submerged period of a tidal cycle. However, the

data used for the flux calculation were from simultaneous periods, so this will not affect the comparison amongst the three sites.

The TKE (Turbulent Kinetic Energy) density can be estimated as:

$$TKE_{density} = 0.5\rho(\overline{u'^2} + \overline{v'^2} + \overline{w'^2}) \qquad (2)$$

Equation 2 is applied for each 5-minute data section. Here, ρ is the fluid density; u', v' and w' are the turbulent fluctuations deviating from 5-minute average values of the eastward, northward and upward flow components, respectively (Thompson et al., 2004).

The bed shear stress τ_b is estimated using Equation (3), where $C_1 = 0.19$ as suggested by Soulsby (1997), and suited to vegetated beds (Thompson et al., 2004):

$$\tau_b = C_1 TKE_{density} \qquad (3)$$

The shear velocity u_* can be estimated from the bed shear stress and the fluid density ρ_f (Equation 4):

$$u_* = \sqrt{\frac{\tau_b}{\rho_f}} \qquad (4)$$

Fugate and Friedrichs (2002) provided an algebraic equation for estimating tidally-averaged settling velocity w_s using an ADV. Voulgaris and Meyers (2004) further expand this method to resolve the tidal variability of the settling velocity (Equation 5), which was adopted in our study:

$$w_s C = \langle w'C' \rangle \qquad (5)$$

Where C is the 5-minute averaged SSC, w' is the vertical fluid velocity fluctuation, C' is the SSC fluctuation estimated from the ADV backscatter strength, and $\langle\ \rangle$ is the symbol indicating time averaging. The settling velocity estimate (Equation 5) can be applied when the

带格式的: 字体: 非倾斜
带格式的: 字体: 非倾斜
带格式的: 字体: 非倾斜
带格式的: 字体: 非倾斜
带格式的: 字体: 非倾斜
带格式的: 字体: 非倾斜

advection transport is minimal compared with the vertical velocity terms (Fugate and Friedrichs, 2002). Using ADV data from pairs of stations, a consistency check was undertaken to evaluate the ratio of the advection term relative to the settling term, as suggested by Fugate and Friedrichs (2002), before the settling velocity was calculated. The flow data and the SSC data obtained by ADV, as well as the distance between the paired stations and the elevations of sensors, were used for this valuation which gives the average ratio of 0.06 ± 0.04 and 0.009 ± 0.006 for the flat-mangrove ~~sites~~ and flat-saltmarsh sites, respectively. Thus, the advection term is two orders of magnitude smaller than the settling term and it is reasonable to estimate settling velocity using the method of Voulgaris and Meyers ~~((~~2004~~))~~.

Bed samples from each site and local water samples were collected to produce a turbidity gradient in the laboratory, for individual calibration of ADV backscatter sensors. SSC was measured by passing a known sample volume through a pre-weighed 0.45 μm poresize glass fiber filter, followed by drying and weighing. Linear relationships were therefore established between the backscatter intensity and the logarithm of SSC for each sensor, as suggested by previous studies (Ha and Maa, 2010, ~~Figure~~Fig. 2).

带格式的: 字体: 非倾斜

带格式的: 字体: 非倾斜

带格式的: 字体: 非倾斜

带格式的: 字体: 非倾斜

带格式的: 字体: 非倾斜

带格式的: 字体: 非倾斜

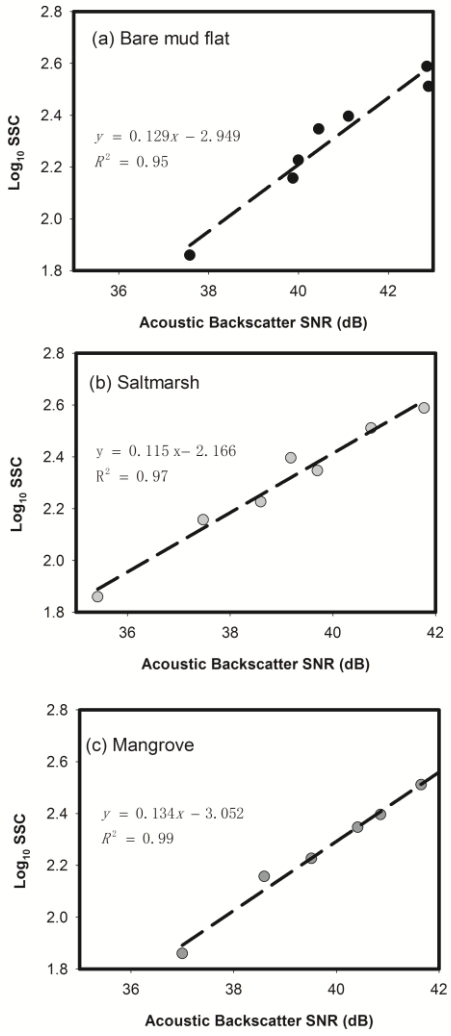

~~Figure~~Fig. ~~2.~~ Calibration between backscatter intensity and suspended sediment concentration for (a) bare mudflat; (b) saltmarsh; and (c) mangrove. Note the x in the equations refers to $Log_{10}SSC$, and SSC is in the unit of mg L^{-1}.

2.4 Vegetation Trapping Experiments

More than 50 saltmarsh grass standings and small branches of mangrove trees were randomly marked and cleaned for field observation. Any sediments attached to these vegetation samples were washed off using clean water in the field before the experiment started. Subsequently, the aboveground parts of 6 vegetation samples (3 mangrove samples and 3 grass samples) were then collected daily using tough scissors after the initial deployment of the instruments. The sediments on the vegetation surface were washed off and collected into cylinders for subsequent filtering and drying to obtain the dry weight of the sediment deposits on the vegetation. The vegetation samples, including leaves and stems, were subsequently dried and weighed to obtain biomass. Note that for conservation purposes, only small branches of the mangrove trees were collected and thus measured weight is mainly from leaves.

The seedlings of mangrove and saltmarsh grass start to grow during this season (Spring). They are much shorter than the natural standings but vital to the development of the ecosystem. In light of the fact that seedlings appear within the near bed whilst the natural standings penetrate the whole water column during the investigation period, it is important to examine the difference between their abilities of trapping sediment using their leaves and stems. *K. obovate* and *S. alterniflora* seedlings were transplanted adjacent to the observation sites and arranged at a density close to the natural status, and used to represent the sediment trapping ability of vegetation at an early stage of life. ~~Some 20 cm, high S~~seedlings of *K. obovata* and *S. alterniflora* were transplanted into Site B and Site C, respectively. For each site, ~~50~~ fifty 20 cm-high seedlings of mangroves or saltmarsh grass, which had been rinsed clean with water, were separately arranged into two quadrates of 200 cm×100 cm, with an individual spacing of 20 cm. Three~~3~~ ~~samples~~ Samples of each type of seedlings were collected in triplicate every day along

批注 **[RV15]:** Avoid starting sentences with numerals.

批注 **[RV16]:** Avoid starting sentences with numerals.

the edge of the plots, together with the natural standings of vegetation to measure the sediment trapped by vegetation using the same method as mentioned before. The mangrove seedlings weare in a similar density as their natural status, but that of the *Spartina* seedlings wasis decreased to allow a comparison between two species.

The instruments recorded from the midnight of 29th/30th April until after the first tidal cycle of 4th May (Table 1), the last point at which water levels were sufficiently high to submerge them.

The sediment mass trapped by the vegetation was measured in this study through the period of the 2nd tidal cycle (occurring in the afternoon of 30 April) to the 11th tidal cycle. The samples were collected every day at noon (Table 1).

Table 1. Description of the field observation deployment

Tidal cycle Number	1	2	3	4	5	6	7	8	9	10	11
Time	01:00 - 03:20	13:00 - 15:00	01:50 - 04:00	13:40 - 15:35	02:30 - 04:40	14:20 - 16:00	03:20 - 05:20	14:40 - 16:40	03:40 - 05:50	N/A	N/A
Date	30/4 AM	30/4 PM	1/5 AM	1/5 PM	2/5 AM	2/5 PM	3/5 AM	3/5 PM	4/5 AM	4/5 PM	5/5 AM
Trapping Experiment		Day 1		Day 2		Day 3		Day 4		Day 5	
Instruments	Recording									Off	
Weather	Cloudy but dry		Rain		Cloudy but dry						Rain

2.5 ~~Supplementary~~ Supporting Measurements

批注 **[RV17]:** Not sue 'supplementary' is the correct term here.

A RTK-GPS (Trimble-SPS881) survey was undertaken to record the relative elevations of the three sites for water level analysis. Plastic accretion stakes (1.5 cm in diameter, 50 cm long, 10 cm exposed, ~~Figure~~Fig. 1b) were inserted into the bed to monitor deposition rates by

measuring the exposed length from May 2012 to May 2014. It is noted that the *Spartina* grass was removed in August 2012 by the local management office and it had recovered by the spring of 2013; as such, the deposition rates of the saltmarsh represent under-estimated values. Surface sediments were collected during instrument deployment for laboratory grain size analysis using a laser grain size analyzer (Helos, manufactured by Sympatec). Biological properties of the vegetation, such as mangrove geometrics (height and diameter of canopy, diameter of trunk), and density and diameter of grass~~,~~ were measured *in situ* using a tape measure. Aboveground biomass of vegetation was measured by harvesting, drying and weighing plant samples.

3 Results

3.1 Tidal-cycle Scale Suspended Sediment Concentration

The variation of suspended sediment concentration (SSC) over 9 tidal cycles is displayed in ~~Figure~~Fig. ~~–~~3. The SSC data exhibit a strong tidal asymmetry, with one exception of the second tidal cycle on the bare mudflat. The overall SSC is higher during the flood phase than the ebb phase for all three sites, which implies a favorable environment for a net sediment input. On average, there is a considerable reduction in SSC between the bare mudflat and the vegetated sites (Table 2). The average SSC reduced nearly 10% from the bare mudflat to the saltmarsh boundary, whilst nearly 20% from the bare mudflat to the mangrove boundary. This pattern implies sediment trapping within the vegetation boundaries at a tidal scale.

Deposition rates over a two-year period were recorded by accretion stakes. The readings of 5 or 6 stakes of each site (see ~~Figure~~Fig. 1 for more details) are averaged and displayed in Table 2. The short-term pattern of SSC variation is generally consistent with long-~~–~~term deposition rates recorded by stakes on the vegetated area and the mudflat, which shows higher

rates at vegetation edges than on the mudflat (Table 2), although the deposition rates may be under-estimated as compaction is not considered.

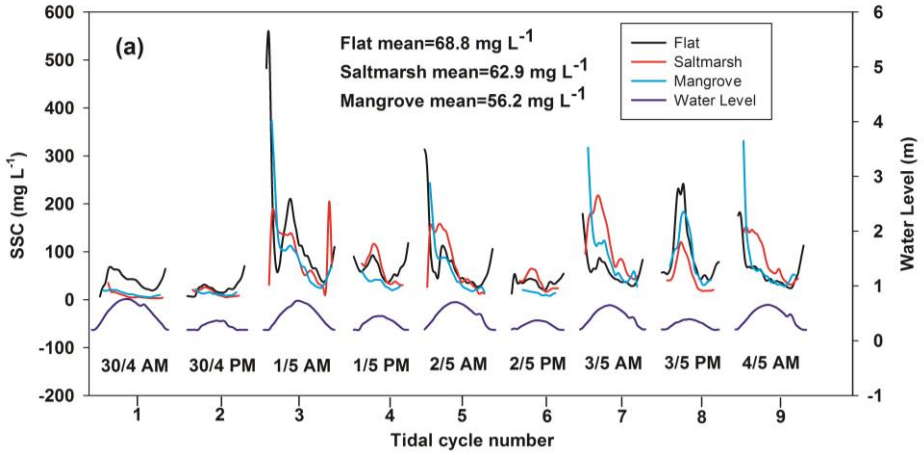

~~Figure~~Fig. 3. The SSC data series over 9 tidal cycles: (a) SSC time series based on acoustic backscatter (ADV); and (b) water level variation. The detailed time is listed in Table 1.

Table 2. Synthesis of the mean parameters associated with suspended sediment transport of the three sites.

Parameter		Flat	Saltmarsh	Mangrove
Grain size (μm)		6.20±0.76	5.79±0.43	6.34±0.90
Deposition rate (cm a^{-1})		1.14±1.20	2.60±0.97*	2.10±0.87
Settling Velocity (mm s^{-1})		1.90	0.87	0.85
SSC (mg L^{-1})		68.8	62.9	56.2
Net SSC flux per tidal cycle (kg/m)	Normal to saltmarsh edge	8.1	3.0	--
	Normal to mangrove edge	4.4	--	3.2
Sediment trapped per tidal cycle (kg/m)		--	5.1	1.2
Deposition tendency	Flood	0. 17	0.21	0.26
	Ebb	0. 23	0.21	0.25
Cumulative S:B ratio	Natural standings	--	0.017	0.016
	Seedlings	--	0.11	0.13

*Note: the deposition rate is under-estimated due to the clearing of grass in August 2012. The stake number is 6 in the saltmarsh site, whilst 5 for the other sites.

3.2 Tidal-cycle Scale Sediment Transport: A Comparison

Detailed flow information has been published in a separate paper (Chen et al., 2016). Here, we provide a brief summary of the horizontal flow conditions. The horizontal flow speeds of the three sites are shown in ~~Figure~~Fig. 4. A considerable reduction in flow speed caused by

带格式的: 字体: 非倾斜

vegetation is readily identified and a rotation of flow direction by vegetation has been related to eddy viscosity and drag forces (Chen et al., 2016).

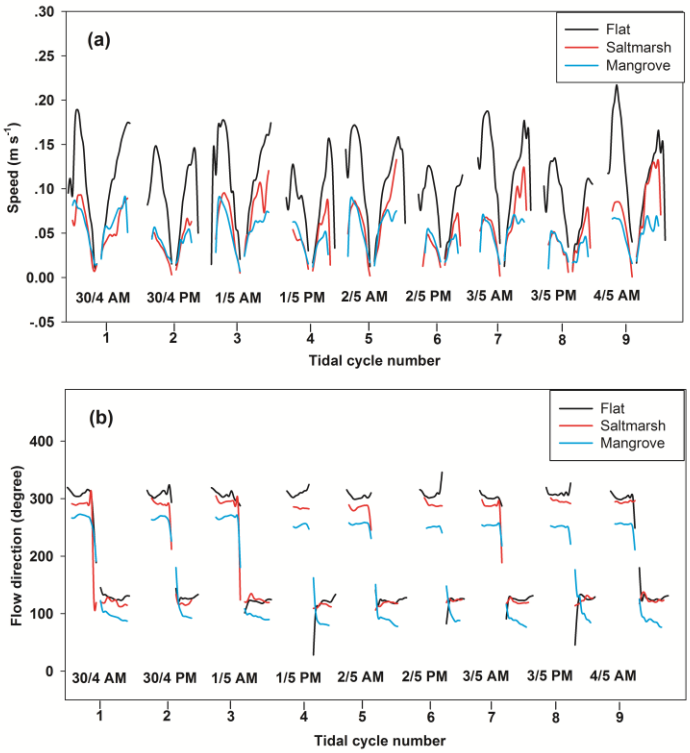

~~Figure~~Fig. 4. The variations of horizontal flow speed and direction throughout 9 tidal cycles (source: Chen et al., 2016): (a) flow speed data; and (b) flow direction data. Note the geographical flow direction uses the north as zero degrees.

Neumeier and Ciavola (2004) noted a relatively uniform vertical velocity profile within saltmarsh grass canopies. Due to the shallow water layer, the SSC is normally regarded as a constant through the vertical profile in modeling or field observations on tidal flats (e.g.,

带格式的: 字体: 非倾斜
带格式的: 字体: 非倾斜
带格式的: 字体: 非倾斜
带格式的: 字体: 非倾斜
带格式的: 字体: 非倾斜

Temmerman et al., 2003; Wang et al., 2012). In addition, based on the consideration of small flow speed magnitude and the relatively low turbidity, a uniform profile assumption is used in this study for SSC flux estimate, based on a combination of flow and SSC data using Equation 1. The SSC flux data for each flood and ebb period is displayed in ~~Figure~~Fig. 5. Due to the flow rotation, the SSC transport normal to the vegetation is mainly presented, but the sediment transport along the vegetation edges is also considered (~~Figure~~Fig. 1b). The SSC fluxes of the bare mudflat site are decomposed according to saltmarsh edge and mangrove edge orientations separately (~~Figure~~Fig. 5). Diurnal inequality results in higher sediment fluxes during the relatively high tides (odd numbers) than the relatively low tides (even numbers). The sediment fluxes are determined by both SSC and flow velocity. Although the SSC values of the bare mudflat are not always higher than the vegetated sites, as indicated by ~~Figure~~Fig. 3 for all tidal cycles, the net sediment trapping of the vegetation edges is likely to be the result of ~~the~~ flow reduction by the vegetation ~~is mainly accounted for by the net sediment trapping of the vegetation edges~~.

Overall, the study area is dominated by a net input of sediments. The highest fluxes occur on the bare mudflat site; this is because when the suspended sediments are transported into the vegetation edges, a large amount of sediment~~s~~ is~~are~~ trapped by the vegetation and only part of the~~m~~ sediment flux is able to pass through the vegetation to reach the upper tidal flat. The bare mudflat site shows different SSC fluxes when considering the main transport directions (~~Figure~~Fig. 5). This site shows a lower net sediment transport towards the mangrove, because the presence of the mangrove edge deviates the flow (257º in flood) away from the main flow direction of 305º in flood on the tidal flat (~~Figure~~Fig. 4b, Chen et al., 2016).

批注 [RV18]: Have I interpreted your sentence correctly?

带格式的： 字体：倾斜

带格式的： 字体：非倾斜

The long-term deposition rates (Table 2) are consistent with the pattern of the flux estimates at tidal cycle scales: relatively low deposition rates are observed on the bare mudflat (1.4 cm a^{-1}) whilst high deposition rates occur at the vegetation edges (> 2 cm a^{-1}); the deposition rate at the saltmarsh edge is higher than that at the mangrove edge, in response to a greater difference in sediment input between the vegetated sites and the bare mudflat site.

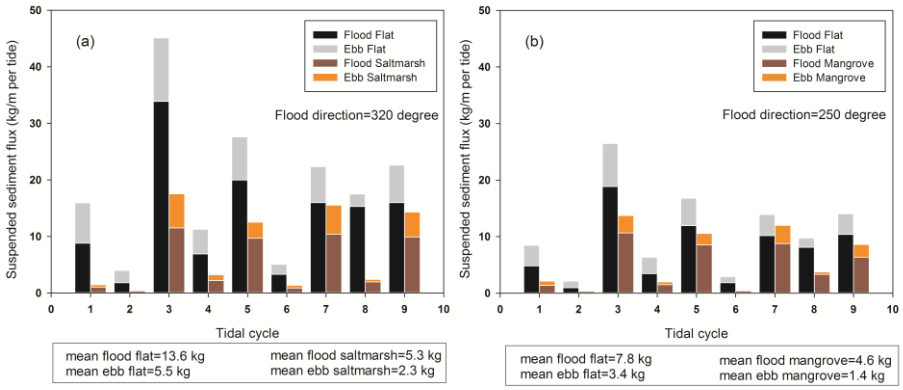

~~Figure~~Fig. 5. Suspended sediment fluxes per unit width estimated at a tidal cycle scale: (a) sediment flux at the bare mudflat site in the direction normal to saltmarsh edge; (b) sediment flux at the saltmarsh site in the direction normal to saltmarsh edge; (c) sediment flux at the bare mudflat site in the direction normal to mangrove edge; and d) SSC flux at the mangrove site in the direction normal to mangrove edge. The flux was estimated to represent the total mass passing a unit width of bed over a time span of either the ebb or flood flow. North represented by zero degrees.

The amount of sediment trapped between the vegetated sites and the bare mudflat sites is estimated using the SSC flux data using Equation 1. The sediment trapped at the vegetation boundaries can be estimated by comparing the difference between the fluxes of the mudflat site

(with subscript of 'mud') and the vegetated sites (with subscript of 'veg'), as described by following (Equation 6):

$$trap = (Flux_{flood,mud} - Flux_{ebb,mud}) - (Flux_{flood,veg} - Flux_{ebb,veg}) \quad (6)$$

The values of sediment trapping ~~,~~ are given in Table 2. This clearly indicates that the presence of vegetation can increase SSC trapping at their front edges. Further, ~~it can be inferred~~ by comparing the SSC fluxes (Table 2), it can be inferred that considerable amount of the sediments transported from the lower part of the tidal flat towards the upper tidal flat are trapped within the front edges of the vegetation, an ~~combination~~ area of 35 m~~eters~~ wide which includ~~inges a combination of~~ ~~the~~ mudflat ~~with~~ and sparse vegetation. ~~The presence of vegetation traps the suspended sediment, resulting in a high deposition at the front and less deposition in the interior of the saltmarsh and the mangrove. This spatial allocation of sediments might benefit the spread of the vegetation.~~ Finally, the saltmarsh front edge, showing a greater trapping ability, is found to be more efficient than the mangrove front edge in trapping sediments. Due to the total amount of sediment flux from the bare mudflat is same for two vegetated sites, coupled with the fact that~~although~~ the mangrove trees trap less sediments normal to their front, more sediments can be transported parallel to the mangrove edge than the saltmarsh edge~~.~~. The transport in~~of~~ this direction can increase the elevation of the whole system and benefiting the neighboring plants. Remote sensing image analysis (Li et al., 2017) shows the mangrove in this area expands in~~at~~ a direction parallel to its front, whilst the saltmarsh advances in a direction normal to its present~~current~~ front. The sediment transport and trapping pattern might explain the different directions of vegetation expansion.

批注 [RV19]: Of what?

批注 [RV20]: This is very difficult to understand. Please rewrite.

批注 [RV21]: Do you observations justify this interpretation? I'm not convinced of this.

批注 [RV22]: Speculation.

批注 [RV23]: This is unconvincing, speculative and poorly justified. Please remove or improve substantially in terms of evidence base.

带格式的: 字体:非倾斜

3.3 EThe enhanced deposition by vegetation as indicated by deposition tendency

In order to quantitatively evaluate the tendency for particles to deposit or resuspend, the ratio of particle settling velocity to the shear velocity $\frac{w_s}{u_*}$ has been proposed by Ortiz et al. (2013) for saltmarsh environments. The estimates of settling velocity and shear velocity for this study were calculated using Equations 2-5 as described in the Methods sSection. In general, when $\frac{w_s}{u_*}$ is above 0.1, the environment is considered to be deposition-dominant (Zong and Nepf, 2010)

Mean $\frac{w_s}{u_*}$ ratios calculated for each flood and ebb tide are displayed in FigureFig. 6. The $\frac{w_s}{u_*}$ ratio of the flood and ebb vary within a range of 0.14 and 0.31 for all sites, implying favorable conditions for deposition. The tidal cycle--averaged values (including flood and ebb phases) of vegetation sites, are 0.25 ± 0.03 and 0.21 ± 0.04 for the mangrove site and the saltmarsh site, respectively, whilst this value is 0.20 ± 0.03 for the bare mudflat site.

带格式的: 字体: 非倾斜

带格式的: 字体: 非倾斜

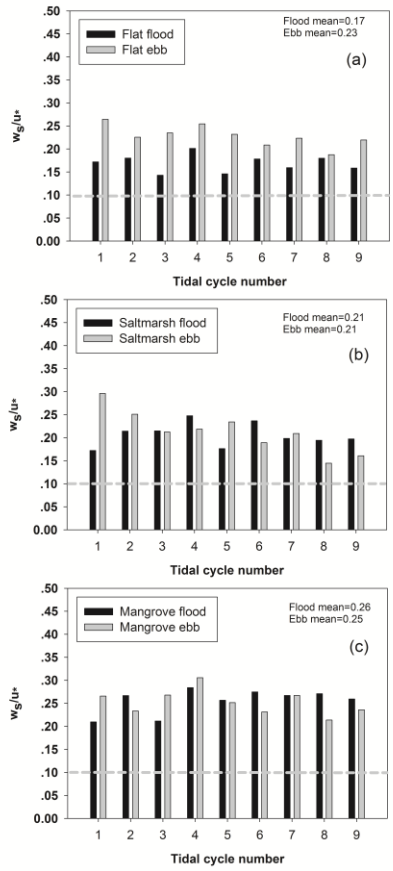

438

439 FigureFig. 6. Deposition tendency of three sites as indicated by $\frac{w_s}{u_*}$ ratio: (a) mudflat; (b)
440 saltmarsh; and (c) mangrove; the dashed line of 0.1 marks the lower limit for 'deposition
441 favorable' conditions, as suggested by Zong and Nepf (2010).

442 3.4 Sediment Trapping by Vegetation, and Precipitation Effects

443 A ratio of sediment mass (S) to biomass (B), i.e. S/B, is proposed in this study, to allow
444 estimates of the ability of vegetation to trap sediments. The S/B ratio is defined as the value of

带格式的: 字体: 小四
带格式的: 字体: 小四
带格式的: 字体: 小四, 非倾斜
带格式的: 字体: 小四
带格式的: 字体: 小四, 非倾斜
带格式的: 字体: 小四

the dry sediment mass washed from the vegetation divided by the dry biomass of the vegetation itself. We choose this ratio because dry sediment mass and dry biomass can be easily measured in laboratory with high accuracy. Further, the data on dry sediment mass and dry biomass have been used in a large number of studies and this allows us to discuss our results using other data sources. The properties of the two vegetation species are listed in Table 3.

Table 3. The biological properties of the investigated mangrove trees and saltmarsh grass

Spartina	Height (m)	Stem density (m^{-2})	Biomass (dry, kg m^{-2})	Coverage (%)	Stem diameter (m)
	1.0	580	2.5	90%	0.008
Mangrove	Height (m)	Stand Density (m^{-2})	Canopy biomass (dry, kg m^{-2})	Canopy closure (%)	Trunk diameter (m)
	1.6	0.8	0.22	80-90%	0.1

Because the samples were collected successively, the S/B ratio data are cumulative, ~~to~~ indicating the continuous sediment trapping by vegetation over tidal cycles. The cumulative S/B ratio of the natural standings and the transplanted seedlings of mangrove trees and saltmarsh grass ~~are illustrated in Figure 7~~ for the observation period are illustrated in ~~Figure~~Fig. 7.

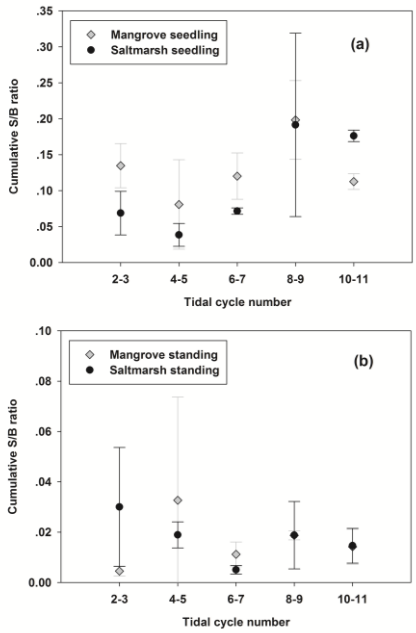

458

459 ~~Figure~~Fig. 7~~:~~. The cumulative sediments trapped by vegetation surfaces, as indicated by the S/B
460 ratio over 10 tidal cycles: (a) seedlings~~;~~ and (b) mature standings. The seedling samples were
461 planted in~~to~~ a matrix of 10 x ~~*~~5 stands within an rectangular area of 100 cm x ~~*~~200 cm. Three~~3~~
462 samples of each vegetation type were collected every day to give the average and standard
463 deviation values in this figure.~~.~~

464

465 Overall, the S/B ratio of natural, high standings is significantly less than that of the
466 seedlings for both types of vegetation (~~Figure~~Fig. 7). This is because the top canopy of the high
467 standings experiences much less submergence than the lower part, and this decreases their
468 efficiency as a sediment trap by unit mass. However, in the light of the large amount of biomass
469 (e.g. aboveground biomass of *Spartina alterniflora* reaches 2.5 kg m^{-2} in this area) of the high

standings and the length of time they are present (from Spring to Autumn) compared to the seedlings (only part of the seedlings are able to survive untiltill Autumn), they perform a more important role overall in trapping sediments on the tidal flat.

The S/B ratio of mangrove and saltmarsh seedlings both vary considerably over the 10 tidal cycles while maintaining similar patterns (FigureFig. 7a). The S/B ratios of the mangrove seedlings are similar to those of the *Spartina* seedlings if the shoot densities are same. The S/B ratio drops to a minimum during tidal cycles 4 and 5, then they increase on the following two days, and decrease slightly again on the last day. This pattern is different from the expected continuous increase and it is highly likely to be associated with precipitation, which took place during tidal cycles 3 and 4, and before tidal cycle 11. The authors observed in the field that the rain drops washed off fine particles attached to the leaves during the low water period. It appears that the sediments become trapped by vegetation during high water levels, and the rain during the emergence hours creates a mechanismway to transport sediment downward ontotowards the bed. Without precipitation, the sediments will be accumulated until an upper limit is reached. The presence of precipitation is able to accelerate this downward transport of sediment. This mechanism may be not only important for the sedimentary process on the tidal flat, but also for the growth of seedlings. High standings show a similar pattern as the seedlings (FigureFig. 7b), except during tidal cycle nNo. 4-5. In general, the high standings show less diurnal variation, as well as lower standard deviations amongst samples. The high standings of saltmarsh grass and mangroves show a decreasing trend in S/B ratio, with a low value occurring on the day after the moderately heavy rain (tidal cycles 4 and 5), together with a general increase after that day. Similarly, the short shower also shows its effect at the end of the observation, slightly decreasing the S/B ratio on the last day. The frequency of measurement sampling is not sufficiently high in

this study to confirm it, but ~~this pattern~~the lag between surface sediment decreases in successive days (Fig. 7) might imply a lag ~~of surface sediment decrease~~ in response to precipitation.

批注 [RV24]: This is rather unclear. Please rephrase and clarify the meaning.

4 Discussion

A complete understanding of the mechanisms mediating sediment accumulation by tidal flat vegetation, particularly the possible impact of vegetation upon suspended particles, is still i~~a~~llusive (Graham and Manning, 2007). Trapping of suspended particles can be caused by both changes to hydraulic forces and by the direct presence of vegetation leaves and stems. In the following sections, the sediment settling caused by hydraulic forces and by the direct trapping by leaves or stems will be discussed separately, together with limitations of this study.

带格式的: 字体: 非倾斜

4.1 Hydraulic Sediment Settling Processes within the Saltmarsh and the Mangrove Fronts

Various devices (e.g., floc cameras) have been used to show that suspended particles settle in a flocculated form within saltmarshes and mangrove swamps (French and Spencer, 1993; Wolanski, 1995; Graham and Manning, 2007). Wolanski (1995) suggested that the settling velocity of suspended particles in mangrove swamps is 1 mm s^{-1} for clay and 5 mm s^{-1} for silt. Voulgaris and Mayers (2004) observed an invariant, tidally-averaged settling velocity of 0.24 mm s^{-1} for flocs on a saltmarsh surface. A more accurate observation of floc settling velocity within a saltmarsh vegetation canopy under turbulent flow conditions was conducted in an annular flume using a flocs camera (Graham and Manning, 2007), which provides a range of 0.004 ~ 3.36 mm s^{-1}, with a mean value of 0.55 mm s^{-1}. Settling velocities estimated based on ADV observations by this study (Table 2) are within the range of previous observations. However, a decrease in the settling velocity of suspended particles from the bare mudflat to the vegetated sites occurs and further explanation is needed for the settling processes.

带格式的: 字体: 非倾斜

带格式的: 字体: 非倾斜

带格式的: 字体: 非倾斜

带格式的: 字体: 非倾斜

带格式的: 字体: 非倾斜

The settling of suspended sediments within the vegetation canopy is related to the generation of turbulence and the wake-sheltering effects in the lee of downstream stems (Shi et al., 1995; Nepf, 1999). In general, the deposition tendency ratio, also known as the inverse movability number forming part of the Rouse parameter (Amos et al., 2010), has a range of 0.002 to 0.3 in aquatic environments and a typical value of 0.02 has been used in flume experiments (Ortiz et al., 2013). Relatively high values of the ratio imply a trend for deposition whilst low values suggest a tendency for resuspension. Deposition has been clearly observed in flumes when ~~this~~ the deposition tendency ratio is above 0.1 (Zong and Nepf, 2010).

The vegetation below the sensors was cleared in this study and, thus, this observation looked into the sediment settling directly driven by hydrodynamics, but not the direct trapping by the vegetation surface. Meanwhile, more than 80% of the turbulent kinetic energy is dissipated by the vegetation in comparison with the mudflat (Chen et al, 2016). Therefore, it is important to use the $\frac{w_s}{u_*}$ ratio to determine the likelihood of deposition.

The most notable pattern revealed by ~~Figure~~Fig. 6 is the change of tidal asymmetry in the $\frac{w_s}{u_*}$ ratio by vegetation. On the bare mudflat, the $\frac{w_s}{u_*}$ ratio shows a strong ebb-dominant characteristic throughout the tidal cycles, consistent with the asymmetry in suspended sediment flux (~~Figure~~Fig. 5). Paired-sample T tests (by SPSS package) are used to exam three sites in terms of the flood-ebb asymmetry. The results show~~s~~ a significant difference between the bare mudflat and the vegetated sites ($P<0.01$, Table 4).

带格式的: 字体: 非倾斜

带格式的: 字体: 非倾斜

带格式的: 字体: 非倾斜

批注 [RV25]: the Rouse parameter…

带格式的: 字体: 非倾斜

带格式的: 字体: 非倾斜

批注 [RV26]: Please present these results in a Table – and refer to the table.

Table 4. Paired samples tests for tidal asymmetry of deposition tendency

	Std. deviation	Std. error mean	t	df	Sig. (P-value)
~~Pair 1:~~ flat vs saltmarsh	0.043	0.014	-3.616	8	0.007
~~Pair 2:~~ flat vs mangrove	0.023	0.075	-8.284	8	<0.001

Thus, a considerable amount of suspended particles, mostly clay and fine silts (Table 2), are transported into the bare mudflat during the flood stage. These particles tend to settle, as indicated by the $\frac{w_s}{u_*}$ ratio (> 0.1 over 9 tidal cycles) during this stage. During the ebb stage however, the $\frac{w_s}{u_*}$ ratio increases considerably, and consequently the majority of deposition occurs during this stage, resulting in a deposition lag.

Tidal asymmetry, as defined by comparing flood and ebb phases through various parameters ~~of~~ in relation to hydrodynamic processes, has been widely recognized for its importance in resulting sedimentation processes (Dronkers, 1986; Scully and Friedrichs, 2007; Brown and Davies, 2010), but hardly considered in flume experiments (Zong and Nepf, 2010; Ortiz et al., 2013). The tidal asymmetry in the deposition tendency can be altered by vegetation. Throughout 9 tidal cycles in our study, the deposition tendency data shows considerable ebb-dominance within the bare mudflat site (~~Figure~~Fig. 6a) whilst the vegetated sites shows ~~the~~ ~~feature~~ either nearly ~~equal~~ symmetrical or flood-dominant deposition tendencies (~~Figure~~Fig.~~s~~ 6b, c ~~and c~~). Differently from the bare mudflat, most of the suspended particles within the vegetated sites therefore deposit during the flood stage when the SSC is high, rather than the ebb stage with

带格式的： 字体：非倾斜

带格式的： 字体：非倾斜

批注 [RV27]: The meaning here is unclear. Please rewrite to clarify.

批注 [RV28]: Don't use 'and' in the Fig. numbering. This should read: (Fig. 6b, c)

554 low SSC, improving the deposition efficiency. This is likely to be an important mechanism
555 throughout which vegetation enhances deposition by regulating hydrodynamics and the
556 consequent $\frac{w_s}{u_*}$ ratio, but has not been reported by previous studies. The presence of vegetation
557 decreases both the settling velocity (Table 2) and the shear velocity (Chen et al., 2016). The
558 improved deposition efficiency implies that shear velocity reduction is greater than the decrease
559 of settling velocity, as a function of the vegetation.

560 4.2 The Potential Contribution of Direct Trapping to Deposition

561 The suspended sediment settling and trapping driven by hydraulics have been extensively
562 studied. However, the sediment directly trapped by vegetation is rarely taken into account.
563 Vegetation occurring on tidal flats has been widely recognized for its ability to increase
564 deposition to adapt to relative sea- -level rise. Accelerated deposition rates have been observed in
565 a number of saltmarshes and mangrove swamps, in comparison with unvegetated tidal flats (e.g.,
566 Childers and Day, 1990; Furukawa and Wolanski, 1996; Christansen et al., 2000; Alongi et al.,
567 2005; Lovelock et al., 2015). The suspended particles can form larger flocs and settle more
568 rapidly to the seabed as the vegetation creates a more favorable environment for sediment
569 settling (Neumeier and Ciavola, 2004; Graham and Manning, 2007; Nepf, 2012; Ortiz et al.,
570 2013). More recently, leaf transport as a source of particulate organic matter (POM) in
571 ecosystems was observed in flume experiments which comparinged mimic mangrove forests and
572 seagrass beds, indicating the mangrove roots werea more efficient at trapping mechanism POM
573 by mangrove roots than theby seagrass beds (Gillis et al., 2013). Along Associated with leaf
574 transport, it can also be readily observed in the field that a thick layer of mud can accumulate on

带格式的: 字体: 非倾斜

带格式的: 字体: 非倾斜

带格式的: 字体: 非倾斜

批注 [RV29]: Unclear. Please rewrite/rephrase.

带格式的: 字体: 非倾斜

the leaf surface. This is another pathway for suspended particles to be trapped by the vegetation system, but is rarely ~~recorded~~ recognized in the literature.

A quantitative measurement of suspended sediment trapped by vegetation stems and leaves in the field has been conducted in this study, and is represented by the S/B ratio (~~Figure~~Fig. 7). Moreover, the amount of sediment trapping over a unit area (1_m_×_1_m) is estimated based on S/B ratio and the biomass data. On average, the difference in S/B ratio of saltmarsh grass between two successive days reaches a value of 0.003 (based on data reported in ~~Figure~~Fig. 7), even when considering the rinsing by rainfall. The maximum accumulated S/B ratio over two successive days reaches 0.014. Considering the dry biomass values of 2.5 kg m^{-2} and based on our observations~~,~~ the aboveground biomass, including stems and leaves, has the potential to trap a maximum of 35 g dry sediments per square meter per day (S/B ratio =0.014)~~, based on our observations~~. The dry density of clay and silt sediments is approximately 1.28 g cm^{-3} and thus the estimated ~~the~~ amount of sediments attached to the vegetation surface have the potential to add up to 0.5 cm to the annual deposition rate during its growing season (6 months~~), ~~). This estimate assuminges complete deposition from the leaves to the bed, ~~although this value~~but could be revised if additional factors (e.g., the water content and bulk density) were considered, and may be ~~lower than predicted~~overestimated.

Spartina alterniflora has been artificially introduced into Chinese tidal flats since 1980s for the purpose of stimulating tidal flat accretion (Chung, 2006). It has been reported that the presence of *Spartina alterniflora* has increased the sedimentation rates of the tidal flats from ~1.5 cm a^{-1} to ~ 3 cm a^{-1} (Wang et al., 2005; Gao et al., 2014). The direct trapping amount of sediments by vegetation, however, remains unknown. Most of the *Spartina alterniflora* saltmarshes appear on the silty or clay mudflats along the east China coast, including Jiangsu

批注 [RV30]: recognized

批注 [RV31]: This sentence is too complex and quite tricky to follow. Please sub-divide and rephrase.

带格式的: 字体: 非倾斜

带格式的: 字体: 非倾斜

Province, Shanghai, Zhejiang Province and Fujian Province (Gao et al., 2014). The total area of this type of saltmarshes sums up to 3.2×10^8 m^2 (Zuo et al., 2012). The aboveground biomass (dry mass) varies within the range of 2000 ~ 2500 g m^{-2} over these regions (Li et al., 2005; Liao et al., 2008; Gao et al., 2016). If the same estimate is undertaken using the S/B ratio of this study (0.014), the *Spartina alterniflora* saltmarshes are expected to result in a maximal direct trapping of 1.9×10^6 tons of sediments over their growing season every year (dry biomass = 2250 g m^{-2}). This value means that the direct trapping of sediments contributes 0.45 cm a^{-1} to the deposition rate; nearly 1/3 of the increased deposition rates reported (Wang et al., 2005; Gao et al., 2014).

The sediment trapped by mangrove trees can also be estimated similarly. The mean density of the mangrove trees is 0.8 trees m^{-2}. The total dry biomass of the canopy is approximately 176 g m^{-2}. If half of the canopy is assumed to be submerged (a factor of 0.5 applied to the biomass), together with the maximum increase of S/B ratio of 0.028 between two succeeding days (based on ~~Figure~~Fig. 7), the potential amount of sediment available from the leaves of mangrove trees is 2.5 g m^{-2} per day at a maximum, which may contribute a maximum of 0.07 cm (in dry mass) annually to deposition rate over an annual period. ~~,~~ This is negligible when compared to the saltmarsh grass. Therefore, the standings of saltmarsh grass contribute substantially to sediment deposition processes, by trapping the sediments via the leaves and stems and then transported to the bed by rainfall rinsing. In contrast, the mangrove trees are less effective in direct trapping sediments via the canopy. It should be noted that most mature mangrove forests worldwide will only rarely be inundated up to the canopy, with most sedimentation occurring due to the slowing down of hydrodynamics between the aerial roots. Our study only attempts to capture the mechanisms for the expanding pioneer zone of mangrove forests which is occupied by short, young mangrove trees. With the future

带格式的: 字体: 非倾斜

带格式的: 字体: 非倾斜

带格式的: 字体: 非倾斜

带格式的: 字体: 非倾斜

development of aerial roots, the sediments trapped by mangrove trees may increase substantially. Meanwhile, the net deposition rate increased by the mangrove trees also provesshows less effective than the saltmarsh grass, although they have more significant influences on the hydrodynamics (Chen et al., 2016). The deposition tendency data in FigureFig. 6 reveals that mangrove trees are more effective than the saltmarsh grass in enhancing sedimentation by hydraulic alteration, but this part is unable to compensate the difference caused by direct trapping. More importantly, the flow rotation by the mangrove trees remarkably reduces the sediment transport flux into the vegetation edge (FigureFig. 5b) and leads to a reducedless efficiency in trapping sediments in a normal direction.

A similar estimate was also used for the amount of sediment trapped by seedlings. The maximum amount of sediment trapped by mangrove seedlings within a day was 4.78 g m^{-2};, higher than the 3.7g m^{-2} value found for grass seedlings of same stem density. The important implication from the seedling observations is that the mangrove seedlings are more efficient in directly trapping sediments, when compared to the more mature trees. The amount of sediment trapped by mangrove seedlings per unit area is almost twice that of the canopy (2.5 g m^{-2} per day). It can therefore be inferred that the both seedlings and aerial roots of some mangrove species, which show similar characteristics to the seedlings, will have a fundamental effect on sedimentation processes.

Although an aerial root system was not observed at the mangrove boundary under this investigation due to the young age of the forest, the biomass distribution of the typical mangrove species in southeast China has been reported by other studies (Lin et al., 1985; 1990; 1992; 1998 Lin et al., 1990; Lin et al., 1992; and Lin et al., 1998, Table 45). For three species in this table, the trunk representstakes the largest percentage of the total aboveground biomass. Secondly,

带格式的: 字体: 非倾斜

带格式的: 字体: 非倾斜

带格式的: 字体: 非倾斜

644 ~~t~~The canopies, mainly consisting of branches and leaves, contain the next largest ~~are in~~
645 ~~secondary place of~~ percentage in the total biomass. The contribution of aboveground roots (or
646 seedlings) varies among species. For these species, the contribution of aboveground roots (or
647 seedlings) is much less than the canopies. If the water level is sufficiently high to reach
648 mangrove canopies, the direct sediment trapping by canopies is more considerable than the
649 aboveground roots (or seedlings). In other words, the relative height of water level to the
650 mangrove trees determines the direct trapping efficiency for these species in Table 45. In
651 contrast, the aboveground roots of *Rhizophora stylosa* show the highest percentage in total
652 aboveground biomass. Therefore, the aboveground root system of *Rhizophora stylosa* is
653 fundamentally important in direct sediment trapping, regardless of water level changes.
654
655 Table 45. The typical mangrove species in Southeast China and their biomass constitutes as
656 indicated by the percentage of total aboveground biomass (data source from Lin et al., 1985;
657 1990; 1992; 1998~~, Lin et al., 1990, Lin et al., 1992 and Lin et al., 1998~~). Note the seedling of
658 *Kandelia obovate* was reported instead of aboveground roots because *Kandelia obovate* trees
659 rarely develop aboveground roots.

Location	Species	Trunk (%)	Branch (%)	Leaf (%)	Aboveground root (%)
Guangdong	*Aegiceras corniculatum*	74.20	13.68	7.29	4.84
Fujian	*Kandelia obovata*	77.78	15.56	6.52	0.19 (seedling)
Hainan	*Bruguiera sexangula*	69.61	22.95	4.39	3.05
Guangxi	*Rhizophora stylosa*	35.41	23.05	3.49	38.04

660

批注 [RV32]: Doesn't make sense. Please rewrite.

带格式的: 字体: 非倾斜

带格式的: 字体: 非倾斜

In terms of the transport of directly trapped sediments, precipitation may play an important role in this process within vegetated tidal flats. On land, raindrops falling on the sediment surface can cause suspension, saltation and bedload movement, particularly in low slope areas, but the maximum raindrop impacts occur for water depths of less than one raindrop diameter (Moss et al., 1979; Proffitt et al., 1991; Beuselinck et al., 2002). Contrary to the terrestrial environment, on vegetated tidal flats the raindrops have limited impact on sediment resuspension because of the deep water layers during high water periods~~;~~ and at low tide, the dense vegetation forms a mat to dissipate the kinetic energy of raindrops. Visual observation of the vegetated sites did not indicate the formation of fast overland flow, which is generally the main factor causing sediment movement on land surfaces. However, the raindrops can still work directly on the bare mudflat surface and influence recently deposited, ~~non-~~unconsolidated sediments as pointed out by Voulgaris and Meyers (2004).

When the vegetated flat was exposed~~emerged~~, the rinsing of the vegetation surface by raindrops results in a direct transport of sediments to the bed. Our experiments show the direct trapping of sediments by the vegetation surface. Precipitation creates a pathway for those particles to be moved onto the bed. Furthermore, the thick sediment layer on the vegetation leaf surfaces might cause a problem for seedling growth by different means, such as reducing photosynthesis or increasing the bending of stems. It has been observed by ecologists that the seedlings of saltmarsh grass and mangrove trees can be smothered due to the thick layer of mud on leaf surfaces (Yihui Zhang, *personal communication*). Therefore, rainfall events, especially moderate ones, can be of fundamental importance to the coastal wetland system and further studies on their frequency and seasonality coupled with tidal characteristics should be considered in the future in order to understand the mechanisms driving the change of coastal ecosystems.

带格式的: 字体: 非倾斜

带格式的: 字体: 非倾斜

带格式的: 字体: 非倾斜

4.3 The Limitations of Field Observations

Instrument availability and the restrictions of *in situ* deployment during this study lead to two primary limitations which should be discussed. Firstly, the number of ADVs available restricted the number of observations possible. Three locations were carefully chosen to form a nearly isoceles triangle, so that the mangrove and the saltmarsh were located on the same contour line (Chen et al., 2016), sharing a mutual control site on the bare mudflat. The elevation difference between the two vegetated flats and the bare mudflat bed is only 0.05 m (Chen et al., 2016). This small elevation difference has minimal influence on the flow direction and the subsequent suspended sediment transport, which can be confirmed through application of Soulsby's drag coefficient calculations, as derived for bedforms (Soulsby, 1997):

$$z_{0b} = a\frac{\Delta H^2}{\lambda} \qquad (7)$$

$$C_{Db} = \left[\frac{0.4}{1+\ln(\frac{z_{0b}}{h})}\right]^2 \qquad (8)$$

where ΔH and λ are the height (0.05 m) and width (35 m), respectively, of the bed form, Z_{0b} is the bed roughness due to bedform, h is the mean water depth and C_{Db} is the drag coefficient attributed to the bedform. The C_{Db} is estimated to be 0.0026 for the 0.05 m elevation difference, which is over an order of magnitude smaller than the drag coefficients (0.04-0.36) associated with the three sites (Chen et al., 2016), indicating that the elevation change has very limited contribution to any frictional term and is unlikely to affect flows. The principle reason for the alteration of flows and suspended sediment transports is therefore attributed to the presence of

带格式的: 字体: 非倾斜

带格式的: 字体: 非倾斜

带格式的: 字体: 非倾斜

带格式的: 字体: 非倾斜

vegetation. ~~and the sharing of a single control point on the bare mudflat is considered reasonable with minimal effects on the sediment transport flux estimates.~~

Secondly, some assumptions have been made regarding likely sediment transport pathways within the tidal flat. Although we acknowledge that the sediment could be transported into and out of the tidal flat via different routes, this question was addressed using previous observations and modeling results. The tidal flat under investigation features a gently seaward sloping topography, and lacks a well-~~-~~developed tidal creek system (Chen et al., 2016). Under these circumstances, modeling (Temmerman et al., 2005b) suggests that flow directions during a tidal cycle are usually perpendicular to the marsh edge with the sedimentation processes controlled by elevation differences and distance from the marsh edge. Thus, our study assumes that suspended sediments are transported into and out of the vegetation via the same route. This assumption might cause some uncertainty of the suspended sediment flux estimates and further work investigating the sediment transport pathway is needed in the future, particularly within coastal wetlands.

5 Conclusions

Field observations were made to compare the sediment transport processes occurring between a bare mudflat, a saltmarsh and a mangrove edge, considering both hydrodynamically induced sediment settling and the direct trapping effects of the vegetation surface. ~~Previous work in the same study area has revealed that the mangrove trees are better at retarding flows and dissipating energy than the saltmarsh grasses (*Chen et al., 2016*). However, t~~The interpretation of the SSC data, together with high-frequency flow ~~information~~measurements ~~(*Chen et al., 2016*)~~, reveals that the saltmarsh grass are more efficient than the mangrove trees at inducing sediment

批注 [RV33]: This sentence is complex and difficult to follow. Please sub-divide and rewrite.

带格式的： 字体：非倾斜

带格式的： 字体：非倾斜

批注 [RV34]: This should focus on your conclusions – drawn from the data presented in this paper – not from previous work.

trapping over a tidal-cycle scale. The main findings of this study are summarized in ~~Figure~~Fig. 8 and outlined below:

1) The SSC data exhibit a strong tidal asymmetry. The SSC is higher during the flood phase than the ebb phase for all three sites, implying a favorable environment for a net sediment input. The mean SSC level is generally high on the mudflat and decreases within the vegetated area, which is generally consistent with the deposition rates of the three sites.
2) Tidal_~~-~~cycle~~-~~scale sediment flux estimates show a depositional environment on the studied tidal flat. The presence of vegetation alters the flow direction and the subsequent suspended sediment transported into the system. Sediment transport fluxes indicate that the saltmarsh edge is more efficient than the mangrove edge at trapping sediment. This pattern is further supported by calculations of sediment fluxes at a tidal scale and deposition rates at a longer timescale. Although the SSC reduction is more pronounced at the mangrove site, the flow rotation caused by the mangrove trees reduces the sediment flux into the mangrove edge itself. Instead, a large portion of suspended sediment~~s~~ is transported along the mangrove edge, which is significantly different from the sediment transport pattern of the saltmarsh edge.
3) The mechanism for acceleration of deposition by tidal flat vegetation can be identified by using two approaches: sediment settling driven by local changes in the hydrodynamics and the direct sediment trapping by vegetation surfaces. Particle settling over a tidal scale was evaluated from deposition tendency. Deposition tendency on the bare mudflat is generally higher during ebb_tides than flood_tides, indicating a tidal asymmetry and a deposition lag during the ebb phase. Tidal flat vegetation is able to mediate the tidal asymmetry of this deposition tendency. Vegetation radically increases this parameter

during floods~~,~~ when the SSC is high, and this creates a more favorable environment for deposition. Eventhough it is more efficient in trapping sediment, the ~~S~~saltmarsh grass is found to be less efficient than the mangrove trees ~~in~~ at altering the deposition tendency of that sediment (Table 2).

4) The sediments trapped on vegetation leaves and stems are also quantified using samples of natural standings and seedlings. Saltmarsh grass has~~illustrates~~ a higher direct sediment trapping ability than mangrove trees. The amount of sediment trapped by the saltmarsh grass surface can contribute a considerable amount to deposition, in particular when associated with rainfall events, whilst the sediment directly trapped by mangrove trees is negligible compared to the observed total annual deposition rate in this particular site where only young mangrove trees occupy the front and very limited biomass is found close to the bed. A new mechanism of direct sediment trapping by the vegetation surface, in combination with precipitation, is proposed by this study, as a supplement to the mechanisms associated with hydrodynamic mediation by vegetation.

批注 [RV35]: Sorry – I though you found it to be more efficient.

批注 [CYN36R35]: We confirm it should be 'less efficient' here, as it talks about the deposition tendency but not the sediment trapping. We hope it is clear now…

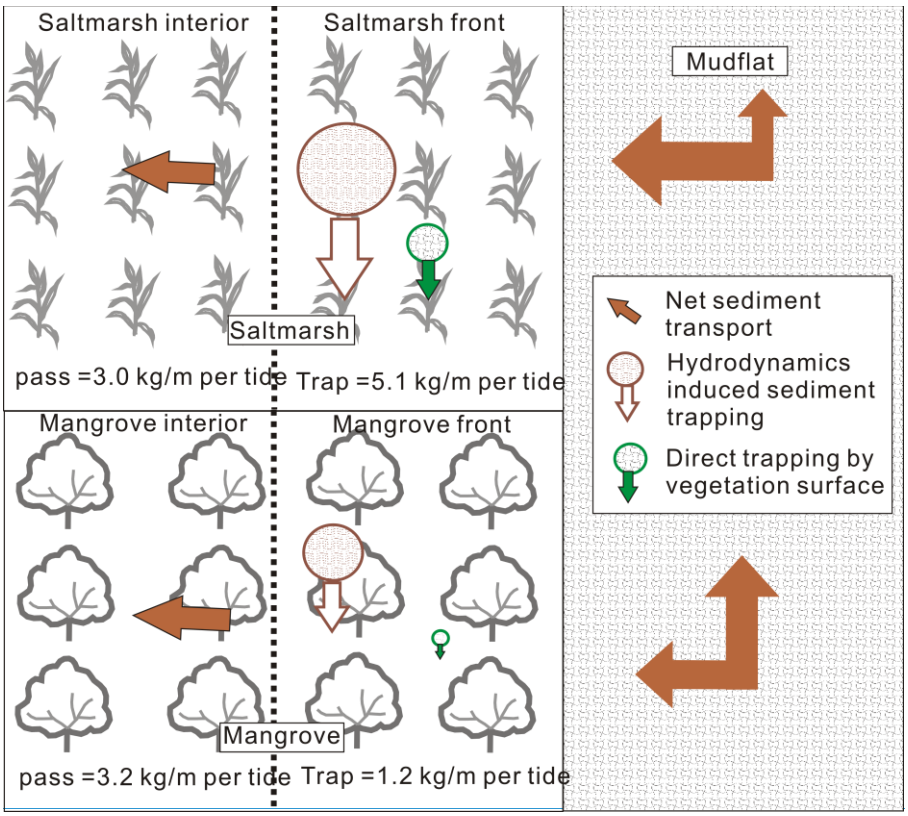
Saltmarsh interior
Saltmarsh front
Mudflat
Saltmarsh
pass =3.0 kg/m per tide
Trap =5.1 kg/m per tide
Net sediment transport
Hydrodynamics induced sediment trapping
Direct trapping by vegetation surface
Mangrove interior
Mangrove front
Mangrove
pass =3.2 kg/m per tide
Trap =1.2 kg/m per tide

765

带格式的: 居中

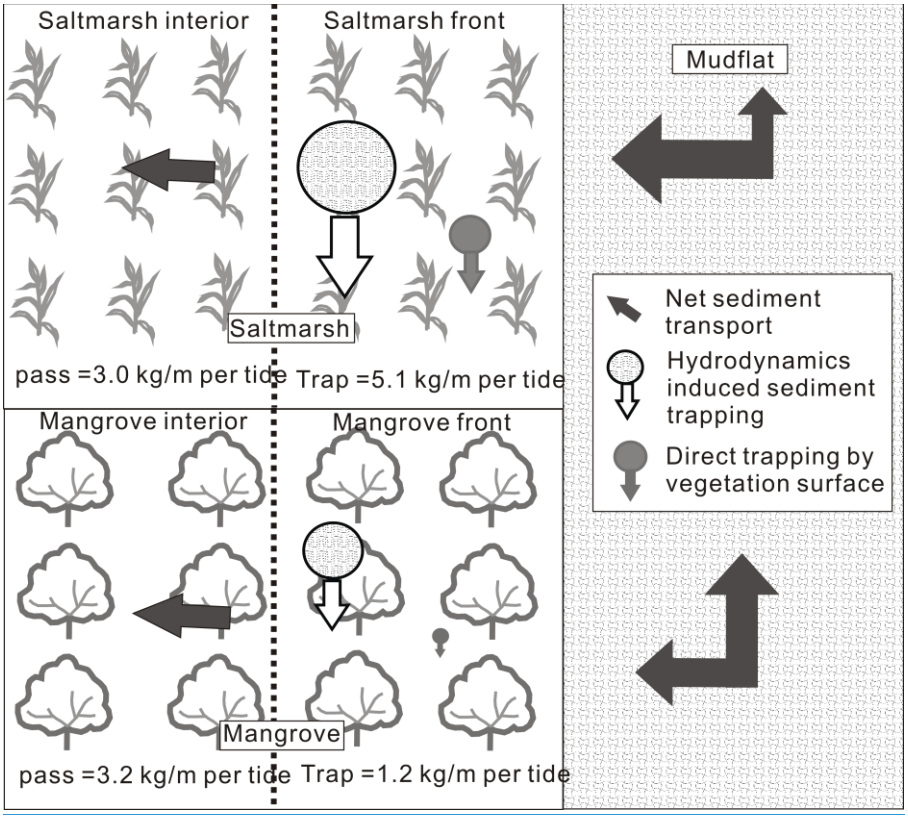

766

767 ~~Figure~~Fig. 8. A summary of the main findings of this study: 1) the suspended sediments are
768 transported from the bare mudflat to the vegetated edges with similar inundation periods, the
769 fluxes can be decomposed into normal and parallel components; 2) a considerable amount of
770 sediment~~s~~ was~~ere~~ trapped at the front of the saltmarsh and the mangrove; 3) the saltmarsh front
771 is more efficient than the mangrove front due to the flow rotation caused by the mangrove; and 4)
772 the sediment trapping is associated with two mechanisms: hydrodynamically induced sediment
773 settling and direct trapping by the vegetation surfaces. The size of the arrow and the circle
774 provides the information on relative magnitudes of these mechanisms.

批注 [RV37]: See earlier comment on colour Fig.s. Please address this through out.

批注 [CYN38R37]: We have replaced this figure with grey-scale one.

Acknowledgments

We would like to thank Dr. Yihui Zhang at Xiamen University and Prof. Dong-Ping Wang at State University of New York at Stony Brook for their valuable comments on inspiring this manuscript. Mr. Yi Li and Mr. Yang Yang (SIO, SOA) are thanked for their support in fieldwork. Thanks extend to the Management Office of Yunxiao Mangrove National Nature Reserve, for the site access. The data used are listed in the tables and figures. This work is funded by NSFC Projects (Grant no. 41006047 and 41776096) and a Fundamental Research Fund of Second Institute of Oceanography (No. JT1505). The authors also thank the anonymous reviewers for their time and thoughtful comments.

References

Alongi, D.M., Pftitzner, J., Trott, L.A., Tirendi, F., Dixon, P., and D.W., Klumpp, 2005.Rapid sediment accumulation and microbial mineralization in forests of the mangrove Kandelia candel in the Jiulongjang Estuary, China. Estuarine. Coastal and Shelf Science 63, 605–618.

Amos, C. L., Villatoro, M., Helsby, R., Thompson, C. E. L., Zaggia, L., and G.,Umgiesser, *et al.*, 2009. The measurement of sand transport in two inlets of venice lagoon, italy. Estuarine Coastal & Shelf Science, 87(2), 225-236.doi: 10.1016/j.ecss.2009.05.016.

Arkema, K.K.,Guannel, G., Verutes, G., Wood, S.A., Guerry, A., Ruckelshaus, M., Kareiva, P., Lacayo, M. and J.M., Silver, 2013. Coastal habitats shield people and property from sea-level rise and storms Nature Climate Change,

796 3, 913-918. doi: 10.1038/NCLIMATE1944

797 Barbier, E.B., Hacker, S.D., Kennedy, C., Koch, E.W., Stier and A.C.B., Silliman, 2011.The
798 value of estuarine and coastal ecosystem services. Ecological Monographs, 81(2), 169-
799 193. doi: 10.1890/10-1510.1

800 Beuselinck, L., G.,Govers, P. B., Hairsine, G.C., Sander, and M. Breynaert, 2002. The influence
801 of rainfall on sediment transport by overland flow over areas of net deposition. Journal of
802 Hydrology, 257, 145-163.doi:10.1016/S0022-1694(01)00548-0.

803 Bouma, T. J., L. A. van Duren, S. Temmerman, T. Claverie, A. Blanco-Garcia, T. Ysebaert, and
804 P. M. J. Herman, 2007. Spatial flow and sedimentation patterns within patches of
805 epibenthic structures: Combining field, flume and modelling experiments, Continental
806 Shelf Research, 27(8), 1020-1045, doi:10.1016/j.csr.2005.12.019.

807 Brown, J.M. and A.G., Davies, 2010. Flood/ebb tidal asymmetry in a shallow sandy estuary and
808 the impact on net sand transport. Geomorphology 114 (2010) 431–439.
809 doi:10.1016/j.geomorph.2009.08.006

810 Cahoon, D. R., Hensel, P. F., Spencer, T., Reed, D. J., McJee, K. and N. Saintilan, 2006. Coastal
811 Wetland Vulnerability to Relative Sea-Level Rise: Wetland Elevation Trends and Process
812 Controls. Verhoeven, J.T.A., Beltman, B., Bobbink, R.,and D.F. Whigham (eds.),
813 Wetlands and Natural Resource Management, Volume 190 of the series Ecological
814 Studies, 271-292.

815 Carus, J., Paul, M., and B., Schroder, 2016. Vegetation as self-adaptive coastal protection:
816 Reduction of current velocity and morphologic plasticity of a brackish marsh pioneer.
817 Ecology and Evolution 2016; 6(6), 1579–1589. doi: 10.1002/ece3.1904

818 Chen, Y., C. E. L. Thompson, and M. B. Collins, 2012. Saltmarsh creek bank stability:
819 Biostabilisation and consolidation with depth, Continental Shelf Research, 35, 64-74, doi:
820 10.1016/j.csr.2011.12.009.

821 Chen, Y., Li, Y., Cai, T., Thompson, C. E. L., and Y. Li, 2016. A comparison of
822 biohydrodynamic interaction within mangrove and saltmarsh boundaries. Earth Surface
823 Processes and Landforms, 41(13): 1967-1979. doi: 10.1002/esp.3964.

824 Childers, D. L., and J. W. Day, 1990. Marsh-water column interactions in two Louisiana
825 sstuaries. I. sediment dynamics. Estuaries, 13(4), 393-403.

826 Christiansen, T., P. L. Wiberg, and T. G. Milligan, 2000. Flow and Sediment Transport on a
827 Tidal Salt Marsh Surface, Estuarine, Coastal and Shelf Science, 50(3), 315-331,
828 doi:10.1006/ecss.2000.0548.

829 Chung, C.H., 2006. Forty years of ecological engineering with Spartina plantations in China.
830 Ecological Engineering, 27, 49–57. doi:10.1016/j.ecoleng.2005.09.012

831 Dronkers, J., 1986. Tidal asymmetry and estuarine morphology. Netherlands Journal of Sea
832 Research, 20 (2/3), 117-131.

833 Fagherazzi, S., Marani, M., and L.K., Blum, 2004. The ecogeomorphology of tidal marshes.
834 Washington, DC: American Geophysical Union, Coastal and Estuarine Studies, 268pp.

835 French, J.R., and T., Spencer, 1993. Dynamics of sedimentation in a tide-dominated back barrier
836 salt marsh, Norfolk, UK. Marine Geology, 110, 315-331.

837 Friess, D. A., K.W. Krauss, E.M. Horstman, T. Balke, T.J. Bouma, D. Galli, and E.L. Webb,
838 2012. Are all intertidal wetlands naturally created equal? Bottlenecks, thresholds and

knowledge gaps to mangrove and saltmarsh ecosystems. Biological Reviews, 87, 346–366. doi:10.1111/j.1469-185X.2011.00198.x

Furukawa, K., and E. Wolanski, 1996. Sedimentation in mangrove forests. Mangroves and Salt Marshes, 1, 3-9.

Furukawa, K., Wolanski, E., and H.Mueller, 1997. Currents and sediment transport in mangrove forests. Estuarine Coastal and Shelf Science, 44(3), 301-310. doi:10.1006/ecss.1996.0120

Fugate, D. C., and C. T. Friedrichs, 2002. Determining concentration and fall velocity of estuarine particle populations using ADV, OBS and LISST, Continental Shelf Research, 22(11-13), 1867-1886, doi:Pii S0278-4343(02)00043-2.

Fugate, D. C., and C. T. Friedrichs, 2003. Controls on suspended aggregate size in partially mixed estuaries, Estuarine, Coastal and Shelf Science, 58(2), 389-404, doi:10.1016/s0272-7714(03)00107-0.

Gao, J., Feng, Z., Chen, L., Wang, Y., Bai, F. and J., Li, 2016. The effect of biomass variations of Spartina alterniflora on the organiccarbon content and composition of a salt marsh in northern JiangsuProvince, China. Ecological Engineering 95, 160–170. doi: 10.1016/j.ecoleng.2016.06.088

Gao, S., Du, Y.F., Xie, W.J., Gao, W.H., Wang, D.D. and X.D., Wu, 2014. Environment-ecosystem dynamic processes of Spartina alterniflora salt-marshes along the eastern China coastlines. Science China: Earth Sciences, 57, 2567–2586, doi: 10.1007/s11430-014-4954-9

Gedan, K. B., M. L.,Kirwan, E., Wolanski, E. B., Barbier, and B. R. Silliman, 2010. The present and future role of coastal wetland vegetation in protecting shorelines: answering recent

challenges to the paradigm. Climatic Change, 106(1), 7-29. doi: 10.1007/s10584-010-0003-7

Gillis, L. G., T. J. Bouma, W. Kiswara, A. D. Ziegler, and P. M. J. Herman, 2014. Leaf transport in mimic mangrove forests and seagrass beds, Mar Ecol Prog Ser, 498, 95-102, doi:10.3354/meps10615.

Goring D. G., and V. I. Nikora, 2002. Despiking acoustic Doppler velocimeter data. Journal of Hydraulic Engineering, ASCE 128: 117-126. doi:10.1061/(ASCE)0733429(2002)128:1(117)

Graham, G. W., and A. J. Manning, 2007. Floc size and settling velocity within a *Spartina anglica* canopy, Continental Shelf Research, 27(8), 1060-1079. doi:10.1016/j.csr.2005.11.017.

Greene, R. S. B. and P. B. Hairsine, 2004. Elementary processes of soil–water interaction and thresholds in soil surface dynamics: a review. Earth Surface Processes and Landforms, 29,1077-1091. doi: 10.1002/esp.1103.

Ha, H. K., and J. P. Y. Maa, 2010. Effects of suspended sediment concentration and turbulence on settling velocity of cohesive sediment, Geosciences Journal, 14(2), 163-171, doi:10.1007/s12303-010-0016-2.

Horstman, E.M., Dohmen-Janssen, C.M., Bouma, T.J., and S. J. M. H. Hulscher, 2015. Tidal-scale flow routing and sedimentation in mangrove forests: Combining field data and numerical modelling, Geomorphology, 228, 244-262. doi:10.1016/j.geomorph.2014.08.011.

882 Kathiresan, K., 2003. How do mangrove forests induce sedimentation? Revista de Biologia
883 Tropical 51, 355-360.

884 Kelleway, J.J., Saintilan, N., Macreadie, P.I., Baldock, J.A. and P.J. Ralph, 2017. Sediment and
885 carbon deposition vary among vegetation assemblages in a coastal salt marsh.
886 Biogeosciences, 14, 3763–3779. doi:10.5194/bg-14-3763-2017

887 Kitheka, J.U., Ongwenyi, G.S., and K.M., Mavuti, 2003. Fluxes and exchange of suspended
888 sediment in tidal inlets draining a degraded mangrove forest in Kenya. Estuarine, Coastal
889 and Shelf Science, 56, 655–667.doi:10.1016/S0272-7714(02)00217-2

890 Leonard, L.A., and M.E. Luther, 1995. Flow hydrodynamics in tidal marsh canopies. Limnology
891 and Oceanography 40: 1474–1484.

892 Li, J., Xu, J., Zhang, D., Yan, X., Tong, Y. and Y., Shen. 2005. Function of Spartina alterniflora
893 salt march and its eco-economic value in south coast of Hangzhou Bay. Areal Research
894 and Development, 24, 58-62. (In Chinese with English abstract).

895 Li, Y., Y., Chen, Y., Li, 2017. Remote sensing analysis of the changes in the junction region of
896 mangrove forests and *Spartina alterniflora* saltmarshes. Marine Science Bulletin, 36,
897 348-359.

898 Liao, C.Z., Luo, Y.Q., Fang, C.M., Chen, J.K., Li, B., 2008. Litter pool sizes, decomposition,
899 and nitrogen dynamics in Spartina alterniflora-invaded and native coastal marshlands of
900 the Yangtze estuary. Oecologia 156, 589–600.

901 Lin, P., 2001. A review on the mangrove research in China. Journal of Xiamen University
902 (Natural Science), 40(2), 592-603.

903 Lin, P., Hu, H., Zheng, W., Li, Z., and Y., Lin, 1998. A study of biomass and energy of
904 mangrove communities in Shenzhen Bay. Scientia Silvae Sinicae, 34, 18-23. (In Chinese
905 with English abstract)

906 Lin, P., Lu, C., Lin, G., Chen, R., and L., Su, 1985. Study on mangrove ecosystem of
907 Jiulongjiang River estuary. Journal of Xiamen University (Natural Science), 24, 508-514.
908 (In Chinese with English abstract)

909 Lin, P., Lu, C., Wang, G. and H., Chen, 1995. Biomass and productivity of *Bruguiera sexangula*
910 mangrove forest in Hainan Island, China. Journal of Xiamen University (Natural Science),
911 29, 209-213. (In Chinese with English abstract)

912 Lin, P., Yin, Y. and C., Lu, 1992. Biomass and productivity of *Rhizophora stylosa* community in
913 Yingluo Bay of Guangxi, China. Journal of Xiamen University (Natural Science), 31,
914 199-202. (In Chinese with English abstract)

915 Liu, Q., 1991. Silt transportation and its influences on submarine scour and silting in Dongshan
916 Bay, Fujian Journal of Oceanography in Taiwan Strait, 10(1), 69-76.

917 Lovelock, C. E., M. F. Adame, V. Bennion, M. Hayes, R. Reef, N. Santini, and D. R. Cahoon ,
918 2015. Sea level and turbidity controls on mangrove soil surface elevation change,
919 Estuarine, Coastal and Shelf Science, 153, 1-9, doi:10.1016/j.ecss.2014.11.026.

920 Luhar, M., and H. M. Nepf, 2013. From the blade scale to the reach scale: A characterization of
921 aquatic vegetative drag, Advances in Water Resources, 51, 305-316,
922 doi:10.1016/j.advwatres.2012.02.002.

923 Mazda, Y., Kanazawa, N., and E.,Wolanski, 1995. Tidal asymmetry in mangrove creeks.
924 Hydrobiologia 295, 51–58.

925 MICZTWR Office, 1990. Multipurpose Investigation of the Coastal Zone and Tidal Wetland
926 Resources– Report of Fujian Province. 575pp. Ocean Press, China.

927 Mitsch, W.J., and J.G. Gosselink, 2007. Wetlands. John Wiley & Sons: Chichester, 619pp.

928 Moller, I., Kudella, M., Rupprecht, F., Spencer, T., Paul, M., van Wesenbeeck, B. K., and S.
929 Schimmels, 2014. Wave attenuation over coastal salt marshes under storm surge
930 conditions. Nature Geoscience, 7(10), 727-731. doi: 10.1038/ngeo2251

931 Moss, A. J., Walker, P. H., and J. Hutka, 1979. Raindrop-simulated transportation in shallow
932 water flows: an experimental study. Sedimentary Geology, 22, 165-184.

933 Nepf, H., 1999. Drag, turbulence, and diffusion in flow through emergent vegetation. Water
934 Resources Research, 35(2), 479-489. doi: 10.1029/1998wr900069.

935 Nepf, H., 2012. Flow and transport in regions with aquatic vegetation. Annual Review of Fluid
936 Mechanics 44: 123–142. doi:10.1146/annurev-fluid-120710-101048.

937 Neumeier, U., and P. Ciavola, 2004, Flow Resistance and Associated Sedimentary Processes in a
938 Spartina maritima Salt-Marsh, J Coastal Res, 20(2), 435-447, doi:10.2112/1551-
939 5036(2004)020(0435:FRAASP)2.0.CO;2.

940 Neumeier, U., and C. L. Amos, 2006.The influence of vegetation on turbulence and flow
941 velocities in European salt-marshes. Sedimentology, 53(2), 259-277. doi: 10.1111/j.1365-
942 3091.2006.00772.x

943 Ortiz, A., Ashton A., and H. Nepf, 2013. Mean and turbulent velocity fields near rigid and
944 flexible plants, and the implications for deposition. Journal of Geophysical Research -
945 Earth Surface 118: 1–15.DOI:10.1002/2013JF002858.

946 Perillo, G. E. M., E. Wolanski, D. R. Cahoon, and M. M. Brinson, 2009. Coastal Wetlands: An
947 Integrated Ecosystem Approach, Elsevier, Elsevier B.V.

948 Proffitt, A. P. B., Rose, C. W., and P. B., Hairsine, 1991. Rainfall detachment and deposition:
949 experiments with low slopes and significant water depth. Soil Science Society of
950 America Journal, 55, 325-332. doi:10.2136/sssaj1991.03615995005500020004x

951 Redfield, A.C., 1972. Development of a New England salt marsh. Ecological Monographs,
952 42,201–237.

953 Saintilan, N., Wilson, N., Rogers, K., Rajkaran, A., and K.W. Krauss, 2014. Mangrove
954 expansion and salt marsh decline at mangrove poleward limits. Global Change Biology,
955 20 (1), 147-157.doi: 10.1111/gcb.12341

956 Scully, M. E., and C. T. Friedrichs, 2007. Sediment pumping by tidal asymmetry in a partially
957 mixed estuary Journal of Geophysical Research, 112, C07028,
958 doi:10.1029/2006JC003784

959 Sheng, J., and A.E.,Hay, 1988. An examination of the spherical scatterer approximation in
960 aqueous suspensions of sand. Journal of the Acoustic Society of America 83 (2), 598–610.

961 Shi, Z., Pethick, J. S., and K., Pye, 1995. Flow structure in and above the various heights of a
962 saltmarsh canopy: a laboratory flume study. Journal of Coastal Research 11(4), 1204–
963 1209.

964 SonTek, 1997. SonTek Doppler current meters: using signal strength data to monitor suspended
965 sediment concentration. SonTek/YSIInc., California, 7pp.

966 Soulsby R., 1997. Dynamics of Marine Sands: A Manual for Practical Applications. Thomas
967 Telford: London, 272pp.

968 Temmerman, S., Bouma, T.J., Govers, G., Wang, Z.B., De Vries, M.B. and P.M.J., Herman,
969 2005a. Impact of vegetation on flow routing and sedimentation patterns: Three-
970 dimensional modeling for a tidal marsh. Journal of Geophysical Research 110, F04019.
971 doi:10.1029/2005JF000301

972 Temmerman, S., Bouma, T.J., Govers, G., and D., Lauwaet, 2005b, Flow paths of water and
973 sediment in a tidal marsh: relations with marsh developmental stage and tidal inundation
974 height. Estuaries 28, 338–352.

975 Temmerman, S., Meire, P., Bouma, T.J., Herman, P.M.J., Ysebaert, T., and H., De Vriend, 2013.
976 Ecosystem-based coastal defence in the face of global change. Nature 504, 79-83.
977 doi:10.1038/nature12859.

978 Thompson, C.E.L., C.L., Amos, and G., Umgiesser, 2004, A Comparison Between Fluid Shear
979 Stress Reduction by Halophytic Plants in Venice Lagoon, Italy and Rustico Bay, Canada
980 - analyses of in situ measurements. Journal of Marine Systems 51, 293-308. Doi:
981 10.1016/j.jmarsys.2004.05.017.

982 van der Wal, D., and K. Pye, 2004. Patterns, rates and possible causes of saltmarsh erosion in the
983 Greater Thames area (UK), Geomorphology, 61(3-4), 373-391,
984 doi:10.1016/j.geomorph.2004.02.005.

985 Vargas-Luna, A., A. Crosato, and W. S. J. Uijttewaal, 2015. Effects of vegetation on flow and
986 sediment transport: comparative analyses and validation of predicting models, Earth Surf
987 ace Processes and Landforms, 40(2), 157-176, doi:10.1002/esp.3633.

988 Vincent, C.E., and A., Downing, 1994. Variability of suspendeds and concentrations, transport
989 and eddy diffusivity under non-breaking waves on the shore face. Continental Shelf
990 Research 14 (2/3), 223–250.

991 Voulgaris, G., and S. T. Meyers, 2004. Temporal variability of hydrodynamics, sediment
992 concentration and sediment settling velocity in a tidal creek, Continental Shelf Research,
993 24, 1659–1683, doi:10.1016/j.csr.2004.05.006.

994 Wang, A., Gao, S., Jia, J., Pan, S., 2005. Contemporary sedimentataion rates on saltmarshes at
995 Wanggang, Jiangsu, China. Journal of Geographical Sciences, 15, 199-209. doi:
996 10.1360/gs050208

997 Wang, A., Ye, X., and J., Chen, 2010. Observations and analyses of floc size and floc settling
998 velocity in coastal salt marsh of Luoyuan Bay, Fujian Province, China. Acta Oceanologia
999 Sinica 29, 116-126. doi: 10.1360/gs050208.

1000 Wang, Y., Gao, S., Jia, J., Thompson, C.E.L., Gao J., and Y. Yang, 2012. Sediment transport
1001 over an accretional intertidal flat with influences of reclamation, Jiangsu coast, China.
1002 Marine Geology 291-294, 147-161. doi:10.1016/j.margeo.2011.01.004.

1003 Wang, Y., Gao, S., Jia, J., Liu Y., and J., Gao, 2014. Remarked morphological change in a large
1004 tidal inlet with low sediment-supply. Continental Shelf Research 90, 79-95.doi:
1005 10.1016/j.csr.2014.02.005

1006 Wolanski, E., 1995. Transport of sediment in mangrove swamps, Hydrobiologia, 295, 31-42.

1007 Wolanski, E., Mazda, Y., King, B., and S., Gay, 1990. Dynamics, flushing and trapping in
1008 Hinchinbrook channel, a giant mangrove swamp, Australia. Estuarine Coastal and Shelf
1009 Science, 31, 555–579.

1010 Wolanski, E., Mazda, Y., Furukawa, K., Ridd, P., Kitheka, J.,Spagnol, S., and T., Stieglitz, 2001.
1011 Water-circulation in mangroves and its implications for Biodiversity. In E. Wolanski
1012 (Ed.), Oceanographic processes of coral reefs: physical and biological links in the Great
1013 Barrier Reef (pp. 53–76). London: CRC Press.

1014 Woodroffe, C.D., Rogers, K., McKee, K.L., Lovelock, C.E., Mendelssohn, I.A. and N. Saintilan,
1015 2016. Mangrove Sedimentation and Response to Relative Sea-Level Rise. Annual
1016 Review of Marine Science, 8, 243–66. Doi: 0.1146/annurev-marine-122414-034025

1017 Zhang, Y., Wang, W., Wu, Q., Fang, B., and P. Lin, 2006. The growth of Kandelia candel
1018 seedlings in mangrove habitats of the Zhangjiang estuary in Fujian, China. Acta
1019 Ecologica Sinica, 26(6), 1648-1655. doi: 10.1016/s1872-2032(06)60028-0

1020 Zhang, Y. H., Huang, G. M., Wang, W. Q., Chen, L. Z., and G.H. Lin, 2012. Interactions
1021 between mangroves and exotic Spartina in an anthropogenically disturbed estuary in
1022 southern China. Ecology, 93(3), 588-597.

1023 Zong, L., and H. Nepf, 2010. Flow and deposition in and around a finite patch of vegetation,
1024 Geomorphology, 116(3-4), 363-372, doi:10.1016/j.geomorph.2009.11.020.

1025 Zuo, P., Zhao, S., Liu, C., Wang,C. and Y., Liang, 2012. Distribution of Spartina spp. along
1026 China's coast. Ecological Engineering, 40,160– 166. doi:10.1016/j.ecoleng.2011.12.014

1027

Accepted revised manuscript with no changes marked
Click here to view linked References

Differential sediment trapping abilities of mangrove and saltmarsh vegetation in a subtropical estuary

Yining Chen[1,2*], Yan Li[1,2], Charlotte Thompson[3], Xinkai Wang [1], Tinglu Cai [1], Yang Chang[1]

[1]Second Institute of Oceanography, SOA, Hangzhou, 310012, China.

[2]State Key Laboratory of Marine and Environmental Science, Xiamen University, Xiamen, 361005, China.

[3]Ocean and Earth Science, University of Southampton, National Oceanography Centre, Southampton, SO14 3ZH, UK.

Corresponding author: Yining Chen (yiningchen5410@hotmail.com; yiningchen@sio.org.cn)

Key Points:

- Compare sediment transport from bare mudflat across mangrove and saltmarsh boundaries.
- Sediment trapping is caused by hydraulic forces and direct trapping by vegetation.
- The saltmarsh edge is more efficient than the mangrove edge at trapping sediments.

Abstract

Saltmarsh and mangrove are common coastal wetland types and their ability to enhance deposition has been investigated extensively, but rarely compared directly. This study carried out *in situ* observations to compare the sediment transport processes between a bare mudflat, a mangrove stand and a saltmarsh stand within a subtropical estuary. Turbidity variations over the latter portion of a spring tide were recorded, alongside measurements of flow data, to estimate sediment trapping by hydraulic forces under similar hydroperiods. In addition, vegetation was transplanted to compare the direct sediment trapping by high- and short-standing seedlings. The suspended sediment concentration (SSC) time series showed an overall reduction between the bare mudflat and the vegetated flats. Suspended sediment flux estimates revealed that a considerable amount of sediment was trapped by the saltmarsh and the mangrove edges. The flux estimates find that the saltmarsh edge is more efficient than the mangrove edge in trapping sediments transported normal to the edge. The sediment trapping mechanisms were considered based on two approaches: the hydrodynamic related sediment settling and direct trapping by vegetation. The calculation of deposition tendency showed that the presence of vegetation altered the flow direction and the tidal asymmetry of the deposition process, resulting in a higher deposition tendency during the flood phase to enhance sediment settling. In addition to sediment settling, vegetation surfaces were found to trap sediments directly. In combination with rinsing by precipitation, these trapped sediments accumulated on the bed and contributed to the deposition. Against the background of similar inundation periods, the saltmarsh grass showed a greater sediment trapping ability than the mangrove trees, in terms of both the hydraulic sediment trapping and the direct trapping by vegetation surface.

Keywords: Sediment trapping; Mangrove; Saltmarsh; Mudflat

1 Introduction

Natural coastal wetlands are widely recognized for their ability to trap sediments (Perillo et al., 2009; Barbier et al., 2011; Moller et al., 2014), as well as for their defense potential against the action of waves and tidal flows (Temmerman et al., 2013; Horstman et al., 2015; Carus et al., 2016). Saltmarshes and mangroves are globally common coastal wetland types, although the latter are mainly restricted to tropical and subtropical regions. In general, mangroves are dominated by halophytic trees and shrubs, whilst saltmarshes are characterized by herbaceous vegetation (Mitsch and Gosselink, 2007). Because of their ability to stabilize the coast by dissipating waves and current energy and enhancing deposition, these two types of habitats can be useful tools for coastal engineers in protecting the coastline (Redfield, 1972; Gedan et al., 2010).

Vegetation occurring along intertidal flats has been recognized as having the ability to stabilize, trap and bind sediments. In general, plants have been observed to directly increase the erosion threshold of bed sediments (Chen et al., 2012), and indirectly trap sediments by providing additional drag force (Leonard and Luther, 1995; Temmerman et al., 2005a; Chen et al., 2016) which mediate flow patterns, and consequently enhance local sediment deposition (Neumeier and Amos, 2006; Horstman et al., 2015). The enhancement of sediment deposition by coastal wetland vegetation has received more extensive attention in recent decades, in part due to the predicted impacts of accelerated sea-level rise due to global warming (van der Wal and Pye, 2004; Cahoon et al., 2006, Arkema et al., 2013; Woodroffe et al., 2016; Kelleyway et al., 2017). For practical purposes, the understanding of the mechanisms of sediment trapping by vegetation is key to the engineering work of coastal stabilization and protection, but the efficiency varies amongst vegetation species (Kathiresan, 2003; Friess et al., 2012; Ortiz et al., 2013).

Previous studies have revealed that heavily vegetated mangrove systems normally trap sediments during the flood tide, and that there is generally no significant export of sediments during the ebb due to the deceleration of the tidal currents by vegetation-induced friction (Wolanski et al., 1990; 2001; Furukawa et al., 1997; Kitheka et al, 2003). At a tidal-scale, field observations also show that mangrove trees are able to create a favorable environment as a sediment sink by modifying flow routing (Horstman et al., 2015). Factors such as vegetation density and biomass, as well as the intertidal position determining submergence/emergence status, and geomorphological setting (e.g., platforms or creeks), all affect the trapping capacity of mangrove trees (Friess et al., 2012).

Saltmarshes and their interaction with sediment dynamics have also been extensively studied (e.g., Leonard and Luther, 1995; Temmerman et al., 2005a; Neumeier and Amos, 2006; Bouma et al., 2007). Previous studies reveal the dampening effects of saltmarsh vegetation on mean flow and turbulent diffusion, resulting in a more favorable environment for deposition (Christiansen et al. 2000; Neumeier and Amos, 2006; Zong and Nepf, 2010; Nepf, 2012). Factors controlling the trapping capacity of saltmarsh grass include density, biomass, the emergence/submergence status and geomorphological setting (Temmerman et al., 2005a, b; Bouma et al., 2007; Nepf, 2012). The differences between the effects of mangroves and saltmarshes are related to the physical structure of the vegetation. The stiff canopy of saltmarshes normally shows a decrease in biomass with height (Neumeier, 2005). The presence of the trunks and aerial roots of mangrove show considerable effects on flow and deposition mediation (e.g. Madza et al., 1995) while the canopy is made up of rigid stems on the bottom and a stiff leaf layer at the top, resulting in an increase in biomass on the top. Therefore, theoretically, the saltmarsh grass shows a more pronounced influence on the bottom of the water column rather

than the top, whilst the mangrove, depending on species, affects the bottom and sometimes the top of the water column, although the regions of the water column affected by vegetation will depend on the relative local tidal levels to the height of trees.

This body of previous work has endeavored to further our understanding of the mechanisms controlling the bio-physical interactions within fluvial systems and coastal wetlands, together with the feedback between vegetation and sediment dynamics. The use of flumes and model vegetation has played an important role in raising our understanding of these detailed mechanisms (Shi et al., 1995; Nepf, 2012; Oritz et al., 2013). However, field observations focused on natural systems and processes are required to further develop these fundamental findings, particularly in regions where different ecosystems overlap. As pointed out by a number of scientists, complex factors such as precipitation, intermittent discharge, bi-directional flows and the consolidation of sediments must also be taken into account during the study of sediment transport on tide-dominated environments (Fagherazzi et al., 2004; Greene and Hairsine, 2004; Chen et al., 2012). These processes drive the evolution of coastal systems over the long term, but cannot be entirely captured by flume observations. Comparisons of the results from field and flume observations (Bouma et al., 2007) found that flume studies are unable to capture all necessary spatial scales, and will always result in some flow artefacts, including lower turbulence intensities than in the field. Vargas-Luna et al. (2015) reviewed a number of physical models in terms of the effects of vegetation on flows and sediment transport and they concluded that 'field measurements are not available, thus, intensive field campaigns including different climatic conditions, vegetation species…are also recommended.' Thus, the aim of this study was to carry out *in situ* observations to compare the sediment transport at the boundaries of a mangrove swamp and an adjacent saltmarsh. The competition between saltmarshes and

mangrove species has been well documented to be associated with the critical bed elevation and the subsequent inundation period (Saintilan et al., 2014). In this study, we focus on a direct comparison between the sediment trapping abilities of the two types of vegetated boundaries with similar inundation periods (i.e. similar bed elevations). A comparison of differences in flow reduction and energy dissipation by saltmarsh and mangrove plants has already been assessed and is presented in a separate paper (Chen et al., 2016).

2 Methods

2.1 Study Site

Yunxiao Mangrove National Natural Reserve, located at the Zhangjiang Estuary in the southeast China coast, was selected as the site to conduct the field measurements (Fig. 1). The tidal flat developing within this reserve is approximately 600 m in width. The upper part of the tidal flat (100-200 m in width) is covered both by mangroves and saltmarshes; the adjacent species make this location an ideal study area for comparative field observations.

The runoff of the Zhangjiang River carries a large amount of fresh water and sediments, with a mean annual water discharge of 9.6×10^8 m^3 and suspended sediment discharge of 3.6×10^8 kg (MICZTWR Office, 1990). The suspended sediment concentration decreases to ~40mg L^{-1} within the estuary and further to ~ 30 mg L^{-1}in Dongshan Bay (MICZTWR Office, 1990; Liu, 1991). The annual precipitation within the estuary region is 700 mm and 80% of it takes place in the wet season (April to September). The study site is home to a tidally-dominated mangrove forest with a fronting saltmarsh; the tidal flat is exposed to irregular semi-diurnal tides with a mean tidal range of 2.3 m. Wave exposure is very limited due to the sheltering effects of Dongshan Bay outside the estuary, except during typhoon seasons which normally occur in

summer. The resulting physical conditions of the estuary therefore favor the deposition of fine-grained sediments, which form a wide range of tidal flats along the main channel (Liu, 1991). The site under investigation is located on a relatively wide tidal flat with a slope of 2-3‰. The bed of this tidal flat consists of fine-grained sediment, mainly clays and silts.

It has been reported that on the southeast coast of China, the rapid spread of the invasive saltmarsh grass *Spartina alterniflora* threatens the local mangroves (Lin, 2001; Zhang et al., 2012). However, the study site is located on a tidal flat that exhibits co-existence of local mangroves and *Spartina alterniflora* saltmarsh. The upper part of the flat is covered by native mangrove species (*Kandelia obovata*, *Aegiceras corniculatum*, and *Avicennia marina*), while the exotic *Spartina alterniflora* occupies part of the mudflat fronting the mangrove forest (Zhang et al., 2012). The saltmarsh grass only covers a small area of the tidal flat during spring and summer, due to human removal as part of managed efforts to maintain a bare mudflat in the lower part of the tidal flat (Zhang et al., 2006).

Fig. 1. Location of study area and field deployment: a) study area: Yunxiao National Mangrove Reserve; b) location of deployments: Site A (bare mudflat), Site B (mangrove boundary) and Site C (saltmarsh boundary)，together with the definition of flow components: U and V are the geographical northing and easting components, V1 and U1 are the components normal and parallel to the mangrove edge, respectively, and V2 and U2 are the components normal and parallel to the saltmarsh edge, respectively; the flood directions of three sites are also marked by arrows: black for mudflat, red for saltmarsh and blue for mangrove; and c) the positions of instruments deployed and the location of seedling transplantation, sites B and C have the same bed elevation, 5 cm above the bed of Site A (the reference for water level measurements)

154

155 The leading edge of the mangrove forest is made up of a mixture of *Kandelia obovata*
156 and *Aegiceras corniculatum*, with a mostly closed canopy (80-90% closed). The mean distance
157 from the bottom of the tree canopy to the bed was 0.4 m. In spring, the trees had a mean height
158 of 1.6 m and a mean canopy width of 1.2 m. Combination of canopy closure percentage and the
159 canopy width gives a density of 0.8 shoots/m^2. The aerial root system is not well developed in
160 the front, due to the presence of young mangrove trees. In addition, aboveground aerial roots of
161 *K. obovata* are generally rare on the mudflats of Southeast China. Seedlings can be observed
162 sparsely within the mangrove forest, with density of 20-30 shoots/m^2.

163 The saltmarsh of *S. alterniflora*, 1.0 m in height, occurs at the seaward front of the
164 mangrove forest, with a high stem density of 580 m^{-2} and a high aboveground biomass (dry) of
165 2.50 kg m^{-2} (Chen et al., 2016). A topographic map of the region indicates a small elevation
166 change (< 0.27%) in the northwest-southeast (NW-SE) direction. When the tidal flat is
167 submerged (2-3 hours every tidal cycle during the observation period, Table 1), the mean water
168 level was 0.43 m above the tidal flat bed, with the maximum water levels reaching 0.76 m (Chen
169 et al., 2016). It should be noted that due to the elevation of the vegetated mudflat, only higher or
170 spring tides are able to reach this part of tidal flat (Fig. 1c).

171 2.2 Location and Time

172 Because spring is the crucial time for the seedlings of mangrove and saltmarsh vegetation
173 to establish, the field observations were carried out during 30th April to 5th May 2014 throughout
174 the latter portion of a spring tide, covering 11 tidal cycles. The weather was cloudy but dry for
175 most of the time, except the second day, during which a moderately heavy rain event (25 mm

over 24 hours) took place, and the last day, during which a short shower took place just before the vegetation samples were collected (after tidal cycle No. 11).

Three locations (Fig. 1) were selected for comparative synchronous measurements, located on the bare mudflat (Site A), within the mangrove edge (Site B) and within the saltmarsh edge (Site C). The distance between the bare mudflat site and the two vegetated flat sites was approximately 35 m. The sites within the mangrove and saltmarsh boundaries are at a distance of 10 m from the vegetation edge, as defined by the start of the closed canopy. The remaining regions between Sites A and B, and Site C are covered by sparse mangrove trees and *Spartina* grass. The fringes of vegetation described in this contribution include both the dense vegetation with closed canopies, as shown in Fig. 1, together with the sparsely vegetated fronting flat. The space between the vegetated sites (B and C) and the bare mudflat location (Site A) confines the vegetation fringes. Site A is 0.05 cm lower in elevation than the other two sites. Site B and Site C have the same elevations as determined by RTK-GPS.

2.3 Sediment Dynamic Observations

The backscatter intensity data of three Acoustic Doppler Velocimeters (ADV) were used to obtain flow data over 9 tidal cycles. The locations were carefully selected to avoid mangrove trees, and the vegetation around the sensors was removed (Chen et al., 2016). These were fixed to stainless steel frames for field deployment. The ADVs (Nortek Vector models, 6MHz) were all positioned 20 cm above the bed to collect data continuously at a frequency of 16Hz. It should be noted that the ADV sensor measures the water volume at a height of 8 cm above the bed (12 cm below the sensor head positioned 20 cm above the bed, Fig. 1c). ADV backscatter intensity data were also used to estimate the suspended sediment concentration (SSC) based on a logarithmic relationship calibrated within the laboratory (Sontek, 1997; Ha and Maa, 2010). The

longest possible data records were extracted and separated into 5-minute intervals to obtain mean values.

The output of the ADV provides three components of current velocity, U, V and W which represent easting, northing and upward components of the flow. A three-dimensional hydrodynamic and sediment transport model has revealed that as long as the water level is below the canopy top, the vegetated areas flood from the unvegetated areas, with flow directions more or less perpendicular to the vegetation edge (Temmerman et al., 2005a*)*. Thus, the flow components are rotated according to the orientation of the vegetation edges for further analyses. The mangrove edge has an orientation of 160°, and the flow components were rotated to generate components parallel (U1) and normal (V1) to this direction. The same procedure was applied to the saltmarsh edge, which has an orientation of 50° (U2 and V2). For simplicity, the three velocity components (u, v and w) of the tidal currents were used in formula as generalized symbols of the velocity components. When the data correlation values exceeded 0.7, the phase-space thresholding method developed by Goring and Nikora (2002) was adopted for despiking noise before the calculation of mean velocities, turbulent velocities and turbidities.

The suspended sediment flux can be expressed as follows (*Wang et al., 2014*):

$$F = \int_T \int_L \int_H CV_0 \, dz\, dx\, dt \qquad (1)$$

Where F is the flux through a cross section with water depth H (dz) and unit width L (dx) over a timescale T (dt) of a flood or ebb flow, C is the SSC converted from ADV backscatter intensity and V_0 is the speed of flow component normal to the vegetation edges. Due to the position of the sensors, the flux only covers the submerged period of a tidal cycle. However, the

data used for the flux calculation were from simultaneous periods, so this will not affect the comparison amongst the three sites.

The TKE (Turbulent Kinetic Energy) density can be estimated as:

$$TKE_{density} = 0.5\rho(\overline{u'^2} + \overline{v'^2} + \overline{w'^2}) \qquad (2)$$

Equation 2 is applied for each 5-minute data section. Here, ρ is the fluid density; u', v' and w' are the turbulent fluctuations deviating from 5-minute average values of the eastward, northward and upward flow components, respectively (Thompson et al., 2004).

The bed shear stress τ_b is estimated using Equation (3), where $C_1 = 0.19$ as suggested by Soulsby (1997), and suited to vegetated beds (Thompson et al., 2004):

$$\tau_b = C_1 TKE_{density} \qquad (3)$$

The shear velocity u_* can be estimated from the bed shear stress and the fluid density ρ_f (Equation 4):

$$u_* = \sqrt{\frac{\tau_b}{\rho_f}} \qquad (4)$$

Fugate and Friedrichs (2002) provided an algebraic equation for estimating tidally-averaged settling velocity w_s using an ADV. Voulgaris and Meyers (2004) further expand this method to resolve the tidal variability of the settling velocity (Equation 5), which was adopted in our study:

$$w_s C = \langle w'C' \rangle \qquad (5)$$

where C is the 5-minute averaged SSC, w' is the vertical fluid velocity fluctuation, C' is the SSC fluctuation estimated from the ADV backscatter strength, and $\langle\ \rangle$ is the symbol indicating time averaging. The settling velocity estimate (Equation 5) can be applied when the

advection transport is minimal compared with the vertical velocity terms (Fugate and Friedrichs, 2002). Using ADV data from pairs of stations, a consistency check was undertaken to evaluate the ratio of the advection term relative to the settling term, as suggested by Fugate and Friedrichs (2002), before the settling velocity was calculated. The flow data and the SSC data obtained by ADV, as well as the distance between the paired stations and the elevations of sensors, were used for this valuation which gives the average ratio of 0.06 ± 0.04 and 0.009 ± 0.006 for the flat-mangrove and flat-saltmarsh sites, respectively. Thus, the advection term is two orders of magnitude smaller than the settling term and it is reasonable to estimate settling velocity using the method of Voulgaris and Meyers (2004).

Bed samples from each site and local water samples were collected to produce a turbidity gradient in the laboratory, for individual calibration of ADV backscatter sensors. SSC was measured by passing a known sample volume through a pre-weighed 0.45 μm poresize glass fiber filter, followed by drying and weighing. Linear relationships were therefore established between the backscatter intensity and the logarithm of SSC for each sensor, as suggested by previous studies (Ha and Maa, 2010, Fig. 2).

Fig. 2. Calibration between backscatter intensity and suspended sediment concentration for (a) bare mudflat; (b) saltmarsh; and (c) mangrove. Note the x in the equations refers to $Log_{10}SSC$, and SSC is in the unit of mg L^{-1}.

2.4 Vegetation Trapping Experiments

More than 50 saltmarsh grass standings and small branches of mangrove trees were randomly marked and cleaned for field observation. Any sediments attached to these vegetation

samples were washed off using clean water in the field before the experiment started. Subsequently, the aboveground parts of 6 vegetation samples (3 mangrove samples and 3 grass samples) were then collected daily using tough scissors after the initial deployment of the instruments. The sediments on the vegetation surface were washed off and collected into cylinders for subsequent filtering and drying to obtain the dry weight of the sediment deposits on the vegetation. The vegetation samples, including leaves and stems, were subsequently dried and weighed to obtain biomass. Note that for conservation purposes, only small branches of the mangrove trees were collected and thus measured weight is mainly from leaves.

The seedlings of mangrove and saltmarsh grass start to grow during this season (Spring). They are much shorter than the natural standings but vital to the development of the ecosystem. In light of the fact that seedlings appear within the near bed whilst the natural standings penetrate the whole water column during the investigation period, it is important to examine the difference between their abilities of trapping sediment using their leaves and stems. *K. obovate* and *S. alterniflora* seedlings were transplanted adjacent to the observation sites and arranged at a density close to the natural status, and used to represent the sediment trapping ability of vegetation at an early stage of life. Seedlings of *K. obovata* and *S. alterniflora* were transplanted into Site B and Site C, respectively. For each site, fifty 20 cm- high seedlings of mangroves or saltmarsh grass, which had been rinsed clean with water, were separately arranged into two quadrates of 200 cm×100 cm, with an individual spacing of 20 cm. Three Samples of each type of seedlings were collected in triplicate every day along the edge of the plots, together with the natural standings of vegetation to measure the sediment trapped by vegetation using the same method as mentioned before. The mangrove seedlings were in a similar density as their natural

status, but that of the *Spartina* seedlings was decreased to allow a comparison between two species.

The instruments recorded from midnight of 29th/30th April until after the first tidal cycle of 4th May (Table 1), the last point at which water levels were sufficiently high to submerge them.

The sediment mass trapped by the vegetation was measured in this study through the period of the 2nd tidal cycle (occurring in the afternoon of 30 April) to the 11th tidal cycle. The samples were collected every day at noon (Table 1).

Table 1. Description of the field observation deployment

Tidal cycle Number	1	2	3	4	5	6	7	8	9	10	11
Time	01:00 - 03:20	13:00 - 15:00	01:50 - 04:00	13:40 - 15:35	02:30 - 04:40	14:20 - 16:00	03:20 - 05:20	14:40 - 16:40	03:40 - 05:50	N/A	N/A
Date	30/4 AM	30/4 PM	1/5 AM	1/5 PM	2/5 AM	2/5 PM	3/5 AM	3/5 PM	4/5 AM	4/5 PM	5/5 AM
Trapping Experiment		Day 1		Day 2		Day 3		Day 4		Day 5	
Instruments	Recording									Off	
Weather	Cloudy but dry		Rain	Cloudy but dry							Rain

2.5 Supporting Measurements

A RTK-GPS (Trimble-SPS881) survey was undertaken to record the relative elevations of the three sites for water level analysis. Plastic accretion stakes (1.5 cm in diameter, 50 cm long, 10 cm exposed, Fig. 1b) were inserted into the bed to monitor deposition rates by measuring the exposed length from May 2012 to May 2014. It is noted that the *Spartina* grass was removed in August 2012 by the local management office and it had recovered by the spring of 2013; as such,

303 the deposition rates of the saltmarsh represent under-estimated values. Surface sediments were
304 collected during instrument deployment for laboratory grain size analysis using a laser grain size
305 analyzer (Helos, manufactured by Sympatec). Biological properties of the vegetation, such as
306 mangrove geometrics (height and diameter of canopy, diameter of trunk), and density and
307 diameter of grass were measured *in situ* using a tape measure. Aboveground biomass of
308 vegetation was measured by harvesting, drying and weighing plant samples.

309 **3 Results**

310 3.1 Tidal-cycle Scale Suspended Sediment Concentration

311 The variation of suspended sediment concentration (SSC) over 9 tidal cycles is displayed
312 in Fig. 3. The SSC data exhibit a strong tidal asymmetry, with one exception of the second tidal
313 cycle on the bare mudflat. The overall SSC is higher during the flood phase than the ebb phase
314 for all three sites, which implies a favorable environment for a net sediment input. On average,
315 there is a considerable reduction in SSC between the bare mudflat and the vegetated sites (Table
316 2). The average SSC reduced nearly 10% from the bare mudflat to the saltmarsh boundary,
317 whilst nearly 20% from the bare mudflat to the mangrove boundary. This pattern implies
318 sediment trapping within the vegetation boundaries at a tidal scale.

319 Deposition rates over a two-year period were recorded by accretion stakes. The readings
320 of 5 or 6 stakes of each site (see Fig. 1 for more details) are averaged and displayed in Table 2.
321 The short-term pattern of SSC variation is generally consistent with long-term deposition rates
322 recorded by stakes on the vegetated area and the mudflat, which shows higher rates at vegetation
323 edges than on the mudflat (Table 2), although the deposition rates may be under-estimated as
324 compaction is not considered.

325

326 Fig. 3. The SSC data series over 9 tidal cycles: (a) SSC time series based on acoustic backscatter
327 (ADV); and (b) water level variation. The detailed time is listed in Table 1.

328

329

330

331 Table 2. Synthesis of the mean parameters associated with suspended sediment transport of the
332 three sites.

Parameter		Flat	Saltmarsh	Mangrove
Grain size (μm)		6.20±0.76	5.79±0.43	6.34±0.90
Deposition rate (cm a^{-1})		1.14±1.20	2.60±0.97*	2.10±0.87
Settling Velocity (mm s^{-1})		1.90	0.87	0.85
SSC (mg L^{-1})		68.8	62.9	56.2
Net SSC flux per tidal cycle (kg/m)	Normal to saltmarsh edge	8.1	3.0	--
	Normal to mangrove edge	4.4	--	3.2
Sediment trapped per tidal cycle (kg/m)		--	5.1	1.2
Deposition tendency	Flood	0. 17	0.21	0.26
	Ebb	0. 23	0.21	0.25
Cumulative S:B ratio	Natural standings	--	0.017	0.016
	Seedlings	--	0.11	0.13

333 *Note: the deposition rate is under-estimated due to the clearing of grass in August 2012. The
334 stake number is 6 in the saltmarsh site, whilst 5 for the other sites.

335

3.2 Tidal-cycle Scale Sediment Transport: A Comparison

Detailed flow information has been published in a separate paper (Chen et al., 2016). Here, we provide a brief summary of the horizontal flow conditions. The horizontal flow speeds of the three sites are shown in Fig. 4. A considerable reduction in flow speed caused by vegetation is readily identified and a rotation of flow direction by vegetation has been related to eddy viscosity and drag forces (Chen et al., 2016).

Fig. 4. The variations of horizontal flow speed and direction throughout 9 tidal cycles (source: Chen et al., 2016): (a) flow speed data; and (b) flow direction data. Note the geographical flow direction uses the north as zero degrees.

Neumeier and Ciavola (2004) noted a relatively uniform vertical velocity profile within saltmarsh grass canopies. Due to the shallow water layer, the SSC is normally regarded as a constant through the vertical profile in modeling or field observations on tidal flats (e.g., Temmerman et al., 2003; Wang et al., 2012). In addition, based on the consideration of small flow speed magnitude and the relatively low turbidity, a uniform profile assumption is used in this study for SSC flux estimate, based on a combination of flow and SSC data using Equation 1. The SSC flux data for each flood and ebb period is displayed in Fig. 5. Due to the flow rotation, the SSC transport normal to the vegetation is mainly presented, but the sediment transport along the vegetation edges is also considered (Fig. 1b). The SSC fluxes of the bare mudflat site are decomposed according to saltmarsh edge and mangrove edge orientations separately (Fig. 5). Diurnal inequality results in higher sediment fluxes during the relatively high tides (odd numbers) than the relatively low tides (even numbers). The sediment fluxes are determined by

both SSC and flow velocity. Although the SSC values of the bare mudflat are not always higher than the vegetated sites, as indicated by Fig. 3 for all tidal cycles, the net sediment trapping by the vegetation edges is likely to be the result of flow reduction by the vegetation.

Overall, the study area is dominated by a net input of sediments. The highest fluxes occur on the bare mudflat site; this is because when the suspended sediments are transported into the vegetation edges, a large amount of sediment is trapped by the vegetation and only part of the sediment flux is able to pass through the vegetation to reach the upper tidal flat. The bare mudflat site shows different SSC fluxes when considering the main transport directions (Fig. 5). This site shows a lower net sediment transport towards the mangrove, because the presence of the mangrove edge deviates the flow (257º in flood) away from the main flow direction of 305º in flood on the tidal flat (Fig. 4b, Chen et al., 2016).

The long-term deposition rates (Table 2) are consistent with the pattern of the flux estimates at tidal cycle scales: relatively low deposition rates are observed on the bare mudflat (1.4 cm a^{-1}) whilst high deposition rates occur at the vegetation edges (> 2 cm a^{-1}); the deposition rate at the saltmarsh edge is higher than that at the mangrove edge, in response to a greater difference in sediment input between the vegetated sites and the bare mudflat site.

Fig. 5. Suspended sediment fluxes per unit width estimated at a tidal cycle scale: (a) sediment flux at the bare mudflat site in the direction normal to saltmarsh edge; (b) sediment flux at the saltmarsh site in the direction normal to saltmarsh edge; (c) sediment flux at the bare mudflat site in the direction normal to mangrove edge; and d) SSC flux at the mangrove site in the direction normal to mangrove edge. The flux was estimated to represent the total mass passing a unit width of bed over a time span of either the ebb or flood flow. North represented by zero degrees.

382

383 The amount of sediment trapped between the vegetated sites and the bare mudflat sites is
384 estimated using the SSC flux data using Equation 1. The sediment trapped at the vegetation
385 boundaries can be estimated by comparing the difference between the fluxes of the mudflat site
386 (with subscript of 'mud') and the vegetated sites (with subscript of 'veg'), as described by
387 following (Equation 6):

388 $$trap = (Flux_{flood,mud} - Flux_{ebb,mud}) - (Flux_{flood,veg} - Flux_{ebb,veg}) \quad (6)$$

389 The values of sediment trapping are given in Table 2. This clearly indicates that the
390 presence of vegetation can increase SSC trapping at their front edges. Further, by comparing the
391 SSC fluxes (Table 2), it can be inferred that a considerable amount of the sediments transported
392 from the lower part of the tidal flat towards the upper tidal flat are trapped within the front edges
393 of the vegetation, an area of 35 m width which includes a combination of mudflat and sparse
394 vegetation. Finally, the saltmarsh front edge, showing a greater trapping ability, is found to be
395 more efficient than the mangrove front edge in trapping sediments. Due to the total amount of
396 sediment flux from the bare mudflat is same for two vegetated sites, coupled with the fact that
397 the mangrove trees trap less sediments normal to their front, more sediments can be transported
398 parallel to the mangrove edge than the saltmarsh edge. The transport in this direction can
399 increase the elevation of the whole system and benefiting the neighboring plants. Remote sensing
400 image analysis (Li et al., 2017) shows the mangrove in this area expands in a direction parallel to
401 its front, whilst the saltmarsh advances in a direction normal to its present front. The sediment
402 transport and trapping pattern might explain the different directions of vegetation expansion.

3.3 Enhanced deposition by vegetation as indicated by deposition tendency

In order to quantitatively evaluate the tendency for particles to deposit or resuspend, the ratio of particle settling velocity to the shear velocity $\frac{w_s}{u_*}$ has been proposed by Ortiz et al. (2013) for saltmarsh environments. The estimates of settling velocity and shear velocity for this study were calculated using Equations 2-5 as described in the Methods section. In general, when $\frac{w_s}{u_*}$ is above 0.1, the environment is considered to be deposition-dominant (Zong and Nepf, 2010)

Mean $\frac{w_s}{u_*}$ ratios calculated for each flood and ebb tide are displayed in Fig. 6. The $\frac{w_s}{u_*}$ ratio of the flood and ebb vary within a range of 0.14 and 0.31 for all sites, implying favorable conditions for deposition. The tidal cycle-averaged values (including flood and ebb phases) of vegetation sites are 0.25 ± 0.03 and 0.21 ± 0.04 for the mangrove site and the saltmarsh site, respectively, whilst this value is 0.20 ± 0.03 for the bare mudflat site.

Fig. 6. Deposition tendency of three sites as indicated by $\frac{w_s}{u_*}$ ratio: (a) mudflat; (b) saltmarsh; and (c) mangrove; the dashed line of 0.1 marks the lower limit for 'deposition favorable' conditions, as suggested by Zong and Nepf (2010).

3.4 Sediment Trapping by Vegetation, and Precipitation Effects

A ratio of sediment mass (S) to biomass (B), S/B, is proposed in this study to allow estimates of the ability of vegetation to trap sediments. The S/B ratio is defined as the value of

the dry sediment mass washed from the vegetation divided by the dry biomass of the vegetation itself. We choose this ratio because dry sediment mass and dry biomass can be easily measured in laboratory with high accuracy. Further, the data on dry sediment mass and dry biomass have been used in a large number of studies and this allows us to discuss our results using other data sources. The properties of the two vegetation species are listed in Table 3.

Table 3. The biological properties of the investigated mangrove trees and saltmarsh grass

Spartina	Height (m)	Stem density (m^{-2})	Biomass (dry, kg m^{-2})	Coverage (%)	Stem diameter (m)
	1.0	580	2.5	90%	0.008
Mangrove	Height (m)	Stand Density (m^{-2})	Canopy biomass (dry, kg m^{-2})	Canopy closure (%)	Trunk diameter (m)
	1.6	0.8	0.22	80-90%	0.1

Because the samples were collected successively, the S/B ratio data are cumulative, indicating the continuous sediment trapping by vegetation over tidal cycles. The cumulative S/B ratio of the natural standings and the transplanted seedlings of mangrove trees and saltmarsh grass for the observation period are illustrated in Fig. 7.

Fig. 7. The cumulative sediments trapped by vegetation surfaces, as indicated by the S/B ratio over 10 tidal cycles: (a) seedlings and (b) mature standings. The seedling samples were planted in a matrix of 10 x 5 stands within an rectangular area of 100 cm x 200 cm. Three samples of each vegetation type were collected every day to give the average and standard deviation values in this figure.

Overall, the S/B ratio of natural, high standings is significantly less than that of the seedlings for both types of vegetation (Fig. 7). This is because the top canopy of the high standings experiences much less submergence than the lower part, and this decreases their efficiency as a sediment trap by unit mass. However, in the light of the large amount of biomass (e.g. aboveground biomass of *Spartina alterniflora* reaches 2.5 kg m^{-2} in this area) of the high standings and the length of time they are present (from Spring to Autumn) compared to the seedlings (only part of the seedlings are able to survive until Autumn), they perform a more important role overall in trapping sediments on the tidal flat.

The S/B ratio of mangrove and saltmarsh seedlings both vary considerably over the 10 tidal cycles while maintaining similar patterns (Fig. 7a). The S/B ratios of the mangrove seedlings are similar to those of the *Spartina* seedlings if the shoot densities are same. The S/B ratio drops to a minimum during tidal cycles 4 and 5, then they increase on the following two days, and decrease slightly again on the last day. This pattern is different from the expected continuous increase and it is highly likely to be associated with precipitation, which took place during tidal cycles 3 and 4, and before tidal cycle 11. The authors observed in the field that the rain drops washed off fine particles attached to the leaves during the low water period. It appears that the sediments become trapped by vegetation during high water levels, and the rain during the emergence hours creates a mechanism to transport sediment downward onto the bed. Without precipitation, the sediments will be accumulated until an upper limit is reached. The presence of precipitation is able to accelerate this downward transport of sediment. This mechanism may be not only important for the sedimentary process on the tidal flat, but also for the growth of seedlings. High standings show a similar pattern as the seedlings (Fig. 7b), except during tidal cycle no. 4-5. In general, the high standings show less diurnal variation, as well as lower

standard deviations amongst samples. The high standings of saltmarsh grass and mangroves show a decreasing trend in S/B ratio, with a low value occurring on the day after the moderately heavy rain (tidal cycles 4 and 5), together with a general increase after that day. Similarly, the short shower also shows its effect at the end of the observation, slightly decreasing the S/B ratio on the last day. The frequency of sampling is not sufficiently high in this study to confirm it, but the lag between surface sediment decreases in successive days (Fig. 7) might imply a lag in response to precipitation.

4 Discussion

A complete understanding of the mechanisms mediating sediment accumulation by tidal flat vegetation, particularly the possible impact of vegetation upon suspended particles, is still illusive (Graham and Manning, 2007). Trapping of suspended particles can be caused by both changes to hydraulic forces and by the direct presence of vegetation leaves and stems. In the following sections, the sediment settling caused by hydraulic forces and by the direct trapping by leaves or stems will be discussed separately, together with limitations of this study.

4.1 Hydraulic Sediment Settling Processes within the Saltmarsh and the Mangrove Fronts

Various devices (e.g., floc cameras) have been used to show that suspended particles settle in a flocculated form within saltmarshes and mangrove swamps (French and Spencer, 1993; Wolanski, 1995; Graham and Manning, 2007). Wolanski (1995) suggested that the settling velocity of suspended particles in mangrove swamps is 1 mm s^{-1} for clay and 5 mm s^{-1} for silt. Voulgaris and Mayers (2004) observed an invariant, tidally-averaged settling velocity of 0.24 mm s^{-1} for flocs on a saltmarsh surface. A more accurate observation of floc settling velocity within a saltmarsh vegetation canopy under turbulent flow conditions was conducted in an

annular flume using a flocs camera (Graham and Manning, 2007), which provides a range of 0.004 ~ 3.36 mm s^{-1}, with a mean value of 0.55 mm s^{-1}. Settling velocities estimated based on ADV observations by this study (Table 2) are within the range of previous observations. However, a decrease in the settling velocity of suspended particles from the bare mudflat to the vegetated sites occurs and further explanation is needed for the settling processes.

The settling of suspended sediments within the vegetation canopy is related to the generation of turbulence and the wake-sheltering effects in the lee of downstream stems (Shi et al., 1995; Nepf, 1999). In general, the deposition tendency ratio, also known as the inverse movability number forming part of the Rouse parameter (Amos et al., 2010), has a range of 0.002 to 0.3 in aquatic environments and a typical value of 0.02 has been used in flume experiments (Ortiz et al., 2013). Relatively high values of the ratio imply a trend for deposition whilst low values suggest a tendency for resuspension. Deposition has been clearly observed in flumes when the deposition tendency ratio is above 0.1 (Zong and Nepf, 2010).

The vegetation below the sensors was cleared in this study and, thus, this observation looked into the sediment settling directly driven by hydrodynamics, but not the direct trapping by the vegetation surface. Meanwhile, more than 80% of the turbulent kinetic energy is dissipated by the vegetation in comparison with the mudflat (Chen et al, 2016). Therefore, it is important to use the $\frac{w_s}{u_*}$ ratio to determine the likelihood of deposition.

The most notable pattern revealed by Fig. 6 is the change of tidal asymmetry in the $\frac{w_s}{u_*}$ ratio by vegetation. On the bare mudflat, the $\frac{w_s}{u_*}$ ratio shows a strong ebb-dominant characteristic throughout the tidal cycles, consistent with the asymmetry in suspended sediment

508 flux (Fig. 5). Paired-sample T tests (by SPSS package) are used to exam three sites in terms of
509 the flood-ebb asymmetry. The results show a significant difference between the bare mudflat and
510 the vegetated sites (P<0.01, Table 4).

511

512

513

514 Table 4. Paired samples tests for tidal asymmetry of deposition tendency

	Std. deviation	Std. error mean	t	df	Sig. (P-value)
flat vs saltmarsh	0.043	0.014	-3.616	8	0.007
flat vs mangrove	0.023	0.075	-8.284	8	<0.001

515

516 Thus, a considerable amount of suspended particles, mostly clay and fine silts (Table 2),
517 are transported into the bare mudflat during the flood stage. These particles tend to settle, as
518 indicated by the $\frac{w_s}{u_*}$ ratio (> 0.1 over 9 tidal cycles) during this stage. During the ebb stage
519 however, the $\frac{w_s}{u_*}$ ratio increases considerably, and consequently the majority of deposition
520 occurs during this stage, resulting in a deposition lag.

521 Tidal asymmetry, as defined by comparing flood and ebb phases through various
522 parameters in relation to hydrodynamic processes, has been widely recognized for its importance
523 in resulting sedimentation processes (Dronkers, 1986; Scully and Friedrichs, 2007; Brown and
524 Davies, 2010), but hardly considered in flume experiments (Zong and Nepf, 2010; Ortiz et al.,
525 2013). The tidal asymmetry in the deposition tendency can be altered by vegetation. Throughout
526 9 tidal cycles in our study, the deposition tendency data shows considerable ebb-dominance

within the bare mudflat site (Fig. 6a) whilst the vegetated sites shows either nearly symmetrical or flood-dominant deposition tendencies (Fig. 6b, c). Differently from the bare mudflat, most of the suspended particles within the vegetated sites therefore deposit during the flood stage when the SSC is high, rather than the ebb stage with low SSC, improving the deposition efficiency. This is likely to be an important mechanism throughout which vegetation enhances deposition by regulating hydrodynamics and the consequent $\frac{w_s}{u_*}$ ratio, but has not been reported by previous studies. The presence of vegetation decreases both the settling velocity (Table 2) and the shear velocity (Chen et al., 2016). The improved deposition efficiency implies that shear velocity reduction is greater than the decrease of settling velocity, as a function of the vegetation.

4.2 The Potential Contribution of Direct Trapping to Deposition

The suspended sediment settling and trapping driven by hydraulics have been extensively studied. However, the sediment directly trapped by vegetation is rarely taken into account. Vegetation occurring on tidal flats has been widely recognized for its ability to increase deposition to adapt to relative sea-level rise. Accelerated deposition rates have been observed in a number of saltmarshes and mangrove swamps, in comparison with unvegetated tidal flats (e.g., Childers and Day, 1990; Furukawa and Wolanski, 1996; Christansen et al., 2000; Alongi et al., 2005; Lovelock et al., 2015). The suspended particles can form larger flocs and settle more rapidly to the seabed as the vegetation creates a more favorable environment for sediment settling (Neumeier and Ciavola, 2004; Graham and Manning, 2007; Nepf, 2012; Ortiz et al., 2013). More recently, leaf transport as a source of particulate organic matter (POM) in ecosystems was observed in flume experiments which compared simulated mangrove forests and seagrass beds, indicating the mangrove roots were more efficient at trapping POM than the

549 seagrass beds (Gillis et al., 2013). Associated with leaf transport, it can be readily observed in the
550 field that a thick layer of mud can accumulate on the leaf surface. This is another pathway for
551 suspended particles to be trapped by the vegetation system, but is rarely recognized in the
552 literature.

553 A quantitative measurement of suspended sediment trapped by vegetation stems and
554 leaves in the field has been conducted in this study, and is represented by the S/B ratio (Fig. 7).
555 Moreover, the amount of sediment trapping over a unit area (1 m × 1 m) is estimated based on
556 S/B ratio and the biomass data. On average, the difference in S/B ratio of saltmarsh grass
557 between two successive days reaches a value of 0.003 (based on data reported in Fig. 7), even
558 when considering the rinsing by rainfall. The maximum accumulated S/B ratio over two
559 successive days reaches 0.014. Considering the dry biomass values of 2.5 kg m^{-2} and based on
560 our observations the aboveground biomass, including stems and leaves, has the potential to trap a
561 maximum of 35 g dry sediments per square meter per day (S/B ratio =0.014). The dry density of
562 clay and silt sediments is approximately 1.28 g cm^{-3} and thus the estimated amount of sediments
563 attached to the vegetation surface have the potential to add up to 0.5 cm to the annual deposition
564 rate during its growing season (6 months). This estimate assumes complete deposition from the
565 leaves to the bed, but could be revised if additional factors (e.g., the water content and bulk
566 density) were considered, and may be overestimated.

567 *Spartina alterniflora* has been artificially introduced into Chinese tidal flats since 1980s
568 for the purpose of stimulating tidal flat accretion (Chung, 2006). It has been reported that the
569 presence of *Spartina alterniflora* has increased the sedimentation rates of the tidal flats from
570 ~1.5 cm a^{-1} to ~ 3 cm a^{-1} (Wang et al., 2005; Gao et al., 2014). The direct trapping amount of
571 sediments by vegetation, however, remains unknown. Most of the *Spartina alterniflora*

saltmarshes appear on the silty or clay mudflats along the east China coast, including Jiangsu Province, Shanghai, Zhejiang Province and Fujian Province (Gao et al., 2014). The total area of this type of saltmarshes sums up to 3.2×10^8 m^2 (Zuo et al., 2012). The aboveground biomass (dry mass) varies within the range of 2000 ~ 2500 g m^{-2} over these regions (Li et al., 2005; Liao et al., 2008; Gao et al., 2016). If the same estimate is undertaken using the S/B ratio of this study (0.014), the *Spartina alterniflora* saltmarshes are expected to result in a maximal direct trapping of 1.9×10^6 tons of sediments over their growing season every year (dry biomass = 2250 g m^{-2}). This value means that the direct trapping of sediments contributes 0.45 cm a^{-1} to the deposition rate; nearly 1/3 of the increased deposition rates reported (Wang et al., 2005; Gao et al., 2014).

The sediment trapped by mangrove trees can also be estimated similarly. The mean density of the mangrove trees is 0.8 trees m^{-2}. The total dry biomass of the canopy is approximately 176 g m^{-2}. If half of the canopy is assumed to be submerged (a factor of 0.5 applied to the biomass), together with the maximum increase of S/B ratio of 0.028 between two succeeding days (based on Fig. 7), the potential amount of sediment available from the leaves of mangrove trees is 2.5 g m^{-2} per day at a maximum, which may contribute a maximum of 0.07 cm (in dry mass) annually to deposition rate over an annual period. This is negligible when compared to the saltmarsh grass. Therefore, the standings of saltmarsh grass contribute substantially to sediment deposition processes, by trapping the sediments via the leaves and stems and then transported to the bed by rainfall rinsing. In contrast, the mangrove trees are less effective in direct trapping sediments via the canopy. It should be noted that most mature mangrove forests worldwide will only rarely be inundated up to the canopy, with most sedimentation occurring due to the slowing down of hydrodynamics between the aerial roots. Our study only attempts to capture the mechanisms for the expanding pioneer zone of

595 mangrove forests which is occupied by short, young mangrove trees. With the future
596 development of aerial roots, the sediments trapped by mangrove trees may increase substantially.
597 Meanwhile, the net deposition rate increased by the mangrove trees also proves less effective
598 than the saltmarsh grass, although they have more significant influences on the hydrodynamics
599 (Chen et al., 2016). The deposition tendency data in Fig. 6 reveals that mangrove trees are more
600 effective than the saltmarsh grass in enhancing sedimentation by hydraulic alteration, but this
601 part is unable to compensate the difference caused by direct trapping. More importantly, the flow
602 rotation by the mangrove trees remarkably reduces the sediment transport flux into the
603 vegetation edge (Fig. 5b) and leads to a reduced efficiency in trapping sediments in a normal
604 direction.

605 A similar estimate was also used for the amount of sediment trapped by seedlings. The
606 maximum amount of sediment trapped by mangrove seedlings within a day was 4.78 g m^{-2};
607 higher than the 3.7g m^{-2} value found for grass seedlings of same stem density. The important
608 implication from the seedling observations is that the mangrove seedlings are more efficient in
609 directly trapping sediments, when compared to the more mature trees. The amount of sediment
610 trapped by mangrove seedlings per unit area is almost twice that of the canopy (2.5 g m^{-2} per
611 day). It can therefore be inferred that the both seedlings and aerial roots of some mangrove
612 species, which show similar characteristics to the seedlings, will have a fundamental effect on
613 sedimentation processes.

614 Although an aerial root system was not observed at the mangrove boundary under this
615 investigation due to the young age of the forest, the biomass distribution of the typical mangrove
616 species in southeast China has been reported by other studies (Lin et al., 1985; 1990; 1992; 1998,
617 Table 5). For three species in this table, the trunk represents the largest percentage of the total

aboveground biomass. The canopies, mainly consisting of branches and leaves, contain the next largest percentage in the total biomass. The contribution of aboveground roots (or seedlings) varies among species. For these species, the contribution of aboveground roots (or seedlings) is much less than the canopies. If the water level is sufficiently high to reach mangrove canopies, the direct sediment trapping by canopies is more considerable than the aboveground roots (or seedlings). In other words, the relative height of water level to the mangrove trees determines the direct trapping efficiency for these species in Table 5. In contrast, the aboveground roots of *Rhizophora stylosa* show the highest percentage in total aboveground biomass. Therefore, the aboveground root system of *Rhizophora stylosa* is fundamentally important in direct sediment trapping, regardless of water level changes.

Table 5. The typical mangrove species in Southeast China and their biomass constitutes as indicated by the percentage of total aboveground biomass (data source from Lin et al., 1985; 1990; 1992; 1998). Note the seedling of *Kandelia obovate* was reported instead of aboveground roots because *Kandelia obovate* trees rarely develop aboveground roots.

Location	Species	Trunk (%)	Branch (%)	Leaf (%)	Aboveground root (%)
Guangdong	*Aegiceras corniculatum*	74.20	13.68	7.29	4.84
Fujian	*Kandelia obovata*	77.78	15.56	6.52	0.19 (seedling)
Hainan	*Bruguiera sexangula*	69.61	22.95	4.39	3.05
Guangxi	*Rhizophora stylosa*	35.41	23.05	3.49	38.04

In terms of the transport of directly trapped sediments, precipitation may play an important role in this process within vegetated tidal flats. On land, raindrops falling on the sediment surface

636 can cause suspension, saltation and bedload movement, particularly in low slope areas, but the
637 maximum raindrop impacts occur for water depths of less than one raindrop diameter (Moss et
638 al., 1979; Proffitt et al., 1991; Beuselinck et al., 2002). Contrary to the terrestrial environment,
639 on vegetated tidal flats the raindrops have limited impact on sediment resuspension because of
640 the deep water layers during high water periods; and at low tide, the dense vegetation forms a
641 mat to dissipate the kinetic energy of raindrops. Visual observation of the vegetated sites did not
642 indicate the formation of fast overland flow, which is generally the main factor causing sediment
643 movement on land surfaces. However, the raindrops can still work directly on the bare mudflat
644 surface and influence recently deposited, unconsolidated sediments as pointed out by Voulgaris
645 and Meyers (2004).

646 When the vegetated flat was exposed, the rinsing of the vegetation surface by raindrops
647 results in a direct transport of sediments to the bed. Our experiments show the direct trapping of
648 sediments by the vegetation surface. Precipitation creates a pathway for those particles to be
649 moved onto the bed. Furthermore, the thick sediment layer on the vegetation leaf surfaces might
650 cause a problem for seedling growth by different means, such as reducing photosynthesis or
651 increasing the bending of stems. It has been observed by ecologists that the seedlings of
652 saltmarsh grass and mangrove trees can be smothered due to the thick layer of mud on leaf
653 surfaces (Yihui Zhang, *personal communication*). Therefore, rainfall events, especially moderate
654 ones, can be of fundamental importance to the coastal wetland system and further studies on their
655 frequency and seasonality coupled with tidal characteristics should be considered in the future in
656 order to understand the mechanisms driving the change of coastal ecosystems.

4.3 The Limitations of Field Observations

Instrument availability and the restrictions of *in situ* deployment during this study lead to two primary limitations which should be discussed. Firstly, the number of ADVs available restricted the number of observations possible. Three locations were carefully chosen to form a nearly isoceles triangle, so that the mangrove and the saltmarsh were located on the same contour line (Chen et al., 2016*)*, sharing a mutual control site on the bare mudflat. The elevation difference between the two vegetated flats and the bare mudflat bed is only 0.05 m *(*Chen et al., 2016*)*. This small elevation difference has minimal influence on the flow direction and the subsequent suspended sediment transport, which can be confirmed through application of Soulsby's drag coefficient calculations, as derived for bedforms *(*Soulsby, 1997*)*:

$$z_{0b} = a\frac{\Delta H^2}{\lambda} \qquad (7)$$

$$C_{Db} = \left[\frac{0.4}{1+\ln(\frac{z_{0b}}{h})}\right]^2 \qquad (8)$$

where ΔH and λ are the height (0.05 m) and width (35 m), respectively, of the bed form, Z_{0b} is the bed roughness due to bedform, h is the mean water depth and C_{Db} is the drag coefficient attributed to the bedform. The C_{Db} is estimated to be 0.0026 for the 0.05 m elevation difference, which is over an order of magnitude smaller than the drag coefficients (0.04-0.36) associated with the three sites *(*Chen et al., 2016*)*, indicating that the elevation change has very limited contribution to any frictional term and is unlikely to affect flows. The principal reason for the

677 alteration of flows and suspended sediment transport is therefore attributed to the presence of
678 vegetation.

679 Secondly, some assumptions have been made regarding likely sediment transport
680 pathways within the tidal flat. Although we acknowledge that the sediment could be transported
681 into and out of the tidal flat via different routes, this question was addressed using previous
682 observations and modeling results. The tidal flat under investigation features a gently seaward
683 sloping topography, and lacks a well-developed tidal creek system (Chen et al., 2016*)*. Under
684 these circumstances, modeling *(*Temmerman et al., 2005b*)* suggests that flow directions during a
685 tidal cycle are usually perpendicular to the marsh edge with the sedimentation processes
686 controlled by elevation differences and distance from the marsh edge. Thus, our study assumes
687 that suspended sediments are transported into and out of the vegetation via the same route. This
688 assumption might cause some uncertainty of the suspended sediment flux estimates and further
689 work investigating the sediment transport pathway is needed in the future, particularly within
690 coastal wetlands.

691

692 **5 Conclusions**

693 Field observations were made to compare the sediment transport processes occurring
694 between a bare mudflat, a saltmarsh and a mangrove edge, considering both hydrodynamically
695 induced sediment settling and the direct trapping effects of the vegetation surface. The
696 interpretation of the SSC data, together with high-frequency flow measurements, reveals that the
697 saltmarsh grass are more efficient than the mangrove trees at inducing sediment trapping over a
698 tidal-cycle scale. The main findings of this study are summarized in Fig. 8 and outlined below:

699 1) The SSC data exhibit a strong tidal asymmetry. The SSC is higher during the flood phase

than the ebb phase for all three sites, implying a favorable environment for a net sediment input. The mean SSC level is generally high on the mudflat and decreases within the vegetated area, which is generally consistent with the deposition rates of the three sites.

2) Tidal cycle-scale sediment flux estimates show a depositional environment on the studied tidal flat. The presence of vegetation alters the flow direction and the subsequent suspended sediment transported into the system. Sediment transport fluxes indicate that the saltmarsh edge is more efficient than the mangrove edge at trapping sediment. This pattern is further supported by calculations of sediment fluxes at a tidal scale and deposition rates at a longer timescale. Although the SSC reduction is more pronounced at the mangrove site, the flow rotation caused by the mangrove trees reduces the sediment flux into the mangrove edge itself. Instead, a large portion of suspended sediment is transported along the mangrove edge, which is significantly different from the sediment transport pattern of the saltmarsh edge.

3) The mechanism for acceleration of deposition by tidal flat vegetation can be identified by using two approaches: sediment settling driven by local changes in the hydrodynamics and the direct sediment trapping by vegetation surfaces. Particle settling over a tidal scale was evaluated from deposition tendency. Deposition tendency on the bare mudflat is generally higher during ebb tides than flood tides, indicating a tidal asymmetry and a deposition lag during the ebb phase. Tidal flat vegetation is able to mediate the tidal asymmetry of this deposition tendency. Vegetation radically increases this parameter during floods when the SSC is high, and this creates a more favorable environment for deposition. Even though it is more efficient in trapping sediment, the saltmarsh grass is found to be less efficient than the mangrove trees at altering the deposition tendency of

723 that sediment (Table 2).

724 4) The sediments trapped on vegetation leaves and stems are also quantified using samples
725 of natural standings and seedlings. Saltmarsh grass has a higher direct sediment trapping
726 ability than mangrove trees. The amount of sediment trapped by the saltmarsh grass
727 surface can contribute a considerable amount to deposition, in particular when associated
728 with rainfall events, whilst the sediment directly trapped by mangrove trees is negligible
729 compared to the observed total annual deposition rate in this particular site where only
730 young mangrove trees occupy the front and very limited biomass is found close to the
731 bed. A new mechanism of direct sediment trapping by the vegetation surface, in
732 combination with precipitation, is proposed by this study, as a supplement to the
733 mechanisms associated with hydrodynamic mediation by vegetation.

734

735 Fig. 8. A summary of the main findings of this study: 1) the suspended sediments are transported
736 from the bare mudflat to the vegetated edges with similar inundation periods, the fluxes can be
737 decomposed into normal and parallel components; 2) a considerable amount of sediment was
738 trapped at the front of the saltmarsh and the mangrove; 3) the saltmarsh front is more efficient
739 than the mangrove front due to the flow rotation caused by the mangrove; and 4) the sediment
740 trapping is associated with two mechanisms: hydrodynamically induced sediment settling and
741 direct trapping by the vegetation surfaces. The size of the arrow and the circle provides the
742 information on relative magnitudes of these mechanisms.

743

Acknowledgments

We would like to thank Dr. Yihui Zhang at Xiamen University and Prof. Dong-Ping Wang at State University of New York at Stony Brook for their valuable comments on inspiring this manuscript. Mr. Yi Li and Mr. Yang Yang (SIO, SOA) are thanked for their support in fieldwork. Thanks extend to the Management Office of Yunxiao Mangrove National Nature Reserve, for the site access. The data used are listed in the tables and figures. This work is funded by NSFC Projects (Grant no. 41006047 and 41776096) and a Fundamental Research Fund of Second Institute of Oceanography (No. JT1505). The authors also thank the anonymous reviewers for their time and thoughtful comments.

References

Alongi, D.M., Pftitzner, J., Trott, L.A., Tirendi, F., Dixon, P., and D.W., Klumpp, 2005.Rapid sediment accumulation and microbial mineralization in forests of the mangrove Kandelia candel in the Jiulongjang Estuary, China. Estuarine. Coastal and Shelf Science 63, 605–618.

Amos, C. L., Villatoro, M., Helsby, R., Thompson, C. E. L., Zaggia, L., and G.,Umgiesser, *et al*., 2009. The measurement of sand transport in two inlets of venice lagoon, italy. Estuarine Coastal & Shelf Science, 87(2), 225-236.doi: 10.1016/j.ecss.2009.05.016.

Arkema, K.K.,Guannel, G., Verutes, G., Wood, S.A., Guerry, A., Ruckelshaus, M., Kareiva, P., Lacayo, M. and J.M., Silver, 2013. Coastal habitats shield people and property from sea-level rise and storms Nature Climate Change, 3, 913-918. doi: 10.1038/NCLIMATE1944

765 Barbier, E.B., Hacker, S.D., Kennedy, C., Koch, E.W., Stier and A.C.B., Silliman, 2011.The
766 value of estuarine and coastal ecosystem services. Ecological Monographs, 81(2), 169-
767 193. doi: 10.1890/10-1510.1

768 Beuselinck, L., G.,Govers, P. B., Hairsine, G.C., Sander, and M. Breynaert, 2002. The influence
769 of rainfall on sediment transport by overland flow over areas of net deposition. Journal of
770 Hydrology, 257, 145-163.doi:10.1016/S0022-1694(01)00548-0.

771 Bouma, T. J., L. A. van Duren, S. Temmerman, T. Claverie, A. Blanco-Garcia, T. Ysebaert, and
772 P. M. J. Herman, 2007. Spatial flow and sedimentation patterns within patches of
773 epibenthic structures: Combining field, flume and modelling experiments, Continental
774 Shelf Research, 27(8), 1020-1045, doi:10.1016/j.csr.2005.12.019.

775 Brown, J.M. and A.G., Davies, 2010. Flood/ebb tidal asymmetry in a shallow sandy estuary and
776 the impact on net sand transport. Geomorphology 114 (2010) 431–439.
777 doi:10.1016/j.geomorph.2009.08.006

778 Cahoon, D. R., Hensel, P. F., Spencer, T., Reed, D. J., McJee, K. and N. Saintilan, 2006. Coastal
779 Wetland Vulnerability to Relative Sea-Level Rise: Wetland Elevation Trends and Process
780 Controls. Verhoeven, J.T.A., Beltman, B., Bobbink, R.,and D.F. Whigham (eds.),
781 Wetlands and Natural Resource Management, Volume 190 of the series Ecological
782 Studies, 271-292.

783 Carus, J., Paul, M., and B., Schroder, 2016. Vegetation as self-adaptive coastal protection:
784 Reduction of current velocity and morphologic plasticity of a brackish marsh pioneer.
785 Ecology and Evolution 2016; 6(6), 1579–1589. doi: 10.1002/ece3.1904

786 Chen, Y., C. E. L. Thompson, and M. B. Collins, 2012. Saltmarsh creek bank stability:
787 Biostabilisation and consolidation with depth, Continental Shelf Research, 35, 64-74, doi:
788 10.1016/j.csr.2011.12.009.

789 Chen, Y., Li, Y., Cai, T., Thompson, C. E. L., and Y. Li, 2016. A comparison of
790 biohydrodynamic interaction within mangrove and saltmarsh boundaries. Earth Surface
791 Processes and Landforms, 41(13): 1967-1979. doi: 10.1002/esp.3964.

792 Childers, D. L., and J. W. Day, 1990. Marsh-water column interactions in two Louisiana
793 sstuaries. I. sediment dynamics. Estuaries, 13(4), 393-403.

794 Christiansen, T., P. L. Wiberg, and T. G. Milligan, 2000. Flow and Sediment Transport on a
795 Tidal Salt Marsh Surface, Estuarine, Coastal and Shelf Science, 50(3), 315-331,
796 doi:10.1006/ecss.2000.0548.

797 Chung, C.H., 2006. Forty years of ecological engineering with Spartina plantations in China.
798 Ecological Engineering, 27, 49–57. doi:10.1016/j.ecoleng.2005.09.012

799 Dronkers, J., 1986. Tidal asymmetry and estuarine morphology. Netherlands Journal of Sea
800 Research, 20 (2/3), 117-131.

801 Fagherazzi, S., Marani, M., and L.K., Blum, 2004. The ecogeomorphology of tidal marshes.
802 Washington, DC: American Geophysical Union, Coastal and Estuarine Studies, 268pp.

803 French, J.R., and T., Spencer, 1993. Dynamics of sedimentation in a tide-dominated back barrier
804 salt marsh, Norfolk, UK. Marine Geology, 110, 315-331.

805 Friess, D. A., K.W. Krauss, E.M. Horstman, T. Balke, T.J. Bouma, D. Galli, and E.L. Webb,
806 2012. Are all intertidal wetlands naturally created equal? Bottlenecks, thresholds and

knowledge gaps to mangrove and saltmarsh ecosystems. Biological Reviews, 87, 346–366. doi:10.1111/j.1469-185X.2011.00198.x

Furukawa, K., and E. Wolanski, 1996. Sedimentation in mangrove forests. Mangroves and Salt Marshes, 1, 3-9.

Furukawa, K., Wolanski, E., and H.Mueller, 1997. Currents and sediment transport in mangrove forests. Estuarine Coastal and Shelf Science, 44(3), 301-310. doi:10.1006/ecss.1996.0120

Fugate, D. C., and C. T. Friedrichs, 2002. Determining concentration and fall velocity of estuarine particle populations using ADV, OBS and LISST, Continental Shelf Research, 22(11-13), 1867-1886, doi:Pii S0278-4343(02)00043-2.

Fugate, D. C., and C. T. Friedrichs, 2003. Controls on suspended aggregate size in partially mixed estuaries, Estuarine, Coastal and Shelf Science, 58(2), 389-404, doi:10.1016/s0272-7714(03)00107-0.

Gao, J., Feng, Z., Chen, L., Wang, Y., Bai, F. and J., Li, 2016. The effect of biomass variations of Spartina alterniflora on the organiccarbon content and composition of a salt marsh in northern JiangsuProvince, China. Ecological Engineering 95, 160–170. doi: 10.1016/j.ecoleng.2016.06.088

Gao, S., Du, Y.F., Xie, W.J., Gao, W.H., Wang, D.D. and X.D., Wu, 2014. Environment-ecosystem dynamic processes of Spartina alterniflora salt-marshes along the eastern China coastlines. Science China: Earth Sciences, 57, 2567–2586, doi: 10.1007/s11430-014-4954-9

Gedan, K. B., M. L.,Kirwan, E., Wolanski, E. B., Barbier, and B. R. Silliman, 2010. The present and future role of coastal wetland vegetation in protecting shorelines: answering recent

challenges to the paradigm. Climatic Change, 106(1), 7-29. doi: 10.1007/s10584-010-0003-7

Gillis, L. G., T. J. Bouma, W. Kiswara, A. D. Ziegler, and P. M. J. Herman, 2014. Leaf transport in mimic mangrove forests and seagrass beds, Mar Ecol Prog Ser, 498, 95-102, doi:10.3354/meps10615.

Goring D. G., and V. I. Nikora, 2002. Despiking acoustic Doppler velocimeter data. Journal of Hydraulic Engineering, ASCE 128: 117-126. doi:10.1061/(ASCE)0733429(2002)128:1(117)

Graham, G. W., and A. J. Manning, 2007. Floc size and settling velocity within a *Spartina anglica* canopy, Continental Shelf Research, 27(8), 1060-1079. doi:10.1016/j.csr.2005.11.017.

Greene, R. S. B. and P. B. Hairsine, 2004. Elementary processes of soil–water interaction and thresholds in soil surface dynamics: a review. Earth Surface Processes and Landforms, 29,1077-1091. doi: 10.1002/esp.1103.

Ha, H. K., and J. P. Y. Maa, 2010. Effects of suspended sediment concentration and turbulence on settling velocity of cohesive sediment, Geosciences Journal, 14(2), 163-171, doi:10.1007/s12303-010-0016-2.

Horstman, E.M., Dohmen-Janssen, C.M., Bouma, T.J., and S. J. M. H. Hulscher, 2015. Tidal-scale flow routing and sedimentation in mangrove forests: Combining field data and numerical modelling, Geomorphology, 228, 244-262. doi:10.1016/j.geomorph.2014.08.011.

Kathiresan, K., 2003. How do mangrove forests induce sedimentation? Revista de Biologia Tropical 51, 355-360.

Kelleway, J.J., Saintilan, N., Macreadie, P.I., Baldock, J.A. and P.J. Ralph, 2017. Sediment and carbon deposition vary among vegetation assemblages in a coastal salt marsh. Biogeosciences, 14, 3763–3779. doi:10.5194/bg-14-3763-2017

Kitheka, J.U., Ongwenyi, G.S., and K.M., Mavuti, 2003. Fluxes and exchange of suspended sediment in tidal inlets draining a degraded mangrove forest in Kenya. Estuarine, Coastal and Shelf Science, 56, 655–667.doi:10.1016/S0272-7714(02)00217-2

Leonard, L.A., and M.E. Luther, 1995. Flow hydrodynamics in tidal marsh canopies. Limnology and Oceanography 40: 1474–1484.

Li, J., Xu, J., Zhang, D., Yan, X., Tong, Y. and Y., Shen. 2005. Function of Spartina alterniflora salt march and its eco-economic value in south coast of Hangzhou Bay. Areal Research and Development, 24, 58-62. (In Chinese with English abstract).

Li, Y., Y., Chen, Y., Li, 2017. Remote sensing analysis of the changes in the junction region of mangrove forests and *Spartina alterniflora* saltmarshes. Marine Science Bulletin, 36, 348-359.

Liao, C.Z., Luo, Y.Q., Fang, C.M., Chen, J.K., Li, B., 2008. Litter pool sizes, decomposition, and nitrogen dynamics in Spartina alterniflora-invaded and native coastal marshlands of the Yangtze estuary. Oecologia 156, 589–600.

Lin, P., 2001. A review on the mangrove research in China. Journal of Xiamen University (Natural Science), 40(2), 592-603.

871 Lin, P., Hu, H., Zheng, W., Li, Z., and Y., Lin, 1998. A study of biomass and energy of
872 mangrove communities in Shenzhen Bay. Scientia Silvae Sinicae, 34, 18-23. (In Chinese
873 with English abstract)

874 Lin, P., Lu, C., Lin, G., Chen, R., and L., Su, 1985. Study on mangrove ecosystem of
875 Jiulongjiang River estuary. Journal of Xiamen University (Natural Science), 24, 508-514.
876 (In Chinese with English abstract)

877 Lin, P., Lu, C., Wang, G. and H., Chen, 1995. Biomass and productivity of *Bruguiera sexangula*
878 mangrove forest in Hainan Island, China. Journal of Xiamen University (Natural
879 Science), 29, 209-213. (In Chinese with English abstract)

880 Lin, P., Yin, Y. and C., Lu, 1992. Biomass and productivity of *Rhizophora stylosa* community in
881 Yingluo Bay of Guangxi, China. Journal of Xiamen University (Natural Science), 31,
882 199-202. (In Chinese with English abstract)

883 Liu, Q., 1991. Silt transportation and its influences on submarine scour and silting in Dongshan
884 Bay, Fujian Journal of Oceanography in Taiwan Strait, 10(1), 69-76.

885 Lovelock, C. E., M. F. Adame, V. Bennion, M. Hayes, R. Reef, N. Santini, and D. R. Cahoon ,
886 2015. Sea level and turbidity controls on mangrove soil surface elevation change,
887 Estuarine, Coastal and Shelf Science, 153, 1-9, doi:10.1016/j.ecss.2014.11.026.

888 Luhar, M., and H. M. Nepf, 2013. From the blade scale to the reach scale: A characterization of
889 aquatic vegetative drag, Advances in Water Resources, 51, 305-316,
890 doi:10.1016/j.advwatres.2012.02.002.

891 Mazda, Y., Kanazawa, N., and E.,Wolanski, 1995. Tidal asymmetry in mangrove creeks.
892 Hydrobiologia 295, 51–58.

MICZTWR Office, 1990. Multipurpose Investigation of the Coastal Zone and Tidal Wetland Resources– Report of Fujian Province. 575pp. Ocean Press, China.

Mitsch, W.J., and J.G. Gosselink, 2007. Wetlands. John Wiley & Sons: Chichester, 619pp.

Moller, I., Kudella, M., Rupprecht, F., Spencer, T., Paul, M., van Wesenbeeck, B. K., and S. Schimmels, 2014. Wave attenuation over coastal salt marshes under storm surge conditions. Nature Geoscience, 7(10), 727-731. doi: 10.1038/ngeo2251

Moss, A. J., Walker, P. H., and J. Hutka, 1979. Raindrop-simulated transportation in shallow water flows: an experimental study. Sedimentary Geology, 22, 165-184.

Nepf, H., 1999. Drag, turbulence, and diffusion in flow through emergent vegetation. Water Resources Research, 35(2), 479-489. doi: 10.1029/1998wr900069.

Nepf, H., 2012. Flow and transport in regions with aquatic vegetation. Annual Review of Fluid Mechanics 44: 123–142. doi:10.1146/annurev-fluid-120710-101048.

Neumeier, U., and P. Ciavola, 2004, Flow Resistance and Associated Sedimentary Processes in a Spartina maritima Salt-Marsh, J Coastal Res, 20(2), 435-447, doi:10.2112/1551-5036(2004)020(0435:FRAASP)2.0.CO;2.

Neumeier, U., and C. L. Amos, 2006.The influence of vegetation on turbulence and flow velocities in European salt-marshes. Sedimentology, 53(2), 259-277. doi: 10.1111/j.1365-3091.2006.00772.x

Ortiz, A., Ashton A., and H. Nepf, 2013. Mean and turbulent velocity fields near rigid and flexible plants, and the implications for deposition. Journal of Geophysical Research - Earth Surface 118: 1–15.DOI:10.1002/2013JF002858.

914 Perillo, G. E. M., E. Wolanski, D. R. Cahoon, and M. M. Brinson, 2009. Coastal Wetlands: An
915 Integrated Ecosystem Approach, Elsevier, Elsevier B.V.

916 Proffitt, A. P. B., Rose, C. W., and P. B., Hairsine, 1991. Rainfall detachment and deposition:
917 experiments with low slopes and significant water depth. Soil Science Society of
918 America Journal, 55, 325-332. doi:10.2136/sssaj1991.03615995005500020004x

919 Redfield, A.C., 1972. Development of a New England salt marsh. Ecological Monographs,
920 42,201–237.

921 Saintilan, N., Wilson, N., Rogers, K., Rajkaran, A., and K.W. Krauss, 2014. Mangrove
922 expansion and salt marsh decline at mangrove poleward limits. Global Change Biology,
923 20 (1), 147-157.doi: 10.1111/gcb.12341

924 Scully, M. E., and C. T. Friedrichs, 2007. Sediment pumping by tidal asymmetry in a partially
925 mixed estuary Journal of Geophysical Research, 112, C07028,
926 doi:10.1029/2006JC003784

927 Sheng, J., and A.E.,Hay, 1988. An examination of the spherical scatterer approximation in
928 aqueous suspensions of sand. Journal of the Acoustic Society of America 83 (2), 598–
929 610.

930 Shi, Z., Pethick, J. S., and K., Pye, 1995. Flow structure in and above the various heights of a
931 saltmarsh canopy: a laboratory flume study. Journal of Coastal Research 11(4), 1204–
932 1209.

933 SonTek, 1997. SonTek Doppler current meters: using signal strength data to monitor suspended
934 sediment concentration. SonTek/YSIInc., California, 7pp.

935 Soulsby R., 1997. Dynamics of Marine Sands: A Manual for Practical Applications. Thomas
936 Telford: London, 272pp.

937 Temmerman, S., Bouma, T.J., Govers, G., Wang, Z.B., De Vries, M.B. and P.M.J., Herman,
938 2005a. Impact of vegetation on flow routing and sedimentation patterns: Three-
939 dimensional modeling for a tidal marsh. Journal of Geophysical Research 110, F04019.
940 doi:10.1029/2005JF000301

941 Temmerman, S., Bouma, T.J., Govers, G., and D., Lauwaet, 2005b, Flow paths of water and
942 sediment in a tidal marsh: relations with marsh developmental stage and tidal inundation
943 height. Estuaries 28, 338–352.

944 Temmerman, S., Meire, P., Bouma, T.J., Herman, P.M.J., Ysebaert, T., and H., De Vriend, 2013.
945 Ecosystem-based coastal defence in the face of global change. Nature 504, 79-83.
946 doi:10.1038/nature12859.

947 Thompson, C.E.L., C.L., Amos, and G., Umgiesser, 2004, A Comparison Between Fluid Shear
948 Stress Reduction by Halophytic Plants in Venice Lagoon, Italy and Rustico Bay, Canada
949 - analyses of in situ measurements. Journal of Marine Systems 51, 293-308. Doi:
950 10.1016/j.jmarsys.2004.05.017.

951 van der Wal, D., and K. Pye, 2004. Patterns, rates and possible causes of saltmarsh erosion in the
952 Greater Thames area (UK), Geomorphology, 61(3-4), 373-391,
953 doi:10.1016/j.geomorph.2004.02.005.

954 Vargas-Luna, A., A. Crosato, and W. S. J. Uijttewaal, 2015. Effects of vegetation on flow and
955 sediment transport: comparative analyses and validation of predicting models, Earth Surf
956 ace Processes and Landforms, 40(2), 157-176, doi:10.1002/esp.3633.

957 Vincent, C.E., and A., Downing, 1994. Variability of suspendeds and concentrations, transport
958 and eddy diffusivity under non-breaking waves on the shore face. Continental Shelf
959 Research 14 (2/3), 223–250.

960 Voulgaris, G., and S. T. Meyers, 2004. Temporal variability of hydrodynamics, sediment
961 concentration and sediment settling velocity in a tidal creek, Continental Shelf Research,
962 24, 1659–1683, doi:10.1016/j.csr.2004.05.006.

963 Wang, A., Gao, S., Jia, J., Pan, S., 2005. Contemporary sedimentataion rates on saltmarshes at
964 Wanggang, Jiangsu, China. Journal of Geographical Sciences, 15, 199-209. doi:
965 10.1360/gs050208

966 Wang, A., Ye, X., and J., Chen, 2010. Observations and analyses of floc size and floc settling
967 velocity in coastal salt marsh of Luoyuan Bay, Fujian Province, China. Acta Oceanologia
968 Sinica 29, 116-126. doi: 10.1360/gs050208.

969 Wang, Y., Gao, S., Jia, J., Thompson, C.E.L., Gao J., and Y. Yang, 2012. Sediment transport
970 over an accretional intertidal flat with influences of reclamation, Jiangsu coast, China.
971 Marine Geology 291-294, 147-161. doi:10.1016/j.margeo.2011.01.004.

972 Wang, Y., Gao, S., Jia, J., Liu Y., and J., Gao, 2014. Remarked morphological change in a large
973 tidal inlet with low sediment-supply. Continental Shelf Research 90, 79-95.doi:
974 10.1016/j.csr.2014.02.005

975 Wolanski, E., 1995. Transport of sediment in mangrove swamps, Hydrobiologia, 295, 31-42.

976 Wolanski, E., Mazda, Y., King, B., and S., Gay, 1990. Dynamics, flushing and trapping in
977 Hinchinbrook channel, a giant mangrove swamp, Australia. Estuarine Coastal and Shelf
978 Science, 31, 555–579.

979 Wolanski, E., Mazda, Y., Furukawa, K., Ridd, P., Kitheka, J.,Spagnol, S., and T., Stieglitz, 2001.
980 Water-circulation in mangroves and its implications for Biodiversity. In E. Wolanski
981 (Ed.), Oceanographic processes of coral reefs: physical and biological links in the Great
982 Barrier Reef (pp. 53–76). London: CRC Press.

983 Woodroffe, C.D., Rogers, K., McKee, K.L., Lovelock, C.E., Mendelssohn, I.A. and N. Saintilan,
984 2016. Mangrove Sedimentation and Response to Relative Sea-Level Rise. Annual
985 Review of Marine Science, 8, 243–66. Doi: 0.1146/annurev-marine-122414-034025

986 Zhang, Y., Wang, W., Wu, Q., Fang, B., and P. Lin, 2006. The growth of Kandelia candel
987 seedlings in mangrove habitats of the Zhangjiang estuary in Fujian, China. Acta
988 Ecologica Sinica, 26(6), 1648-1655. doi: 10.1016/s1872-2032(06)60028-0

989 Zhang, Y. H., Huang, G. M., Wang, W. Q., Chen, L. Z., and G.H. Lin, 2012. Interactions
990 between mangroves and exotic Spartina in an anthropogenically disturbed estuary in
991 southern China. Ecology, 93(3), 588-597.

992 Zong, L., and H. Nepf, 2010. Flow and deposition in and around a finite patch of vegetation,
993 Geomorphology, 116(3-4), 363-372, doi:10.1016/j.geomorph.2009.11.020.

994 Zuo, P., Zhao, S., Liu, C., Wang,C. and Y., Liang, 2012. Distribution of Spartina spp. along
995 China's coast. Ecological Engineering, 40,160– 166. doi:10.1016/j.ecoleng.2011.12.014

996

Figure 1

Click here to download high resolution image

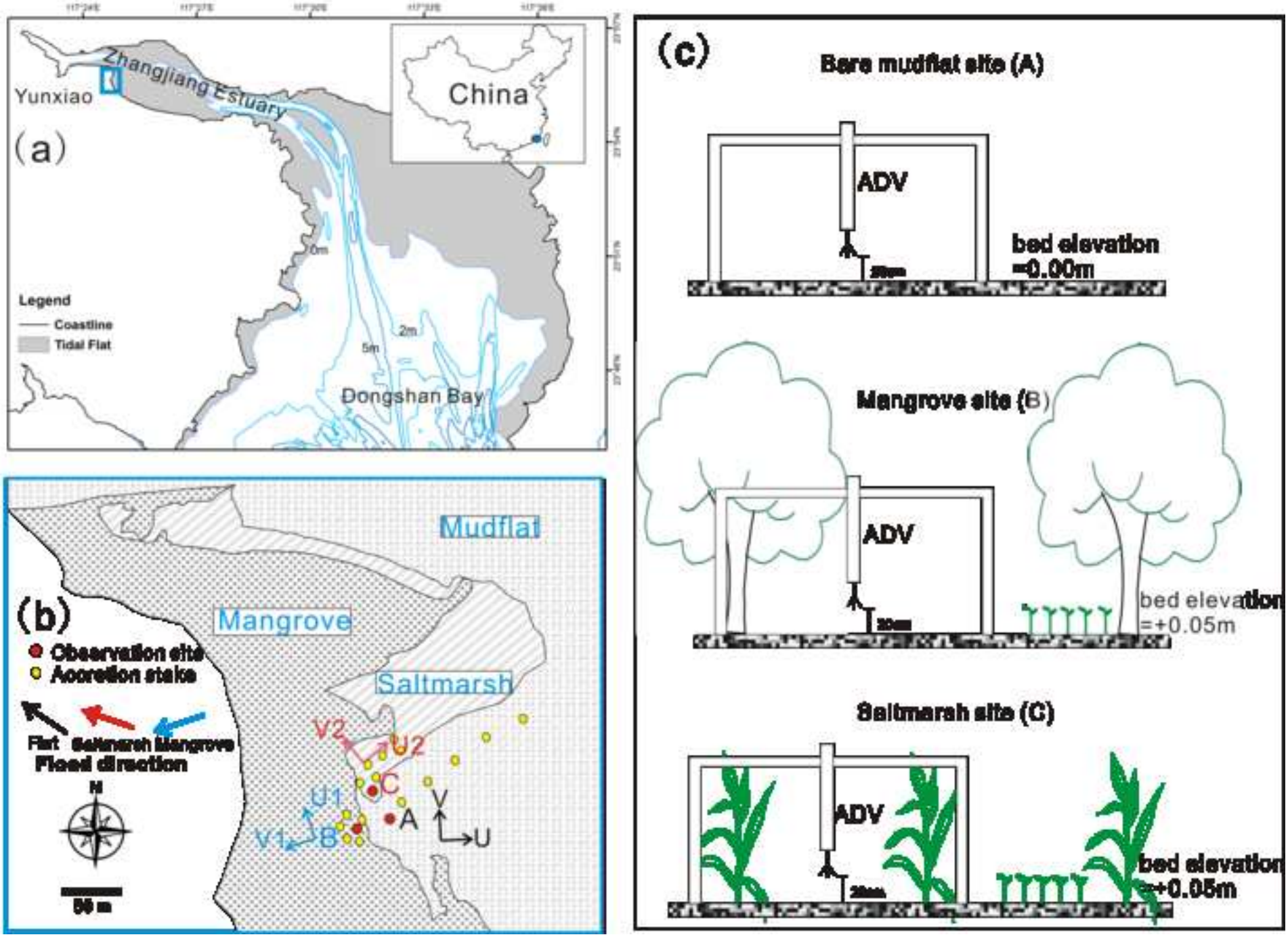

Figure 3

Click here to download high resolution image

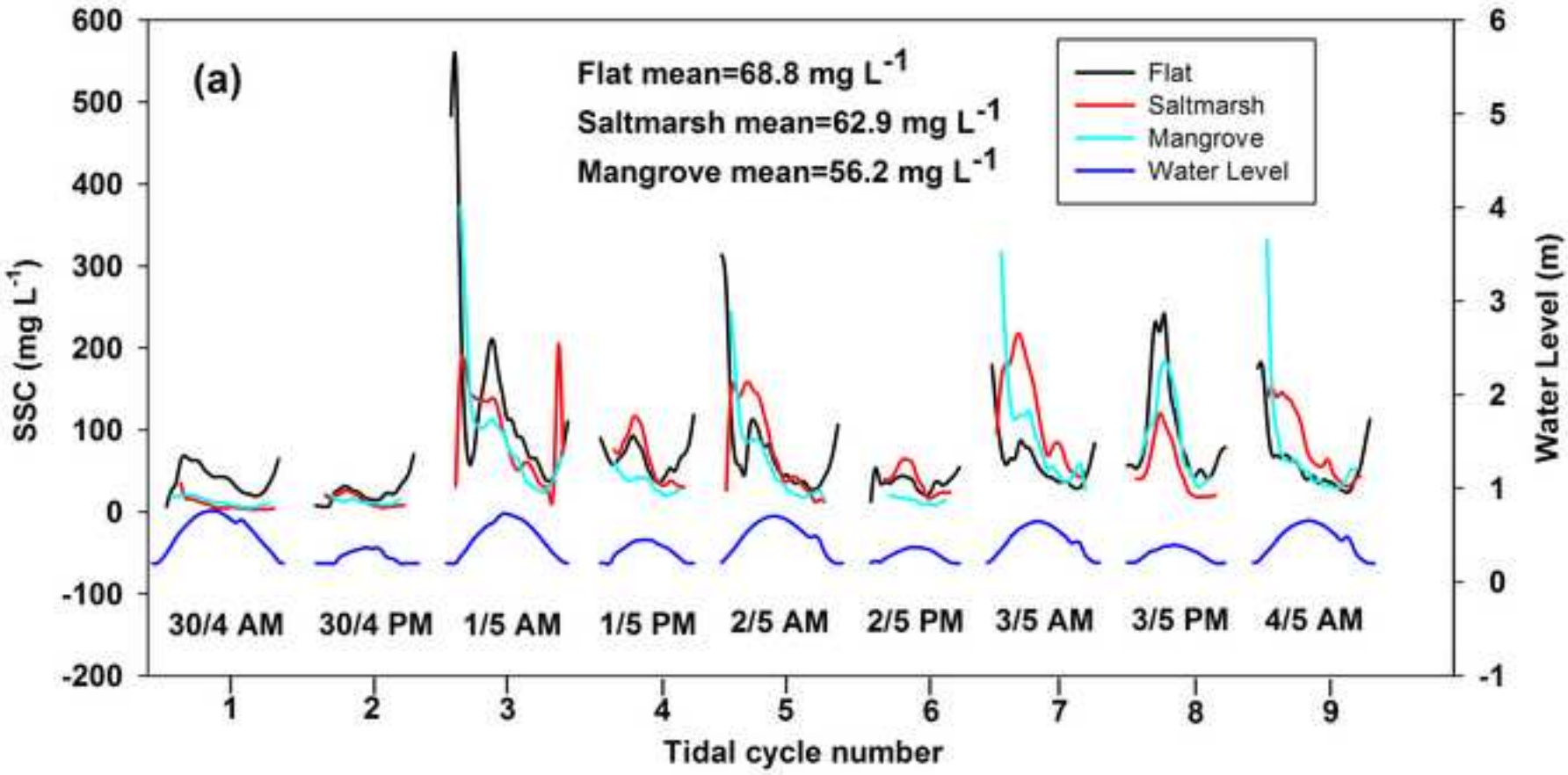

Figure 4

Click here to download high resolution image

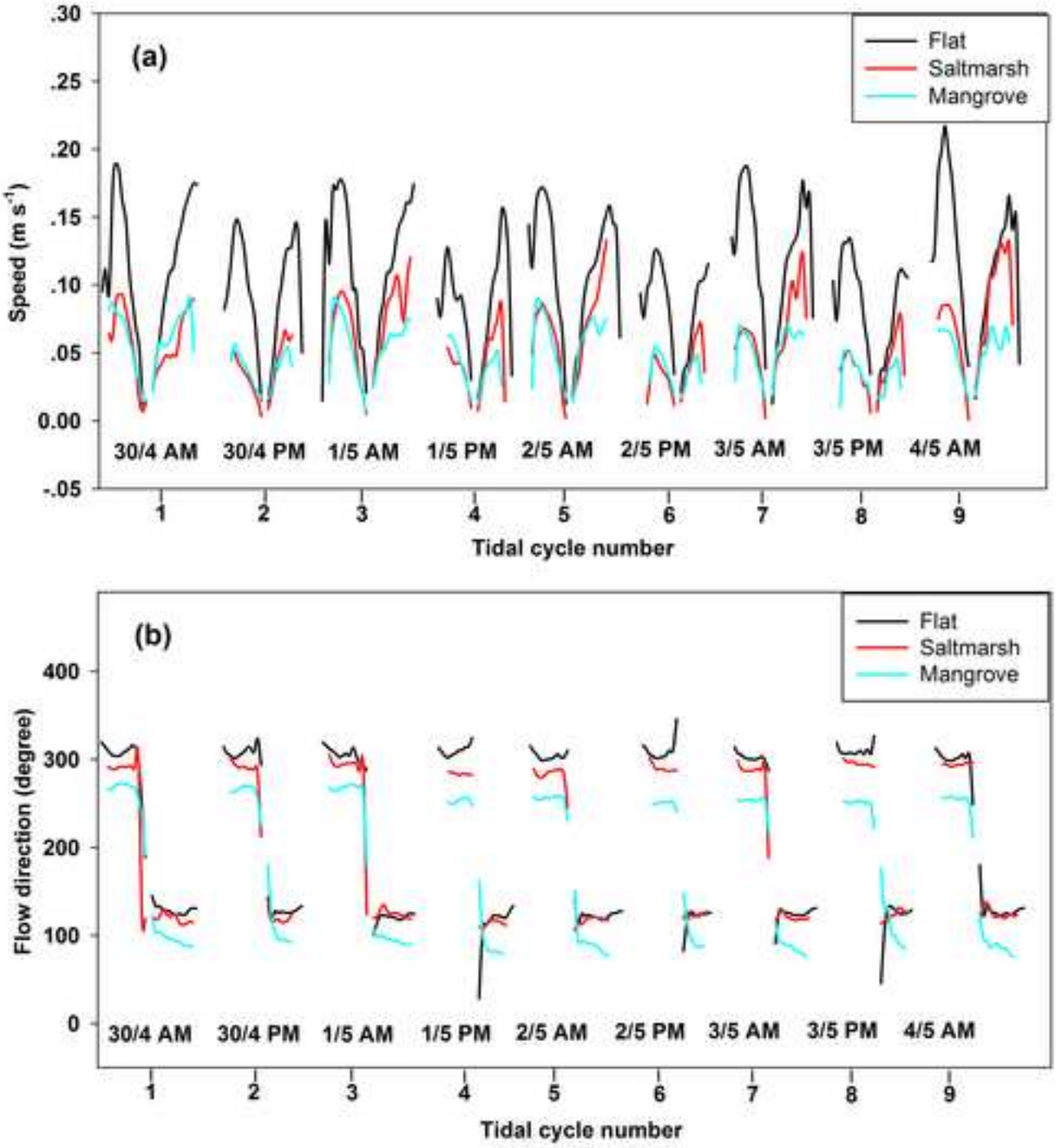

Figure 5

Click here to download high resolution image

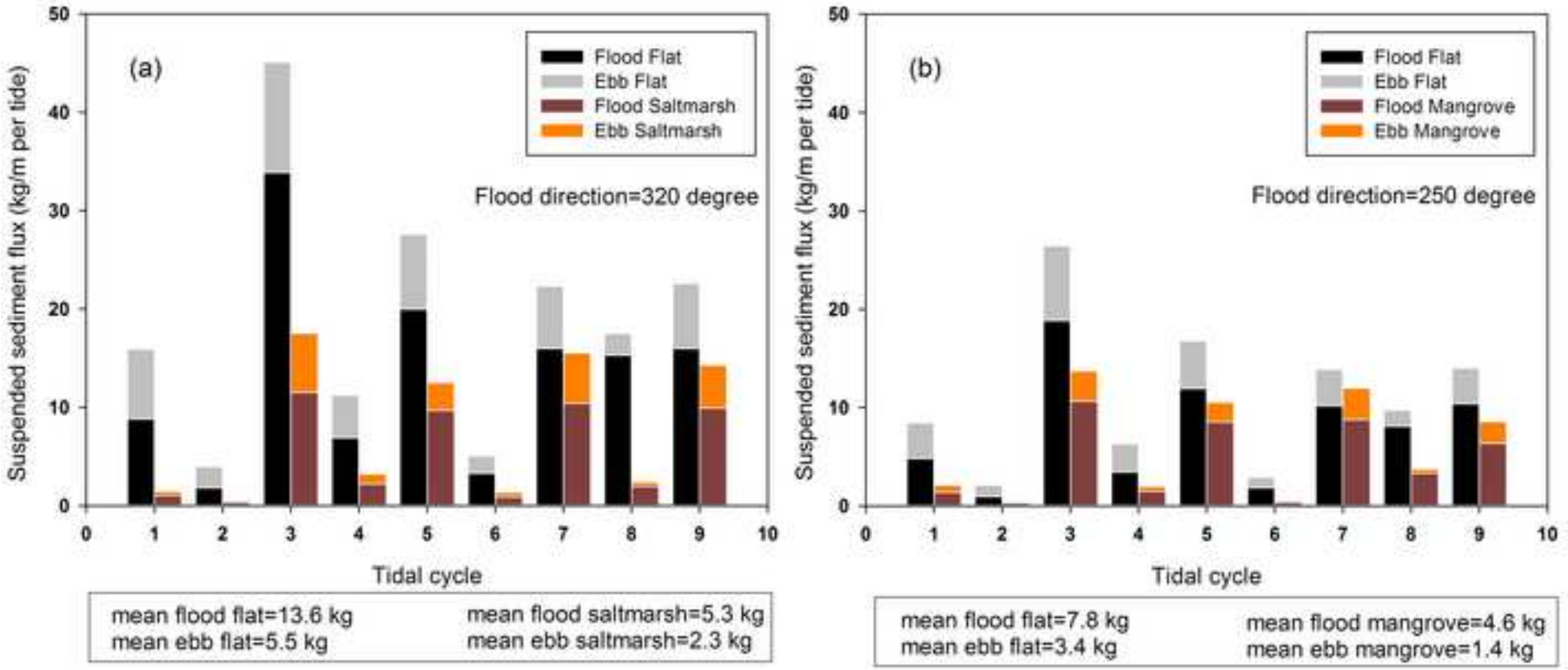

Figure 2

Click here to download high resolution image

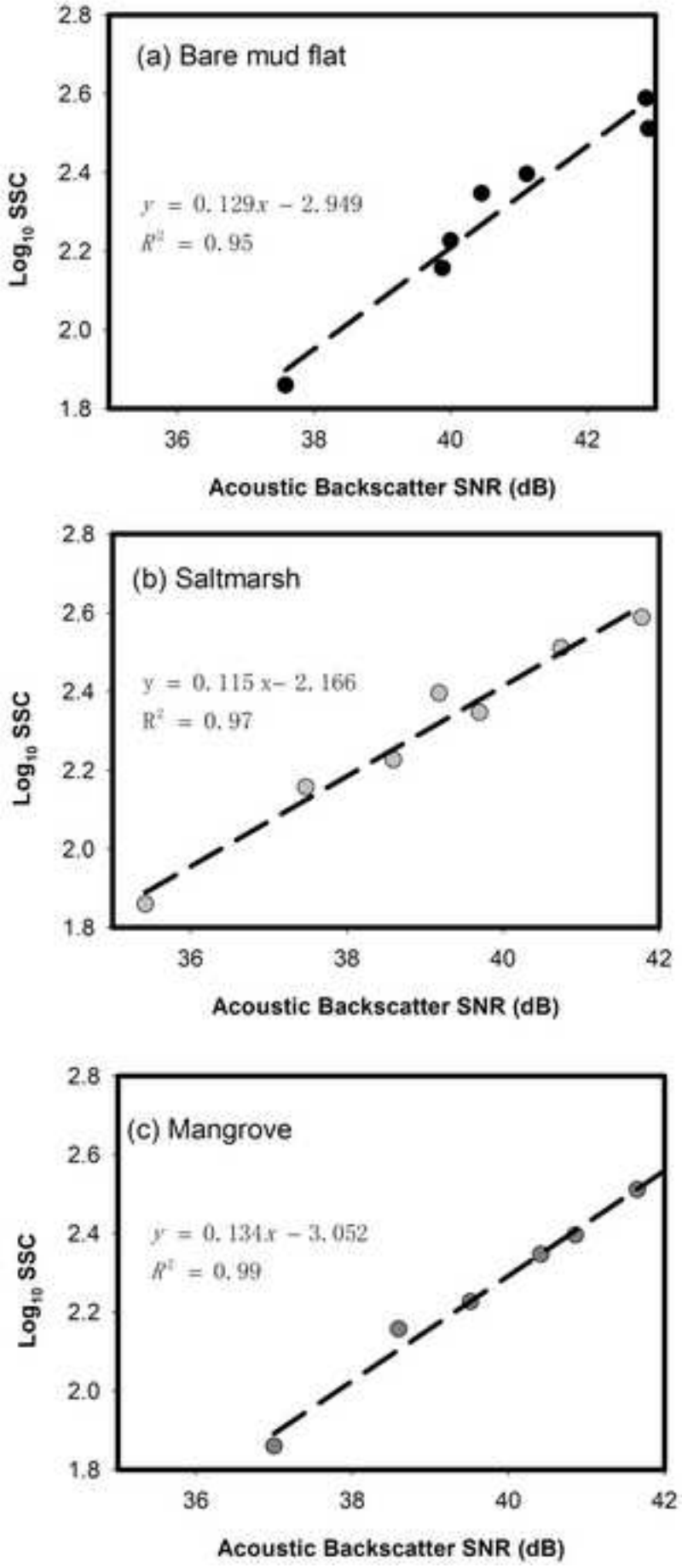

Figure 6

Click here to download high resolution image

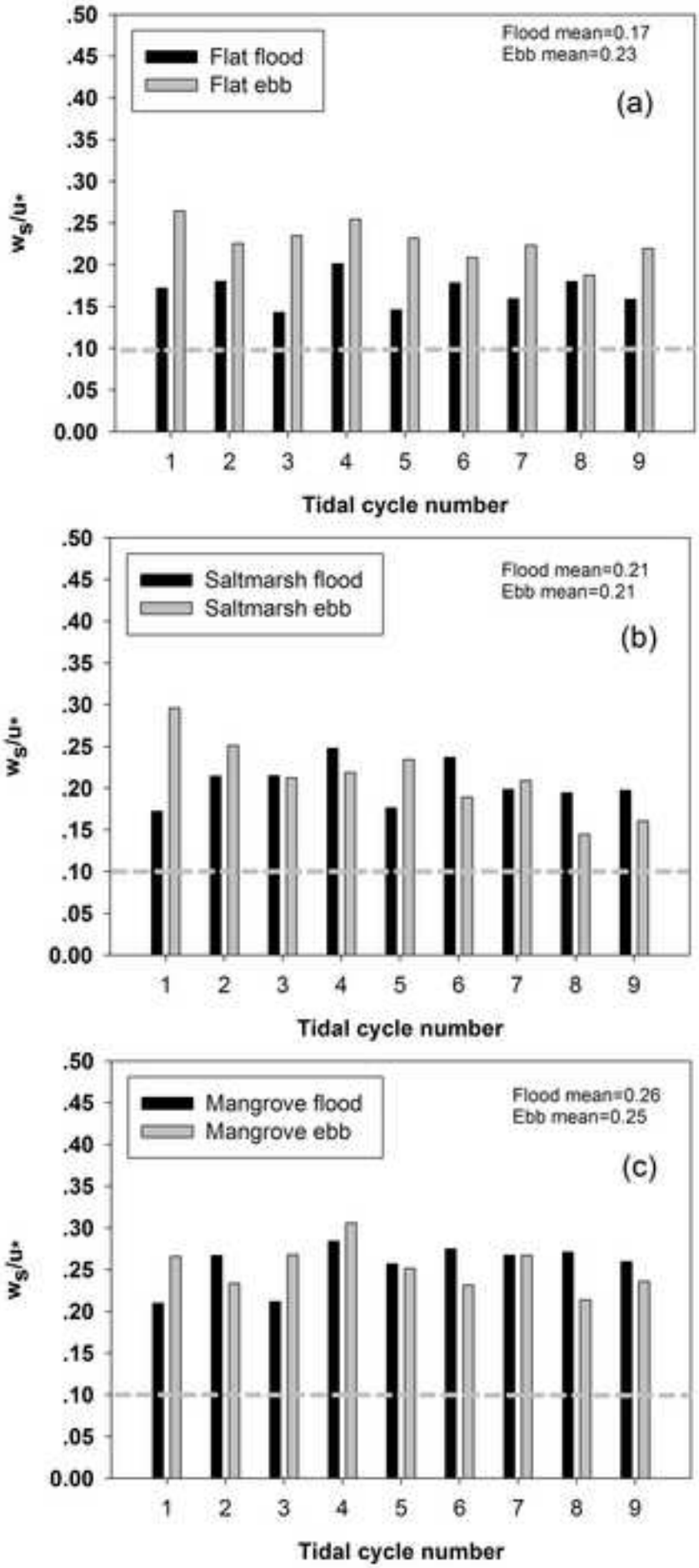

Figure 7

Click here to download high resolution image

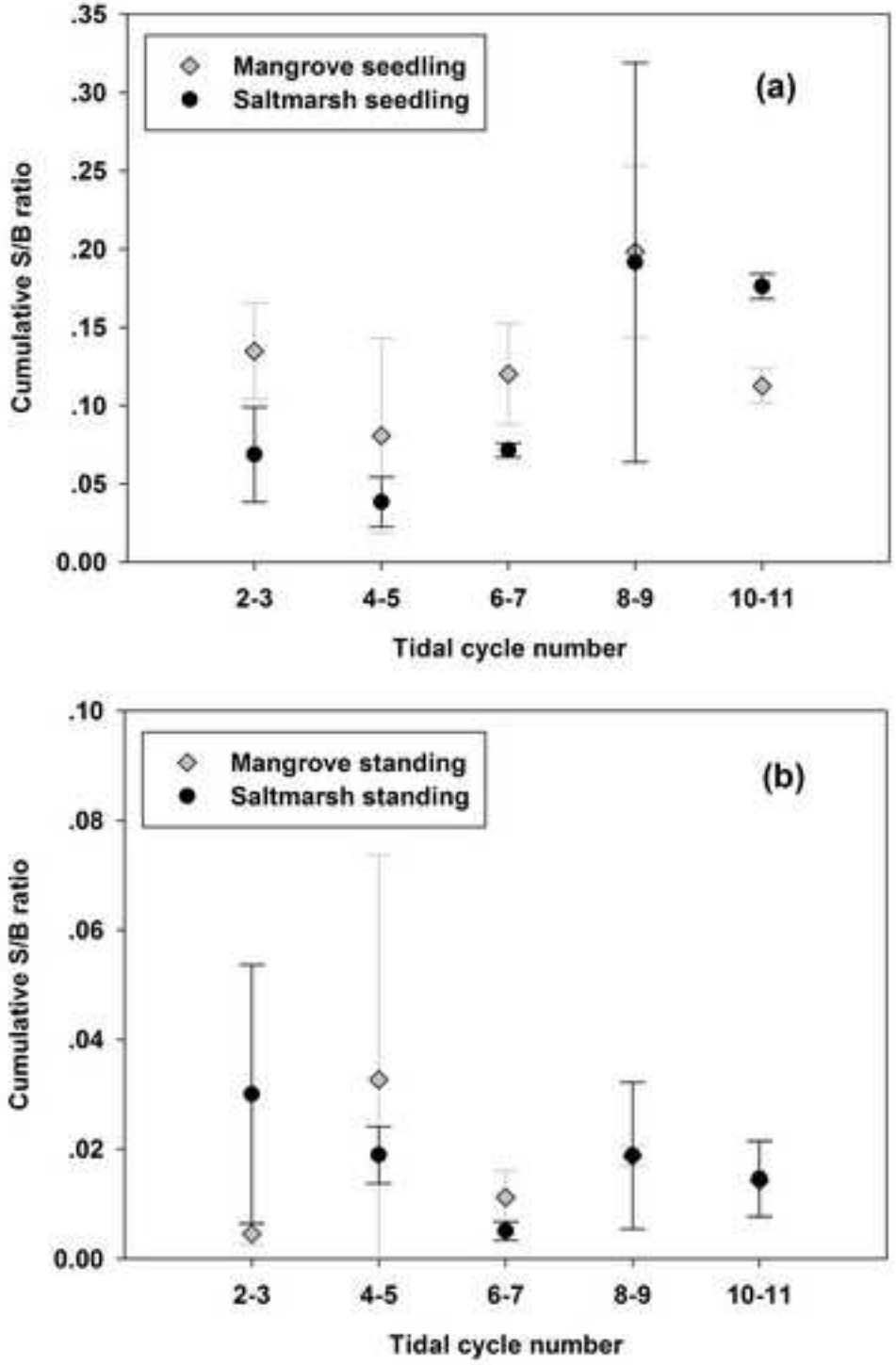

Figure 8

Click here to download high resolution image